

Supporting Information

Design and photophysical studies of Iridium(III)-Cobalt(III) dyads and their application for dihydrogen photo-evolution

Cédric Lentz,^a Olivier Schott,^b Thomas Auvray,^b Garry S. Hanan,^{b*} Benjamin Elias^{a*}

^a Institute of Condensed Matter and Nanosciences, Molecular Chemistry, Materials and Catalysis (IMCN/MOST), UCLouvain, Place Louis Pasteur 1, bte L4.01.02, B-1348 Louvain-la-Neuve (Belgium)

^b Département de Chimie, Université de Montréal, 2900 Boulevard Edouard-Montpetit, Montréal, Québec H3T 1J4 (Canada)

Table of Content

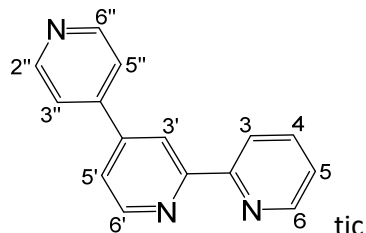
Synthetic procedures.....	2
1) Ligands.....	2
2) Ir(III) photosensitizers.....	3
3) Ir(III)-Co(III) dyads.....	8
¹ H NMR Spectra	11
Crystallographic study	26
Cyclic voltammetry.....	32
1) Ir(III) photosensitizers.....	32
2) Ir(III)-Co(III) dyads.....	35
Absorption and emission spectra of Ir(III) photosensitizers	37
Absorption spectra of Ir(III)-Co(III) dyads.....	40
Acid titrations data	43
Theoretical model	61
Photo-catalyzed hydrogen production.....	101
References.....	115

Synthetic procedures

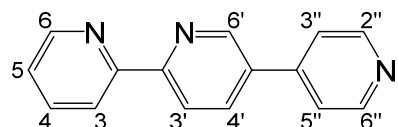
4-Bromo-2,2'-bipyridine¹ and 5-bromo-2,2'-bipyridine² were synthesized as previously described. Precursors [Ir(ppy)₂Cl]₂, [Ir(ppyF)₂Cl]₂ and [Ir(piq)₂Cl]₂ were obtained according to Nonoyama's procedure.³ Co(III) complexes were synthesized as previously described.⁴ All the procedures applied to synthesize the Ir(III) photosensitizers and the Ir(III)-Co(III) dyads were performed in the dark.

1) Ligands

2244tpy. In a Schlenk flask were successively added 4-bromo-2,2'-bipyridine (102.3 mg, 0.435 mmol), 1,2-dimethoxyethane (9.0 mL), water (1.2 mL), K₂CO₃ (120.9 mg, 0.875 mmol) and 4-pyridylboronic acid (70.1 mg, 0.570 mmol). The mixture was degassed and put under Argon before adding [Pd(PPh₃)₄] (51.2 mg, 0.0443 mmol). The reaction mixture was degassed again and refluxed for 4 days under Argon. The mixture was poured onto water (30 mL). The solid was filtered on Celite, washed successively with water and ethyl acetate. The organic layer was separated and the aqueous phase extracted with ethyl acetate (3 x 30 mL). The organic layers were combined, dried over MgSO₄ and concentrated under reduced pressure. The product was purified by chromatography column on silica using CH₂Cl₂:MeOH / 95:5 as eluent. The fraction with R_f = 0.3 was collected and evaporated (m = 84.2 mg – 82.9 %). ¹H NMR (CDCl₃), δ/ppm: 8.77 (dd, 1H, H-6', J_{6'-5'} = 5.1 Hz, J_{6'-3'} = 0.7 Hz), 8.74 (dd, 2H, H-2'' + H-6'', J_{2''/6''-3''/5''} = 4.5 Hz, J_{2''/6''-5''/3''} = 1.7 Hz), 8.69 (m, 2H, H-6 + H-3'), 8.45 (dd, 1H, H-3, J₃₋₄ = 7.9 Hz, J₃₋₅ = 1.1 Hz), 7.84 (ddd, 1H, H-4, J₄₋₃ = 7.9 Hz, J₄₋₅ = 7.7 Hz, J₄₋₆ = 1.8 Hz), 7.64 (dd, 2H, H-3'' + H-5'', J_{3''/5''-2''/6''} = 4.5 Hz, J_{5''/3''-2''/6''} = 1.7 Hz), 7.53 (dd, 1H, H-5', J_{5'-6'} = 5.1 Hz, J_{5'-3'} = 1.9 Hz), 7.33 (ddd, 1H, H-5, J₅₋₄ = 7.7 Hz, J₅₋₆ = 4.8 Hz, J₅₋₃ = 1.1 Hz).

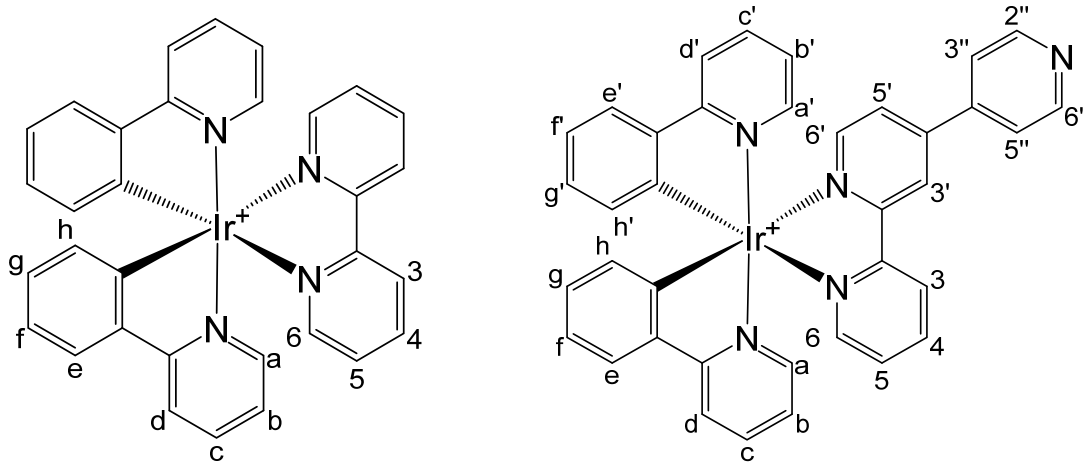


2254tpy. In a Schlenk flask were successively added 5-bromo-2,2'-bipyridine (60.1 mg, 0.256 mmol), 1,2-dimethoxyethane (5.3 mL), water (0.7 mL), K₂CO₃ (72.9 mg, 0.528 mmol) and 4-pyridylboronic acid (42.3 mg, 0.344 mmol). The mixture was degassed and put under Argon before adding [Pd(PPh₃)₄] (32.1 mg, 0.0278 mmol). The reaction mixture was degassed again and refluxed for 4 days under Argon. The mixture was poured onto water (30 mL). The solid was filtered on Celite and washed successively with water and ethyl acetate. The organic layer was separated and the aqueous phase extracted with ethyl acetate (3 x 30 mL). The organic layers were combined, dried over MgSO₄ and concentrated under reduced pressure. The product was purified by chromatography column on silica using CH₂Cl₂:MeOH / 95:5 as eluent. The fraction with a R_f = 0.3 was collected and evaporated (m = 48.6 mg – 81.5 %). ¹H NMR (CDCl₃), δ/ppm: 8.97 (d, 1H, H-6', J_{6'-4'} = 2.4 Hz, J_{6'-3'} = 0.5 Hz), 8.73 (m, 3H, H-2'' + H-6'' + H-6), 8.55 (dd, H-3', J_{3'-4'} = 8.3 Hz, J_{3'-6'} = 0.5 Hz), 8.46 (dd, 1H, H-3, J₃₋₄ = 7.9 Hz, J₃₋₅ = 1.1 Hz), 8.08 (dd, 1H, H-4', J_{4'-3'} = 8.3 Hz, J_{4'-6'} = 2.4 Hz), 7.86 (dd, 1H, H-4, J₄₋₃ = 7.9 Hz, J₄₋₅ = 7.6 Hz, J₄₋₆ = 1.8 Hz), 7.60 (dd, 2H, H-3'' + H-5'', J_{3''/5''-2''/6''} = 4.5 Hz, J_{5''/3''-2''/6''} = 1.7 Hz), 7.36 (1H, ddd, H-5, J₅₋₄ = 7.6 Hz, J₅₋₆ = 4.8 Hz, J₅₋₃ = 1.1 Hz).



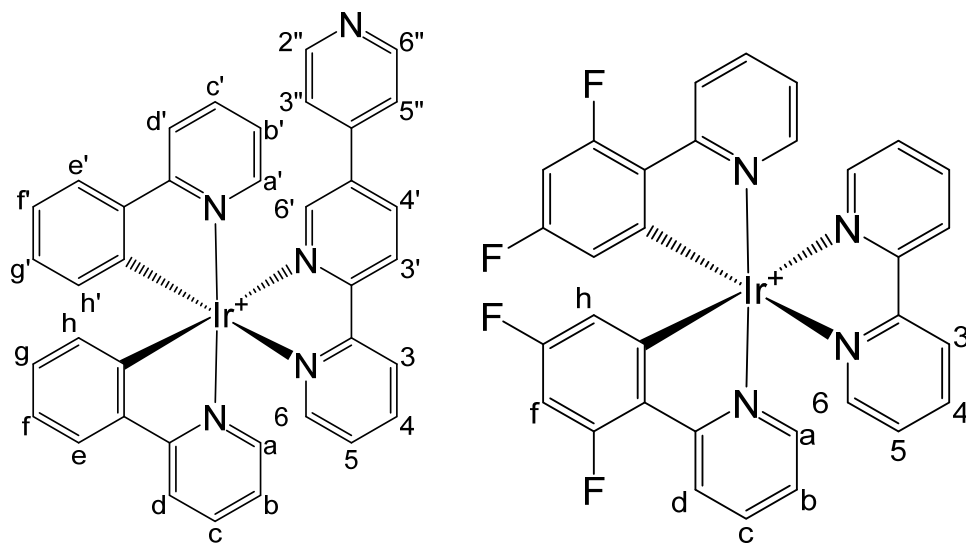
2) Ir(III) photosensitizers

Irppy-bpy. $[\text{Ir}(\text{ppy})_2\text{Cl}]_2$ (0.0571 mg, 0.0532 mmol) and 2,2'-bipyridine (20.0 mg, 0.128 mmol) were suspended in ethyleneglycol (7.0 mL). The mixture was refluxed overnight under Argon. The solution was cooled to room temperature and a saturated aqueous solution of NH_4PF_6 (6.0 mL) was added for precipitation. The solid was centrifuged, washed with water (3X) and dried under reduced pressure. HRMS (ESI): m/z calculated for $[\text{C}_{32}\text{H}_{24}^{193}\text{IrN}_4 - \text{PF}_6]^+$, 657.16247 ; found: 657.16221, m/z calculated for $[\text{C}_{22}\text{H}_{16}^{193}\text{IrN}_2 - \text{PF}_6 - \text{bpy}]^+$, 501.09372 ; found: 501.09222. ^1H NMR (CD_3CN), δ/ppm : 8.53 (dd, 2H, H -3, $J_{3-4} = 8.1$ Hz, $J_{3-5} = 1.3$ Hz), 8.12 (ddd, 2H, H -4, $J_{4-3} = 8.1$ Hz, $J_{4-5} = 7.9$ Hz, $J_{4-6} = 1.7$ Hz), 8.06 (dd, 2H, H -d, $J_{d-c} = 8.5$ Hz, $J_{d-b} = 1.6$ Hz), 7.98 (dd, 2H, H -6, $J_{6-5} = 5.5$ Hz, $J_{6-4} = 1.7$ Hz), 7.85 (ddd, 2H, H -c, $J_{c-d} = 8.5$ Hz, $J_{c-b} = 7.6$ Hz, $J_{c-a} = 1.6$ Hz), 7.80 (dd, 2H, H -e, $J_{e-f} = 7.8$ Hz, $J_{e-g} = 1.4$ Hz), 7.60 (dd, 2H, H -a, $J_{a-b} = 5.8$ Hz, $J_{a-c} = 1.6$ Hz), 7.50 (ddd, 2H, H -5, $J_{5-4} = 7.9$ Hz, $J_{5-6} = 5.5$ Hz, $J_{5-3} = 1.3$ Hz), 7.04 (ddd, 2H, H -f, $J_{f-e} = 7.8$ Hz, $J_{f-g} = 7.5$ Hz, $J_{f-h} = 1.3$ Hz), 7.02 (ddd, 2H, H -b, $J_{b-c} = 7.6$ Hz, $J_{b-a} = 5.8$ Hz, $J_{b-d} = 1.6$ Hz), 6.92 (ddd, 2H, H -g, $J_{g-f} = J_{g-h} = 7.5$ Hz, $J_{g-e} = 1.4$ Hz), 6.28 (dd, 2H, H -h, $J_{h-g} = 7.5$ Hz, $J_{h-f} = 1.3$ Hz).



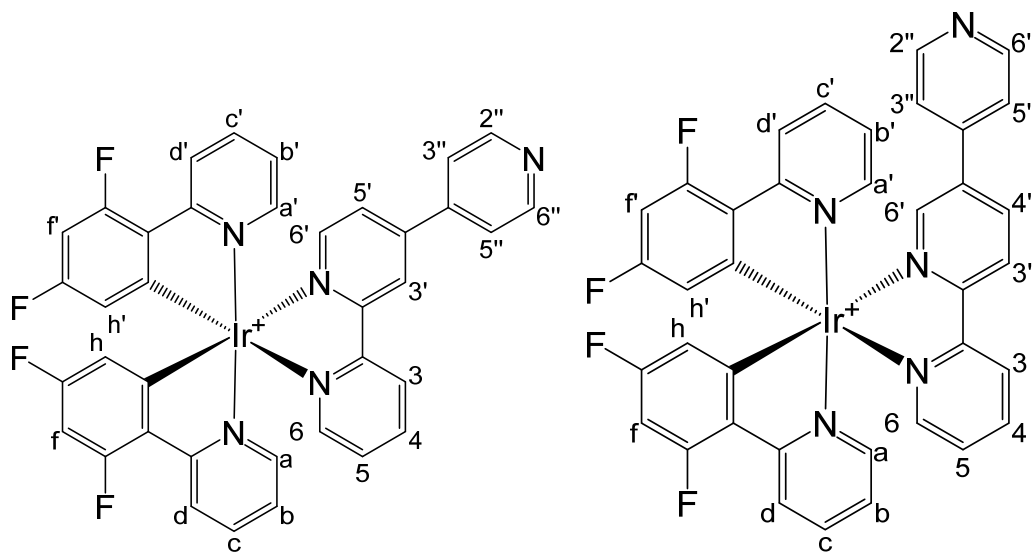
Irppy-2244tpy. $[\text{Ir}(\text{ppy})_2\text{Cl}]_2$ (47.0 mg, 0.0438 mmol) and 2,2';4',4''-terpyridine (22.5 mg, 0.0965 mmol) were suspended in ethyleneglycol (6.0 mL). The mixture was refluxed overnight under Argon. The solution was cooled to room temperature and a saturated aqueous solution of NH_4PF_6 (5.0 mL) was added for precipitation. The solid was centrifuged, washed with water (3X) and dried under reduced pressure. HRMS (ESI): m/z calculated for $[\text{C}_{37}\text{H}_{27}^{193}\text{IrN}_5 - \text{PF}_6]^+$, 734.18902 ; found: 734.18860, m/z calculated for $[\text{C}_{22}\text{H}_{16}^{193}\text{IrN}_2 - \text{PF}_6 - 2244\text{-tpy}]^+$, 501.09372 ; found: 501.09245. ^1H NMR (CD_3CN), δ/ppm : 8.79 (m, 3H, H -3' + H -2'' + H -6''), 8.71 (dd, 1H, H -3, $J_{3-4} = 8.1$ Hz, $J_{3-5} = 0.5$ Hz), 8.17 (ddd, 1H, H -4, $J_{4-3} = 8.1$ Hz, $J_{4-5} = 7.7$ Hz, $J_{4-6} = 1.1$ Hz), 8.08 (m, 2H, H -d + H -d'), 8.05 (d, 1H, H -6', $J_{6-5'} = 5.8$ Hz), 8.02 (dd, 1H, H -6, $J_{6-5} = 5.5$ Hz, $J_{6-4} = 1.1$ Hz), 7.84 (m, 4H, H -c + H -c' + H -e + H -e'), 7.78 (m, 3H, H -5' + H -3'' + H -5''), 7.65 (m, 2H, H -a + H -a'), 7.54 (ddd, 1H, H -5, $J_{5-4} = 7.7$ Hz, $J_{5-6} = 5.5$ Hz, $J_{5-3} = 0.5$ Hz), 7.05 (m, 4H, H -f + H -f' + H -b + H -b'), 6.94 (m, 2H, H -g + H -g'), 6.30 (m, 2H, H -h + H -h').

Irppy-2254tpy. $[\text{Ir}(\text{ppy})_2\text{Cl}]_2$ (53.0 mg, 0.0494 mmol) and 2,2';5',4''-terpyridine (25.5 mg, 0.109 mmol) were suspended in ethyleneglycol (6.0 mL). The mixture was refluxed overnight under Argon. The solution was cooled to room temperature and a saturated aqueous solution of NH_4PF_6 (5.0 mL) was added for precipitation. The solid was centrifuged, washed with water (3X) and dried under reduced pressure. HRMS (ESI): m/z calculated for $[\text{C}_{37}\text{H}_{27}^{193}\text{IrN}_5 - \text{PF}_6]^+$, 734.18902 ; found: 734.18906, m/z calculated for $[\text{C}_{22}\text{H}_{16}^{193}\text{IrN}_2 - \text{PF}_6 - 2254\text{-tpy}]^+$, 501.09372 ; found: 501.09293. ^1H NMR (CD_3CN), δ/ppm : 8.62 (m, 3H, $H\text{-}3' + H\text{-}2'' + H\text{-}6''$), 8.57 (dd, 1H, $H\text{-}3$, $J_{3\text{-}4} = 8.1$ Hz, $J_{3\text{-}5} = 0.6$ Hz), 8.42 (dd, 1H, $H\text{-}4'$, $J_{4'\text{-}3'} = 8.5$ Hz, $J_{4'\text{-}6'} = 2.0$ Hz), 8.18 (d, 1H, $H\text{-}6'$, $J_{6'\text{-}4'} = 2.0$ Hz), 8.15 (ddd, 1H, $H\text{-}4$, $J_{4\text{-}3} = 8.1$ Hz, $J_{4\text{-}5} = 7.8$ Hz, $J_{4\text{-}6} = 1.6$ Hz), 8.07 (m, 2H, $H\text{-}d + H\text{-}d'$), 8.02 (dd, 1H, $H\text{-}6$, $J_{6\text{-}5} = 5.4$ Hz, $J_{6\text{-}4} = 1.6$ Hz), 7.84 (m, 4H, $H\text{-}c + H\text{-}c' + H\text{-}e + H\text{-}e'$), 7.67 (m, 2H, $H\text{-}a + H\text{-}a'$), 7.53 (ddd, 1H, $H\text{-}5$, $J_{5\text{-}4} = 7.8$ Hz, $J_{5\text{-}6} = 5.4$ Hz, $J_{5\text{-}3} = 0.6$ Hz), 7.30 (dd, 2H, $H\text{-}3'' + H\text{-}5''$, $J_{3''/5''\text{-}2''/6''} = 4.5$ Hz, $J_{5''/3''\text{-}2''/6''} = 1.7$ Hz), 7.05 (m, 4H, $H\text{-}f + H\text{-}f' + H\text{-}b + H\text{-}b'$), 6.94 (m, 2H, $H\text{-}g + H\text{-}g'$), 6.33 (m, 2H, $H\text{-}h + H\text{-}h'$).



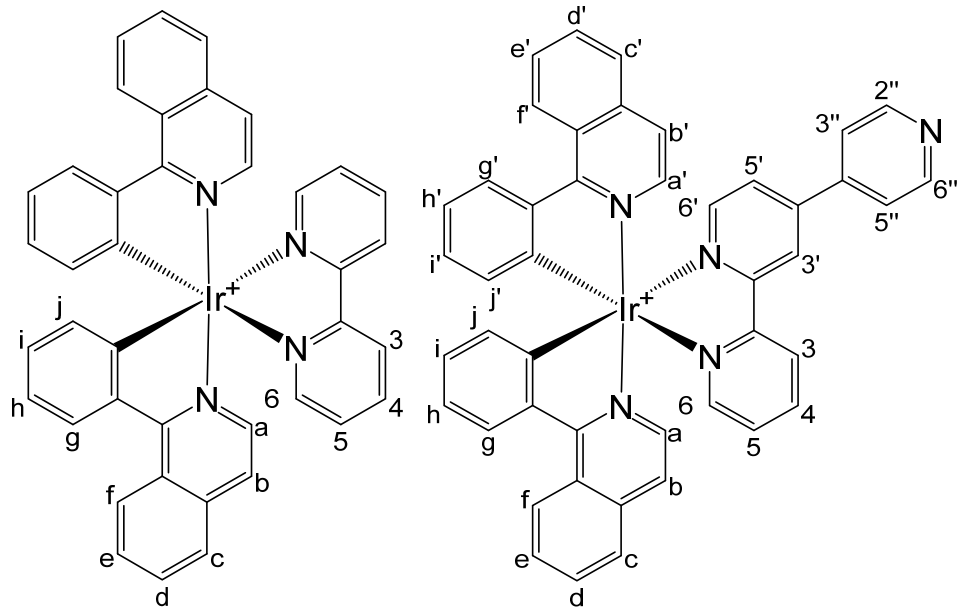
IrppyF2-bpy. $[\text{Ir}(\text{ppyF}_2)_2\text{Cl}]_2$ (71.0 mg, 0.0584 mmol) and 2,2'-bipyridine (22.1 mg, 0.141 mmol) were suspended in ethyleneglycol (7.0 mL). The mixture was refluxed overnight under Argon. The solution was cooled to room temperature and a saturated aqueous solution of NH_4PF_6 (6.0 mL) was added for precipitation. The solid was centrifuged, washed with water (3X) and dried under reduced pressure. HRMS (ESI): m/z calculated for $[\text{C}_{32}\text{H}_{20}\text{F}_4^{193}\text{IrN}_4 - \text{PF}_6]^+$, 729.12478 ; found: 729.12459, m/z calculated for $[\text{C}_{22}\text{H}_{12}\text{F}_4^{193}\text{IrN}_2 - \text{PF}_6 - \text{bpy}]^+$, 573.05604 ; found: 573.05446. ^1H NMR (CD_3CN), δ/ppm : 8.53 (dd, 2H, $H\text{-}3$, $J_{3\text{-}4} = 8.1$ Hz, $J_{3\text{-}5} = 1.1$ Hz), 8.32 (dd, 2H, $H\text{-}d$, $J_{d\text{-}c} = 8.4$ Hz, $J_{d\text{-}b} = 0.7$ Hz), 8.16 (ddd, 2H, $H\text{-}4$, $J_{4\text{-}3} = 8.1$ Hz, $J_{4\text{-}5} = 7.8$ Hz, $J_{4\text{-}6} = 1.4$ Hz), 8.01 (dd, 2H, $H\text{-}6$, $J_{6\text{-}5} = 5.5$ Hz, $J_{6\text{-}4} = 1.4$ Hz), 7.91 (ddd, 2H, $H\text{-}c$, $J_{c\text{-}d} = 8.5$ Hz, $J_{c\text{-}b} = 7.5$ Hz, $J_{c\text{-}a} = 1.2$ Hz), 7.61 (dd, 2H, $H\text{-}a$, $J_{a\text{-}b} = 5.8$ Hz, $J_{a\text{-}c} = 1.2$ Hz), 7.53 (ddd, 2H, $H\text{-}5$, $J_{5\text{-}4} = 7.8$ Hz, $J_{5\text{-}6} = 5.5$ Hz, $J_{5\text{-}3} = 1.1$ Hz), 7.07 (ddd, 2H, $H\text{-}b$, $J_{b\text{-}c} = 7.5$ Hz, $J_{b\text{-}a} = 5.8$ Hz, $J_{b\text{-}d} = 0.7$ Hz), 6.71 (ddd, 2H, $H\text{-}f$, $J_{f\text{-}F} = 12.7$ Hz, $J_{f\text{-}h} = 9.4$ Hz, $J_{f\text{-}h} = 2.4$ Hz), 5.73 (dd, 2H, $H\text{-}h$, $J_{h\text{-}F} = 8.6$ Hz, $J_{h\text{-}f} = 2.4$ Hz).

IrppyF₂-2244tpy. [Ir(ppyF₂)₂Cl]₂ (56.2 mg, 0.0462 mmol) and 2,2';4',4''-terpyridine (23.6 mg, 0.101 mmol) were suspended in ethyleneglycol (6.0 mL). The mixture was refluxed overnight under Argon. The solution was cooled to room temperature and a saturated aqueous solution of NH₄PF₆ (5.0 mL) was added for precipitation. The solid was centrifuged, washed with water (3X) and dried under reduced pressure. HRMS (ESI): m/z calculated for [C₃₇H₂₃F₄¹⁹³IrN₅ – PF₆]⁺, 806.15133 ; found: 806.15063, m/z calculated for [C₂₂H₁₂F₄¹⁹³IrN₂ – PF₆ – 2244-tpy]⁺, 573.05604 ; found: 573.05454. ¹H NMR (CD₃CN), δ/ppm: 8.83 (m, 3H, H-3' + H-2'' + H-6''), 8.75 (d, 1H, H-3, J₃₋₄ = 8.1 Hz, J₃₋₅ = 0.6 Hz), 8.37 (m, 2H, H-d + H-d'), 8.24 (ddd, 1H, H-4, J₄₋₃ = 8.1 Hz, J₄₋₅ = 7.8 Hz, J₄₋₆ = 1.2 Hz), 8.11 (d, 1H, H-6', J_{6'-5'} = 5.8 Hz), 8.02 (dd, 1H, H-6, J₆₋₅ = 5.4 Hz, J₆₋₄ = 1.2 Hz), 7.95 (m, 2H, H-c + H-c'), 7.84 (dd, 1H, J_{5'-6'} = 5.8 Hz, J_{5'-3'} = 1.9 Hz), 7.82 (dd, 2H, H-3'' + H-5'', J_{3''/5''-2''/6''} = 4.5 Hz, J_{5''/3''-2''/6''} = 1.7 Hz), 7.69 (m, 2H, H-a + H-a'), 7.61 (ddd, 1H, H-5, J₅₋₄ = 7.8 Hz, J₅₋₆ = 5.4 Hz, J₅₋₃ = 0.6 Hz), 7.12 (m, 2H, H-b + H-b'), 6.75 (m, 2H, H-H-f + H-f'), 5.79 (m, 2H, H-h + H-h').



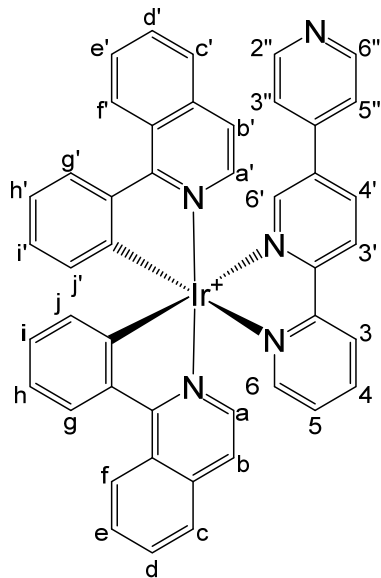
IrppyF₂-2254tpy. [Ir(ppyF₂)₂Cl]₂ (53.7 mg, 0.0442 mmol) and 2,2';5',4''-terpyridine (21.6 mg, 0.0926 mmol) were suspended in ethyleneglycol (6.0 mL). The mixture was refluxed overnight under Argon. The solution was cooled to room temperature and a saturated aqueous solution of NH₄PF₆ (5.0 mL) was added for precipitation. The solid was centrifuged, washed with water (3X) and dried under reduced pressure. HRMS (ESI): m/z calculated for [C₃₇H₂₃F₄¹⁹³IrN₅ – PF₆]⁺, 806.15133 ; found: 806.15068, m/z calculated for [C₂₂H₁₂F₄¹⁹³IrN₂ – PF₆ – 2254-tpy]⁺, 573.05604 ; found: 573.04591. ¹H NMR (CD₃CN), δ/ppm: 8.65 (m, 3H, H-3' + H-2'' + H-6''), 8.59 (d, 1H, H-3, J₃₋₄ = 8.1 Hz, J₃₋₅ = 0.4 Hz), 8.42 (dd, 1H, H-4', J_{4'-3'} = 8.5 Hz, J_{4'-6'} = 2.1 Hz), 8.32 (m, 2H, H-d + H-d'), 8.20 (m, 2H, H-4 + H-6'), 8.03 (dd, 1H, H-6, J₆₋₅ = 5.5 Hz, J₆₋₄ = 0.8 Hz), 7.91 (m, 2H, H-c + H-c'), 7.69 (m, 2H, H-a + H-a'), 7.53 (ddd, 1H, H-5, J₅₋₄ = 7.6 Hz, J₅₋₆ = 5.5 Hz, J₅₋₃ = 0.4 Hz), 7.40 (dd, 2H, H-3'' + H-5'', J_{3''/5''-2''/6''} = 4.5 Hz, J_{5''/3''-2''/6''} = 1.6 Hz), 7.09 (m, 2H, H-b + H-b'), 6.71 (m, 2H, H-f + H-f'), 5.76 (m, 2H, H-h + H-h').

Irpiq-bpy. $[\text{Ir}(\text{piq})_2\text{Cl}]_2$ (0.0322 mg, 0.0253 mmol) and 2,2'-bipyridine (9.4 mg, 0.0602 mmol) were suspended in ethyleneglycol (3.0 mL). The mixture was refluxed overnight under Argon. The solution was cooled to room temperature and a saturated aqueous solution of NH_4PF_6 (3.0 mL) was added for precipitation. The solid was centrifuged, washed with water (3X), dried under reduced pressure and washed again with diethylether (3X). HRMS (ESI): m/z calculated for $[\text{C}_{40}\text{H}_{28}^{193}\text{IrN}_4 - \text{PF}_6]^+$, 755.19144 ; found: 755.19342, m/z calculated for $[\text{C}_{30}\text{H}_{20}^{193}\text{IrN}_2 - \text{PF}_6 - \text{bpy}]^+$, 601.12502 ; found: 601.12306. ^1H NMR (CD_3CN), δ/ppm : 9.02 (m, 2H, $H\text{-c}/H\text{-f}$), 8.54 (dd, 2H, $H\text{-3}$, $J_{3\text{-}4} = 8.1$ Hz, $J_{3\text{-}5} = 1.0$ Hz), 8.38 (dd, 2H, $H\text{-g}$, $J_{g\text{-}h} = 8.2$ Hz, $J_{g\text{-}i} = 1.0$ Hz), 8.11 (ddd, 2H, $H\text{-4}$, $J_{4\text{-}3} = 8.1$ Hz, $J_{4\text{-}5} = 7.8$ Hz, $J_{4\text{-}6} = 1.1$ Hz), 7.99 (m, 2H, $H\text{-f}/H\text{-c}$), 7.87 (dd, 2H, $H\text{-6}$, $J_{6\text{-}5} = 5.4$ Hz, $J_{6\text{-}4} = 1.1$ Hz), 7.84 (m, 4H, $H\text{-d} + H\text{-e}$), 7.51 (d, 2H, $H\text{-b}$, $J_{b\text{-a}} = 6.4$ Hz), 7.46 (ddd, 2H, $H\text{-5}$, $J_{5\text{-}4} = 7.8$ Hz, $J_{5\text{-}6} = 5.4$ Hz, $J_{5\text{-}3} = 1.0$ Hz), 7.42 (d, 2H, $H\text{-a}$, $J_{a\text{-b}} = 6.4$ Hz), 7.14 (ddd, 2H, $H\text{-h}$, $J_{h\text{-g}} = 8.2$ Hz, $J_{h\text{-i}} = 7.8$ Hz, $J_{h\text{-j}} = 1.1$ Hz), 6.88 (ddd, 2H, $H\text{-i}$, $J_{i\text{-h}} = 7.8$ Hz, $J_{i\text{-j}} = 7.6$ Hz, $J_{i\text{-g}} = 1.0$ Hz), 6.31 (dd, 2H, $H\text{-j}$, $J_{j\text{-i}} = 7.6$ Hz, $J_{j\text{-h}} = 1.1$ Hz).



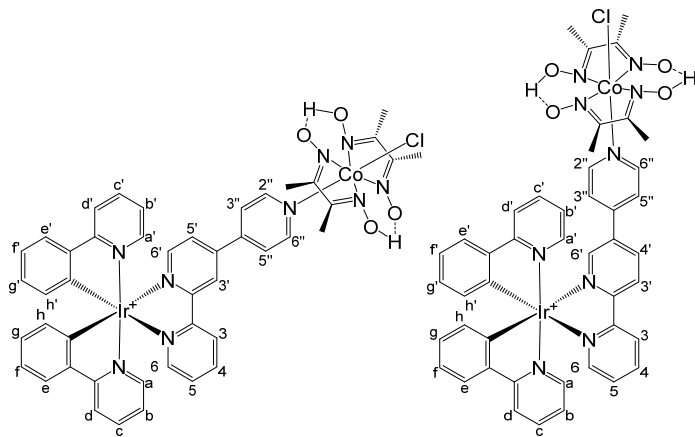
Irpiq-2244tpy. $[\text{Ir}(\text{piq})_2\text{Cl}]_2$ (49.7 mg, 0.0391 mmol) and 2,2';4',4''-terpyridine (20.3 mg, 0.0870 mmol) were suspended in ethyleneglycol (5.0 mL). The mixture was refluxed overnight under Argon. The solution was cooled to room temperature and a saturated aqueous solution of NH_4PF_6 (6.0 mL) was added for precipitation. The solid was centrifuged, washed with water (3X), dried under reduced pressure and washed again with diethylether (3X). HRMS (ESI): m/z calculated for $[\text{C}_{45}\text{H}_{31}^{193}\text{IrN}_5 - \text{PF}_6]^+$, 834.22032 ; found: 834.21994, m/z calculated for $[\text{C}_{30}\text{H}_{20}^{193}\text{IrN}_2 - \text{PF}_6 - 2244\text{tpy}]^+$, 601.12502 ; found: 601.12264. ^1H NMR (CD_3CN), δ/ppm : 9.03 (m, 2H, $H\text{-f} + H\text{-f}'$), 8.81 (d, 1H, $H\text{-3}'$, $J_{3\text{-}5'} = 1.6$ Hz), 8.78 (dd, 2H, $H\text{-2}'' + H\text{-6}''$, $J_{2''/6''-3''/5''} = 4.5$ Hz, $J_{6''/2''-3''/5''} = 1.7$ Hz), 8.74 (dd, 1H, $H\text{-3}$, $J_{3\text{-}4} = 8.1$ Hz, $J_{3\text{-}5} = 0.5$ Hz), 8.40 (m, 2H, $H\text{-g} + H\text{-g}'$), 8.16 (ddd, 1H, $H\text{-4}$, $J_{4\text{-}3} = 8.1$ Hz, $J_{4\text{-}5} = 7.8$ Hz, $J_{4\text{-}6} = 1.5$ Hz), 8.00 (m, 2H, $H\text{-c} + H\text{-c}'$), 7.96 (d, 1H, $H\text{-6}'$, $J_{6\text{-}5'} = 5.8$ Hz), 7.91 (dd, 1H, $H\text{-6}$, $J_{6\text{-}5} = 5.6$ Hz, $J_{6\text{-}4} = 1.5$ Hz), 7.84 (m, 4H, $H\text{-d} + H\text{-d}' + H\text{-e} + H\text{-e}'$), 7.76 (dd, 2H, $H\text{-3}'' + H\text{-5}''$, $J_{3''/5''-2''/6''} = 4.5$ Hz, $J_{5''/3''-2''/6''} = 1.7$ Hz), 7.75 (dd, 1H, $H\text{-5}'$, $J_{5\text{-}6'} = 5.8$ Hz, $J_{5\text{-}3'} = 1.6$ Hz), 7.55 (m, 2H, $H\text{-a/b} + H\text{-a'/b'}$), 7.50 (ddd, 1H, $H\text{-5}$, $J_{5\text{-}4} = 7.8$ Hz, $J_{5\text{-}6} = 5.6$ Hz, $J_{5\text{-}3} = 0.5$ Hz), 7.44 (m, 2H, $H\text{-b/a} + H\text{-b'/a'}$), 7.15 (m, 2H, $H\text{-h} + H\text{-h}'$), 6.90 (m, 2H, $H\text{-i} + H\text{-i}'$), 6.32 (m, 2H, $H\text{-j} + H\text{-j}'$).

Irpiq-2254tpy. $[\text{Ir}(\text{piq})_2\text{Cl}]_2$ (39.1 mg, 0.0307 mmol) and 2,2';5',4''-terpyridine (17.0 mg, 0.0729 mmol) were suspended in ethyleneglycol (4.0 mL). The mixture was refluxed overnight under Argon. The solution was cooled to room temperature and a saturated aqueous solution of NH_4PF_6 (5.0 mL) was added for precipitation. The solid was centrifuged, washed with water (3X), dried under reduced pressure and washed again with diethylether (3X). HRMS (ESI): m/z calculated for $[\text{C}_{45}\text{H}_{31}^{193}\text{IrN}_5 - \text{PF}_6]^+$, 832.21799 ; found: 834.21985, m/z calculated for $[\text{C}_{30}\text{H}_{20}^{193}\text{IrN}_2 - \text{PF}_6 - 2254\text{tpy}]^+$, 601.12502 ; found: 601.12291. ^1H NMR (CD_3CN), δ/ppm : 9.02 (m, 2H, $H\text{-}f + H\text{-}f'$), 8.65 (d, 1H, $H\text{-}3'$, $J_{3'\text{-}4'} = 8.5$ Hz), 8.59 (m, 3H, $H\text{-}3 + H\text{-}2'' + H\text{-}6''$), 8.41 (dd, 1H, $H\text{-}4'$, $J_{4'\text{-}3'} = 8.5$ Hz, $J_{4'\text{-}6'} = 2.2$ Hz), 8.40 (m, 2H, $H\text{-}g + H\text{-}g'$), 8.14 (ddd, 1H, $H\text{-}4$, $J_{4\text{-}3} = 8.0$ Hz, $J_{4\text{-}5} = 7.8$ Hz, $J_{4\text{-}6} = 1.2$ Hz), 7.99 (m, 2H, $H\text{-}c + H\text{-}c'$), 7.96 (d, 1H, $H\text{-}6'$, $J_{6'\text{-}4'} = 2.2$ Hz), 7.93 (dd, 1H, $H\text{-}6$, $J_{6\text{-}5} = 5.4$ Hz, $J_{6\text{-}4} = 1.2$ Hz), 7.83 (m, 4H, $H\text{-}d + H\text{-}d' + H\text{-}e + H\text{-}e'$), 7.57 (m, 2H, $H\text{-}a/b + H\text{-}a'/b'$), 7.50 (ddd, 1H, $H\text{-}5$, $J_{5\text{-}4} = 7.8$ Hz, $J_{5\text{-}6} = 5.4$ Hz, $J_{5\text{-}3} = 0.6$ Hz), 7.43 (m, 2H, $H\text{-}b/a + H\text{-}b'/a'$), 7.24 (dd, 2H, $H\text{-}3'' + H\text{-}5''$, $J_{3''/5''\text{-}2''/6''} = 4.5$ Hz, $J_{5''/3''\text{-}2''/6''} = 1.7$ Hz), 7.16 (m, 2H, $H\text{-}h + H\text{-}h'$), 6.91 (m, 2H, $H\text{-}i + H\text{-}i'$), 6.34 (m, 2H, $H\text{-}j + H\text{-}j'$).



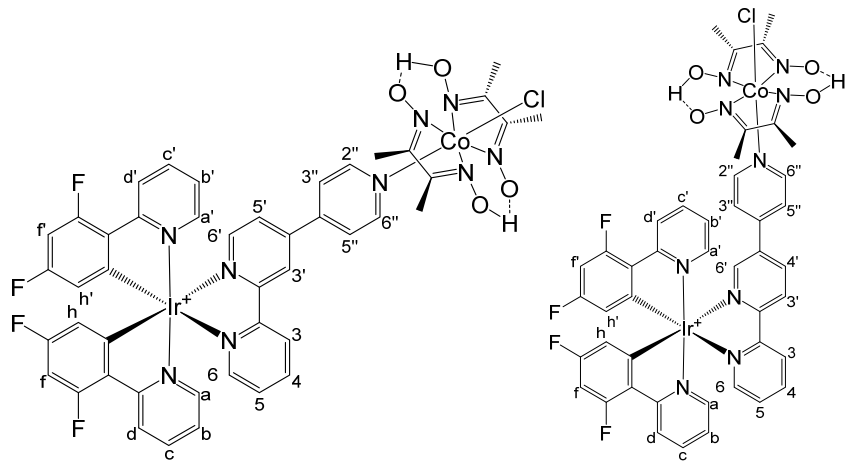
3) Ir(III)-Co(III) dyads

Irppy-2244tpy-Co. To a suspension of Co(dmgH)(dmgH₂)Cl₂ (10.0 mg, 0.0277 mmol) in methanol (3.5 mL) was added Et₃N (3.7 μL, 0.0265 mmol). The mixture was stirred at room temperature for 15 min. until a brown solution was obtained. A solution of Irppy-2244tpy (22.7 mg, 0.0258 mmol) in dichloromethane (3.5 mL) was slowly added to this solution and the mixture was stirred at room temperature for 1h30. A stream of air was passed through the solution for 15 min. and diethylether was added for precipitation. The yellow-orange precipitate was centrifuged and washed with diethylether. The product was dissolved in acetone to remove impurities. The crude product was purified by column chromatography on SiO₂ (CH₂Cl₂/MeOH : 95/5). HRMS (ESI): m/z calculated for [C₄₅H₄₁Cl⁵⁹Co¹⁹³IrN₉O₄ – PF₆]⁺, 1058.19258 ; found: 1058.19288, m/z calculated for [C₃₇H₂₇¹⁹³IrN₅ – PF₆ – Co(dmgH)₂Cl]⁺, 734.18902 ; found: 734.18881. ¹H NMR (acetone-d₆), δ/ppm: 9.26 (s, 1H, H-3'), 9.15 (dd, 1H, H-3, J₃₋₄ = 8.0 Hz, J₃₋₅ = 0.7 Hz), 8.36 (d, 2H, H-2'' + H-6'', J_{2''/6''-3''/5''} = 6.2 Hz), 8.32 (ddd, 1H, H-4, J₄₋₃ = 8.0 Hz, J₄₋₅ = 7.9 Hz, J₄₋₆ = 1.3 Hz), 8.25 (m, 2H, H-d + H-d'), 8.21 (d, 1H, H-6', J_{6'-5'} = 5.8 Hz), 8.13 (dd, 1H, H-6, J₆₋₅ = 5.3 Hz, J₆₋₄ = 1.3 Hz), 8.04 (m, 3H, H-5' + H-3'' + H-5''), 7.95 (m, 2H, H-c + H-c'), 7.90 (m, 2H, H-e + H-e'), 7.83 (m, 2H, H-a + H-a'), 7.75 (ddd, 1H, H-5, J₅₋₄ = 7.9 Hz, J₅₋₆ = 5.3 Hz, J₅₋₃ = 0.7 Hz), 7.13 (m, 2H, H-b + H-b'), 7.04 (m, 2H, H-f + H-f'), 6.92 (m, 2H, H-g + H-g'), 6.34 (m, 2H, H-h + H-h'), 2.33 (s, 12H, -CH₃ dmgh).



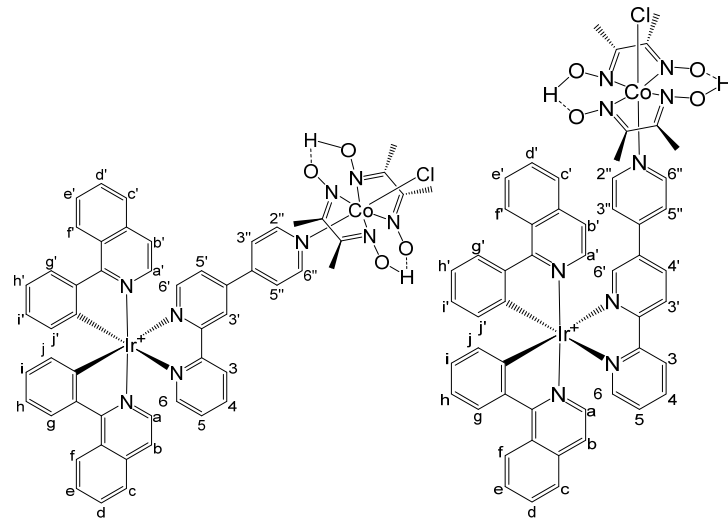
Irppy-2254tpy-Co. To a suspension of Co(dmgH)(dmgH₂)Cl₂ (11.6 mg, 0.0321 mmol) in methanol (4.0 mL) was added Et₃N (4.3 μL, 0.0309 mmol). The mixture was stirred at room temperature for 15 min. until a brown solution was obtained. A solution of Irppy-2254tpy (26.2 mg, 0.0298 mmol) in dichloromethane (4.0 mL) was slowly added to this solution and the mixture was stirred at room temperature for 1h30. A stream of air was passed through the solution for 15 min. and diethylether was added for precipitation. The yellow-orange precipitate was centrifuged and washed with diethylether. The product was dissolved in acetone to remove impurities. The crude product was purified by column chromatography on SiO₂ (CH₂Cl₂/MeOH : 95/5). HRMS (ESI): m/z calculated for [C₄₅H₄₁Cl⁵⁹Co¹⁹³IrN₉O₄ – PF₆]⁺, 1058.19258 ; found: 1058.19244, m/z calculated for [C₃₇H₂₇¹⁹³IrN₅ – PF₆ – Co(dmgH)₂Cl]⁺, 734.18902 ; found: 734.18871. ¹H NMR (acetone-d₆), δ/ppm: 8.99 (d, 1H, H-3', J_{3-4'} = 8.6 Hz), 8.92 (dd, 1H, H-3, J₃₋₄ = 8.1 Hz, J₃₋₅ = 0.5 Hz), 8.65 (dd, 1H, H-4', J_{4'-3'} = 8.6 Hz, J_{4'-6'} = 2.1 Hz), 8.36 (d, 1H, H-6', J_{6'-4'} = 2.1 Hz), 8.32 (ddd, 1H, H-4, J₄₋₃ = 8.1 Hz, J₄₋₅ = 7.8 Hz, J₄₋₆ = 1.3 Hz), 8.23 (m, 2H, H-d + H-d'), 8.19 (dd, 2H, H-2'' + H-6'', J_{2''/6''-3''/5''} = 5.6 Hz, J_{2''/6''-5''/3''} = 1.4 Hz), 8.13 (dd, 1H, H-6, J₆₋₅ = 5.4 Hz, J₆₋₄ = 1.3 Hz), 7.91 (m, 6H, H-a + H-a' + H-c + H-c' + H-e + H-e'), 7.75 (ddd, 1H, H-5, J₅₋₄ = 7.8 Hz, J₅₋₆ = 5.4 Hz, J₅₋₃ = 0.5 Hz), 7.47 (dd, 2H, H-3'' + H-5'', J_{3''/5''-2''/6''} = 5.6 Hz, J_{5''/3''-2''/6''} = 1.4 Hz), 7.09 (m, 4H, H-f + H-f' + H-b + H-b'), 6.93 (m, 2H, H-g + H-g'), 6.36 (m, 2H, H-h + H-h'), 2.32 (s, 12H, -CH₃ dmgh).

IrppyF₂-2244tpy-Co. To a suspension of Co(dmgH)(dmgH₂)Cl₂ (8.4 mg, 0.0277 mmol) in methanol (3.0 mL) was added Et₃N (3.1 μL, 0.0222 mmol). The mixture was stirred at room temperature for 15 min. until a brown solution was obtained. A solution of IrppyF₂-2244tpy (20.6 mg, 0.0217 mmol) in dichloromethane (3.0 mL) was slowly added to this solution and the mixture was stirred at room temperature for 1h30. A stream of air was passed through the solution for 15 min. and diethylether was added for precipitation. The yellow-orange precipitate was centrifuged and washed with diethylether. The product was dissolved in acetone to remove impurities. The crude product was purified by column chromatography on SiO₂ (CH₂Cl₂/MeOH : 95/5). HRMS (ESI): m/z calculated for [C₄₅H₃₇Cl⁵⁹CoF₄¹⁹³IrN₉O₄ – PF₆]⁺, 1130.15489 ; found: 1130.15521, m/z calculated for [C₃₇H₂₃F₄¹⁹³IrN₅ – PF₆ – Co(dmgH)₂Cl]⁺, 806.15133 ; found: 806.15109. ¹H NMR (acetone-d₆), δ/ppm: 9.21 (d, 1H, H-3', J_{3'-5'} = 1.2 Hz), 9.08 (dd, 1H, H-3, J₃₋₄ = 8.1 Hz, J₃₋₅ = 0.7 Hz), 8.37 (m, 6H, H-2'' + H-6'' + H-4 + H-d + H-d' + H-6'), 8.24 (dd, 1H, H-6, J₆₋₅ = 5.4 Hz, J₆₋₄ = 1.2 Hz), 8.06 (m, 3H, H-c + H-c' + H-5'), 8.00 (dd, 3H, H-3'' + H-5'', J_{3''/5''-2''/6''} = 5.4 Hz, J_{3''/5''-6''/2''} = 1.5 Hz), 7.92 (m, 2H, H-a + H-a'), 7.79 (ddd, 1H, H-5, J₅₋₄ = 7.7 Hz, J₅₋₆ = 5.4 Hz, J₅₋₃ = 0.7 Hz), 7.22 (m, 2H, H-b + H-b'), 6.78 (m, 2H, H-f + H-f'), 5.79 (m, 2H, H-h + H-h'), 2.34 (s, 12H, -CH₃ dmgh).



IrppyF₂-2254tpy-Co. To a suspension of Co(dmgH)(dmgH₂)Cl₂ (7.9 mg, 0.0219 mmol) in methanol (3.0 mL) was added Et₃N (2.9 μL, 0.0208 mmol). The mixture was stirred at room temperature for 15 min. until a brown solution was obtained. A solution of IrppyF₂-2254tpy (19.4 mg, 0.0204 mmol) in dichloromethane (3.0 mL) was slowly added to this solution and the mixture was stirred at room temperature for 1h30. A stream of air was passed through the solution for 15 min. and diethylether was added for precipitation. The yellow-orange precipitate was centrifuged and washed with diethylether. The product was dissolved in acetone to remove impurities. The crude product was purified by column chromatography on SiO₂ (CH₂Cl₂/MeOH : 95/5). HRMS (ESI): m/z calculated for [C₄₅H₃₇Cl⁵⁹CoF₄¹⁹³IrN₉O₄ – PF₆]⁺, 1130.15489 ; found: 1130.15505, m/z calculated for [C₃₇H₂₃F₄¹⁹³IrN₅ – PF₆ – Co(dmgH)₂Cl]⁺, 806.15133 ; found: 806.15089. ¹H NMR (acetone-d₆), δ/ppm: 9.04 (d, 1H, H-3', J_{3'-4'} = 8.6 Hz), 8.97 (dd, 1H, H-3, J₃₋₄ = 8.1 Hz, J₃₋₅ = 0.6 Hz), 8.72 (dd, 1H, H-4', J_{4'-3'} = 8.6 Hz, J_{4'-6'} = 2.0 Hz), 8.52 (d, 1H, H-6', J_{6'-4'} = 2.0 Hz), 8.38 (m, 3H, H-4 + H-d + H-d'), 8.24 (dd, 1H, H-6, J₆₋₅ = 5.5 Hz, J₆₋₄ = 0.9 Hz), 8.21 (dd, 2H, H-2'' + H-6'', J_{2''/6''-3''/5''} = 5.6 Hz, J_{2''/6''-5''/3''} = 1.4 Hz), 7.97 (m, 4H, H-a + H-a' + H-c + H-c'), 7.80 (ddd, 1H, H-5, J₅₋₄ = 7.6 Hz, J₅₋₆ = 5.5 Hz, J₅₋₃ = 0.6 Hz), 7.62 (dd, 2H, H-3'' + H-5'', J_{3''/5''-2''/6''} = 5.6 Hz, J_{3''/5''-2''/6''} = 1.4 Hz), 7.20 (m, 2H, H-b + H-b'), 6.77 (m, 2H, H-f + H-f'), 5.78 (m, 2H, H-h + H-h'), 2.32 (s, 12H, -CH₃ dmgh).

Irpiq-2244tpy-Co. To a suspension of Co(dmgH)(dmgH₂)Cl₂ (8.5 mg, 0.0235 mmol) in methanol (3.0 mL) was added Et₃N (3.1 μL, 0.0222 mmol). The mixture was stirred at room temperature for 15 min. until a brown solution was obtained. A solution of Irpiq-2244tpy (21.6 mg, 0.0221 mmol) in dichloromethane (3.0 mL) was slowly added to this solution and the mixture was stirred at room temperature for 1h30. A stream of air was passed through the solution for 15 min. and diethylether was added for precipitation. The orange precipitate was centrifuged and washed with diethylether. The product was dissolved in acetone to remove impurities. The crude product was purified by column chromatography on SiO₂ (CH₂Cl₂/MeOH : 95/5). HRMS (ESI): m/z calculated for [C₅₃H₄₅³⁷Cl⁵⁹Co¹⁹³IrN₉O₄ – PF₆]⁺, 1158.22388 ; found: 1158.22434, m/z calculated for [C₄₅H₃₁¹⁹³IrN₅ – PF₆ – Co(dmgH)₂Cl]⁺, 834.22032 ; found: 834.22027. ¹H NMR (acetone-d₆), δ/ppm: 9.24 (d, 1H, H-3', J_{3'-5'} = 1.6 Hz), 9.10 (m, 3H, H-3 + H-f + H-f'), 8.43 (m, 2H, H-g + H-g'), 8.36 (d, 2H, H-2'' + H-6'', J_{2''/6''-3''/5''} = 6.4 Hz), 8.32 (ddd, 1H, H-4, J₄₋₃ = J₄₋₅ = 8.0 Hz, J₄₋₆ = 1.5 Hz), 8.07 (m, 3H, H-6' + H-c + H-c'), 7.99 (m, 4H, H-5' + H-6 + H-3'' + H-5''), 7.91 (m, 4H, H-d + H-d' + H-e + H-e'), 7.70 (m, 3H, H-5 + H-a/b + H-a'/b'), 7.55 (m, 2H, H-b/a + H-b'/a'), 7.15 (m, 2H, H-h + H-h'), 6.91 (m, 2H, H-i + H-i'), 6.37 (m, 2H, H-j + H-j'), 2.33 (s, 12H, -CH₃ dmgh).



Irpiq-2254tpy-Co. To a suspension of Co(dmgH)(dmgH₂)Cl₂ (6.6 mg, 0.0183 mmol) in methanol (2.5 mL) was added Et₃N (2.4 μL, 0.0172 mmol). The mixture was stirred at room temperature for 15 min. until a brown solution was obtained. A solution of Irpiq-2254tpy (16.8 mg, 0.0172 mmol) in dichloromethane (2.5 mL) was slowly added to this solution and the mixture was stirred at room temperature for 1h30. A stream of air was passed through the solution for 15 min. and diethylether was added for precipitation. The orange precipitate was centrifuged and washed with diethylether. The product was dissolved in acetone to remove impurities. The crude product was purified by column chromatography on SiO₂ (CH₂Cl₂/MeOH : 95/5). HRMS (ESI): m/z calculated for [C₅₃H₄₅³⁷Cl⁵⁹Co¹⁹³IrN₉O₄ – PF₆]⁺, 1158.22388 ; found: 1158.22415, m/z calculated for [C₄₅H₃₁¹⁹³IrN₅ – PF₆ – Co(dmgH)₂Cl]⁺, 834.22032 ; found: 834.22024. ¹H NMR (acetone-d₆), δ/ppm: 9.10 (m, 2H, H-f + H-f'), 9.03 (d, 1H, H-3', J_{3'-4'} = 8.6 Hz), 8.96 (d, 1H, H-3, J₃₋₄ = 8.1 Hz), 8.66 (dd, 1H, H-4', J_{4'-3'} = 8.6 Hz, J_{4'-6'} = 2.0 Hz), 8.45 (m, 2H, H-g + H-g'), 8.32 (ddd, 1H, H-4, J₄₋₃ = 8.1 Hz, J₄₋₅ = 8.0 Hz, J₄₋₆ = 1.5 Hz), 8.17 (dd, 2H, H-2'' + H-6'', J_{2''/6''-3''/5''} = 5.6 Hz, J_{2''/6''-5''/3''} = 1.4 Hz), 8.13 (d, 1H, H-6', J_{6'-4'} = 2.0 Hz), 8.05 (m, 3H, H-6 + H-c + H-c'), 7.92 (m, 4H, H-d + H-d' + H-e + H-e'), 7.75 (m, 3H, H-5 + H-a/b + H-a'/b'), 7.54 (m, 2H, H-b/a + H-b'/a'), 7.42 (dd, 2H, H-3'' + H-5'', J_{5''/3''-2''/6''} = 5.6 Hz, J_{5''/3''-2''/6''} = 1.4 Hz), 7.18 (m, 2H, H-h + H-h'), 6.94 (m, 2H, H-i + H-i'), 6.39 (m, 2H, H-j + H-j'), 2.30 (s, 12H, -CH₃ dmgh).

¹H NMR Spectra

Irppy-2244tpy

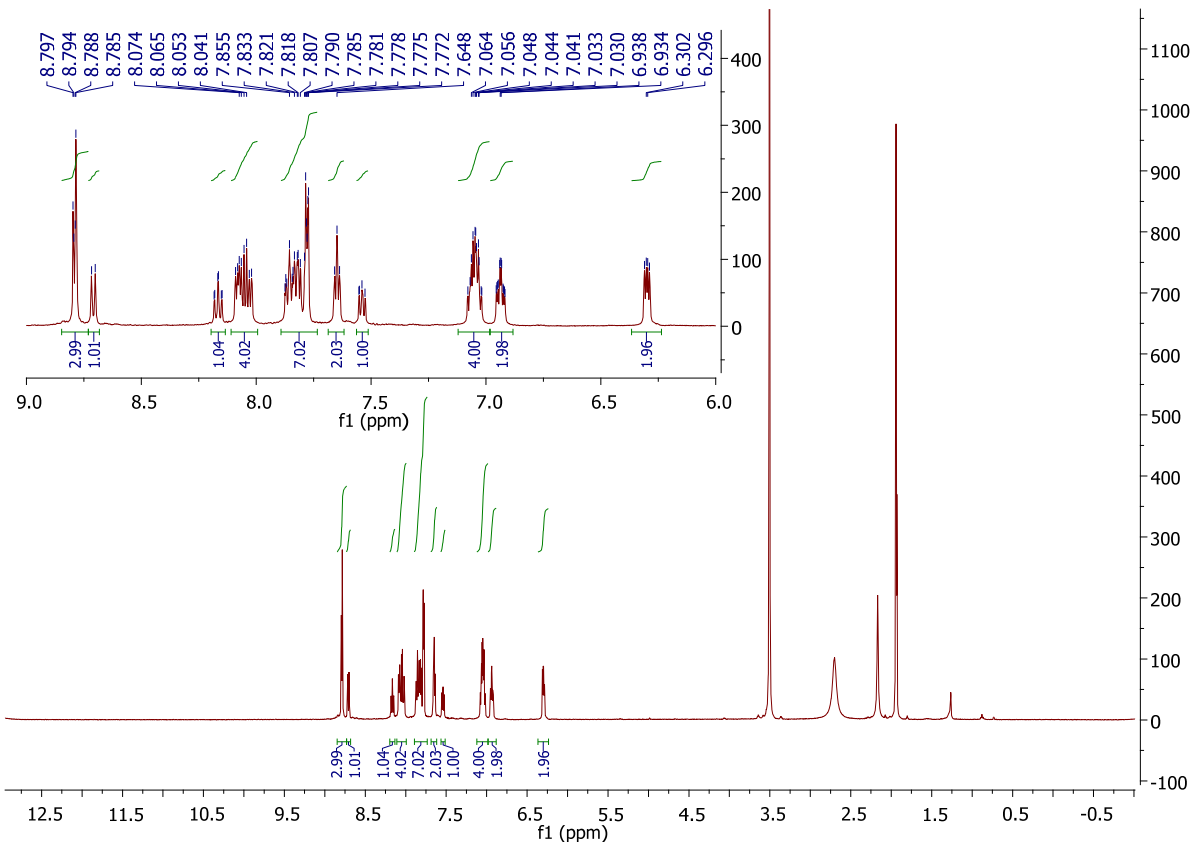


Figure S1 ¹H NMR spectra of Irppy-2244tpy

lrppy-2254tpy

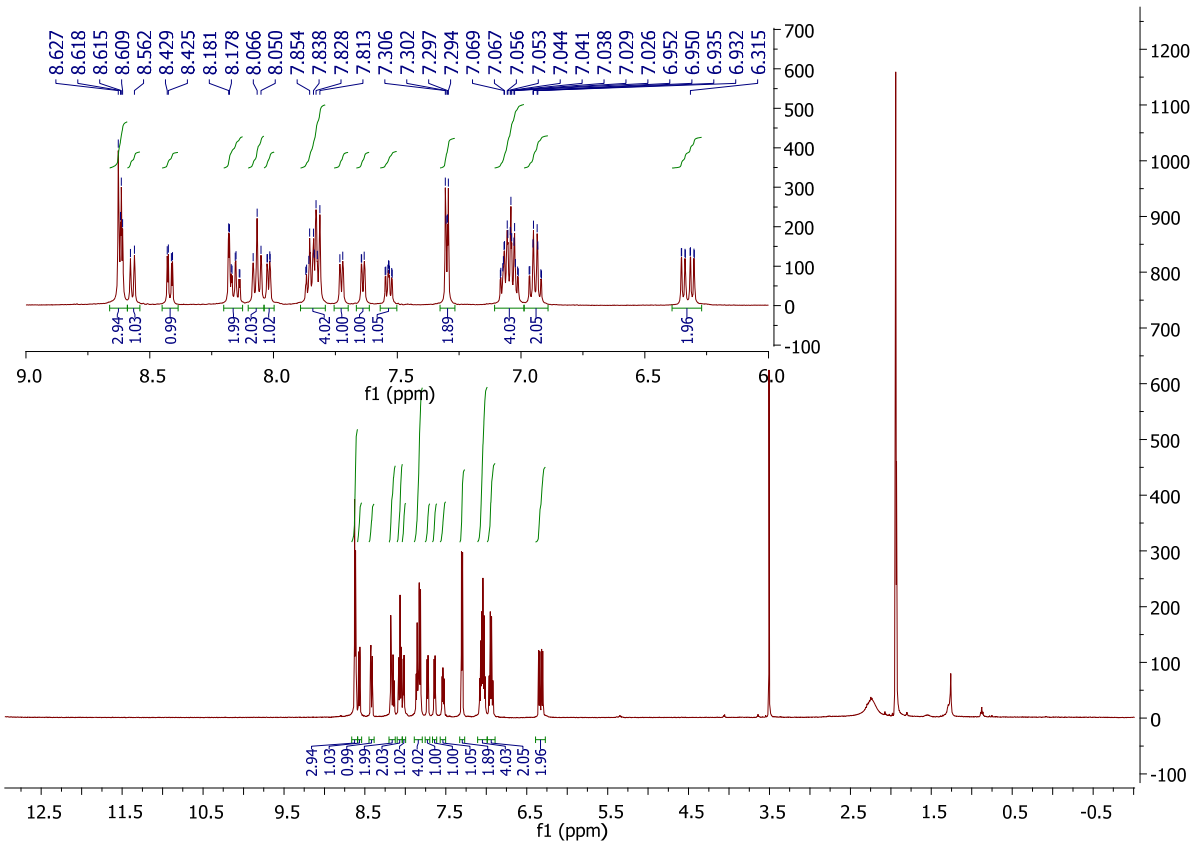


Figure S2 ^1H NMR spectra of Irppy-2254tpy

Irppy-bpy

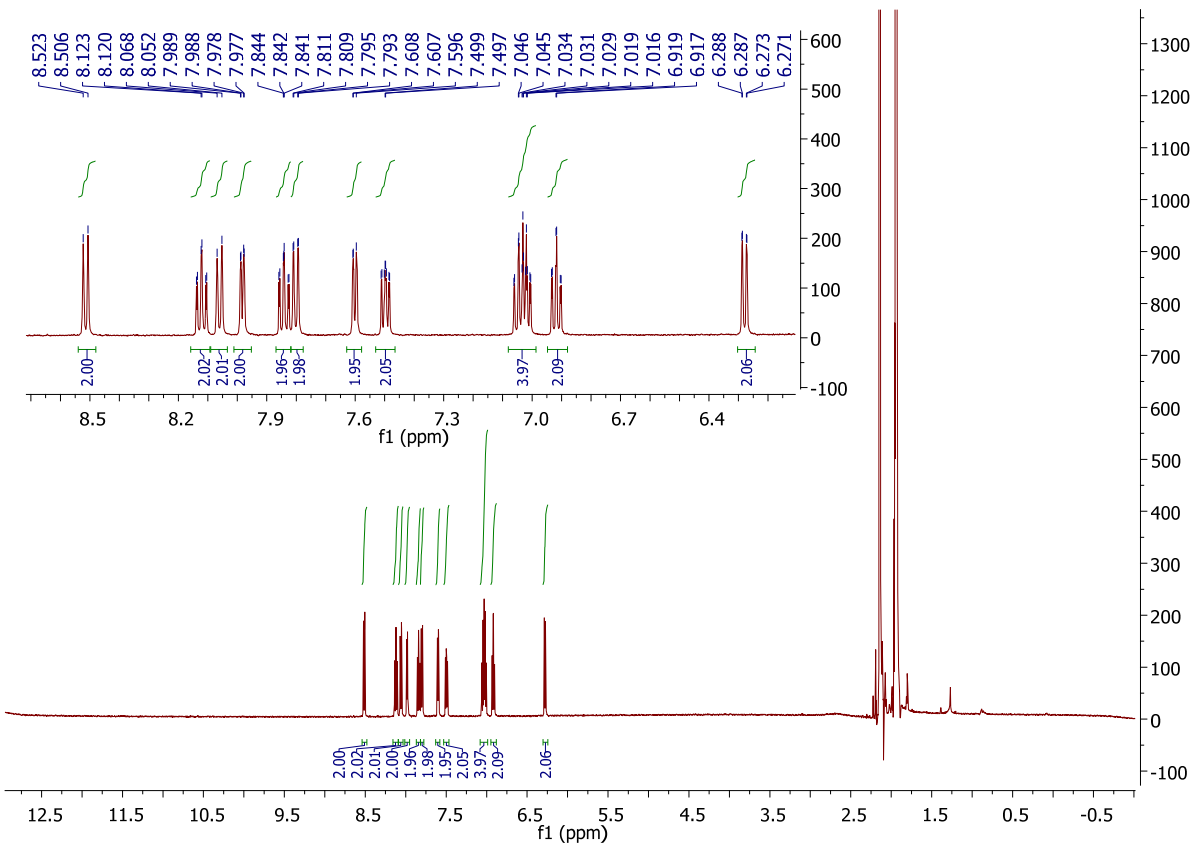


Figure S3 ¹H NMR spectra of Irppy-bpy

IrppyF₂-2244tpy

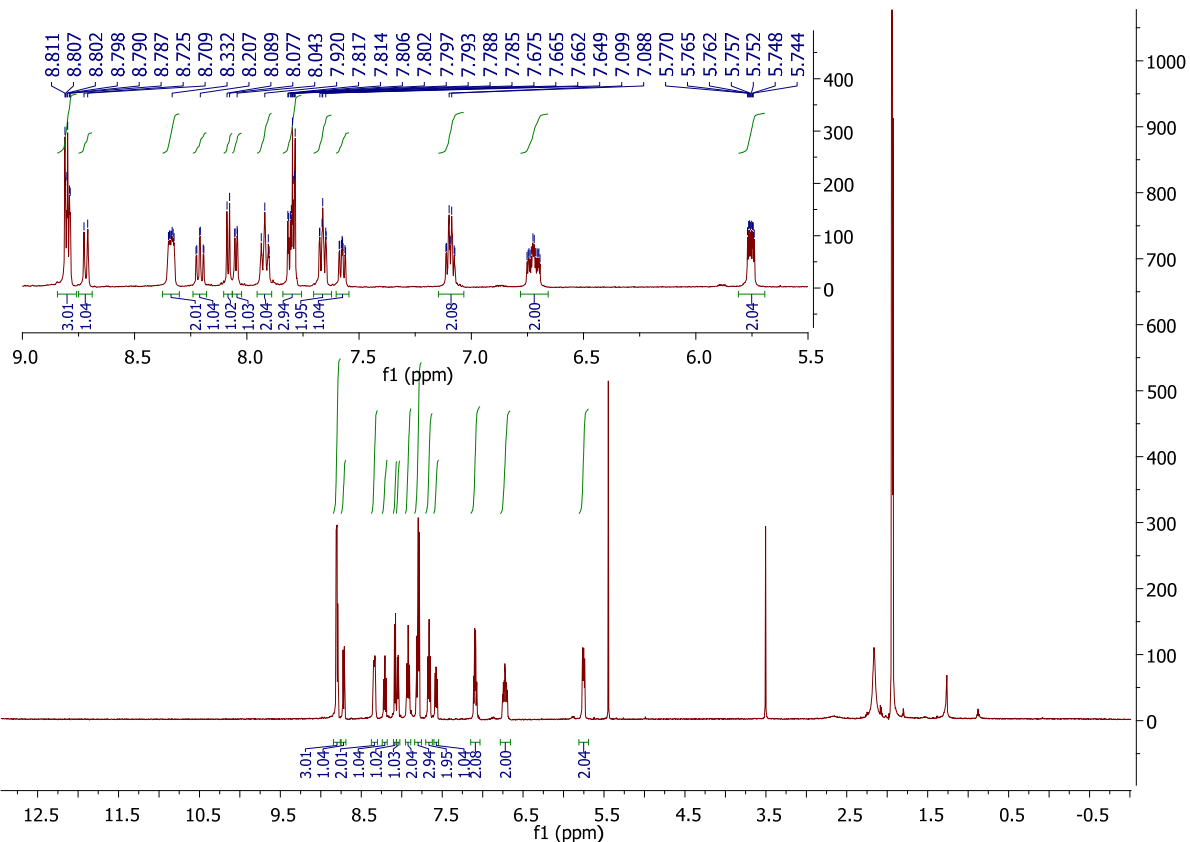


Figure S4 ¹H NMR spectra of IrppyF₂-2244tpy

IrppyF₂-2254tpy

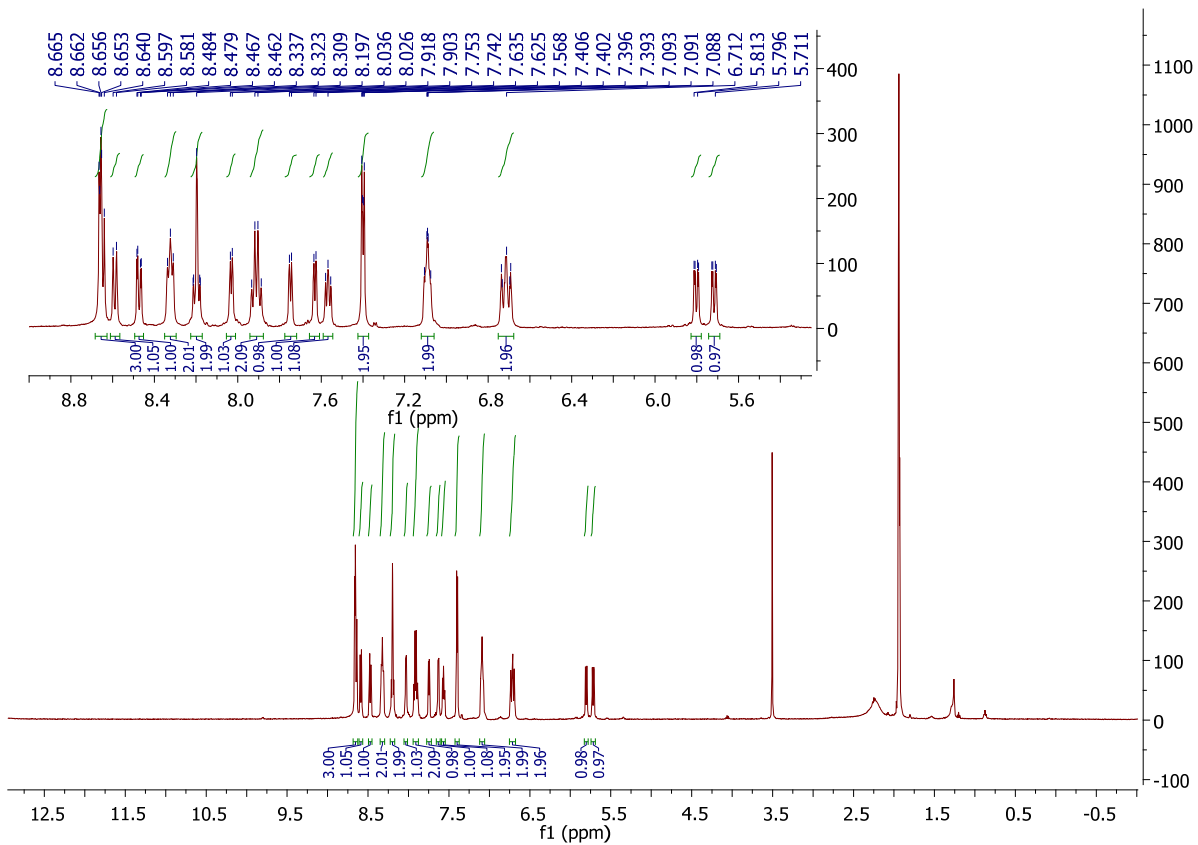


Figure S5 ¹H NMR spectra of IrppyF₂-2254tpy

IrppyF₂-bpy

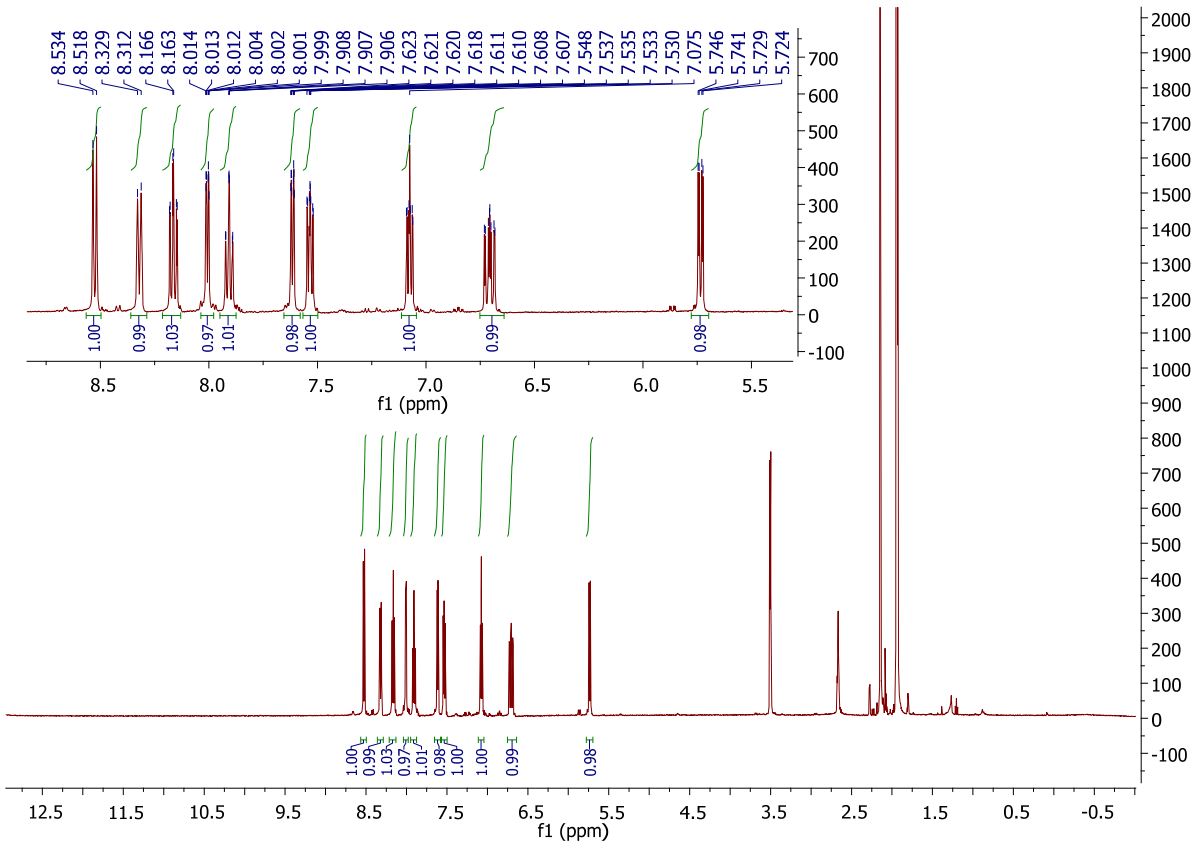


Figure S6 ^1H NMR spectra of IrppyF₂-bpy

Irpiq-2244tpy

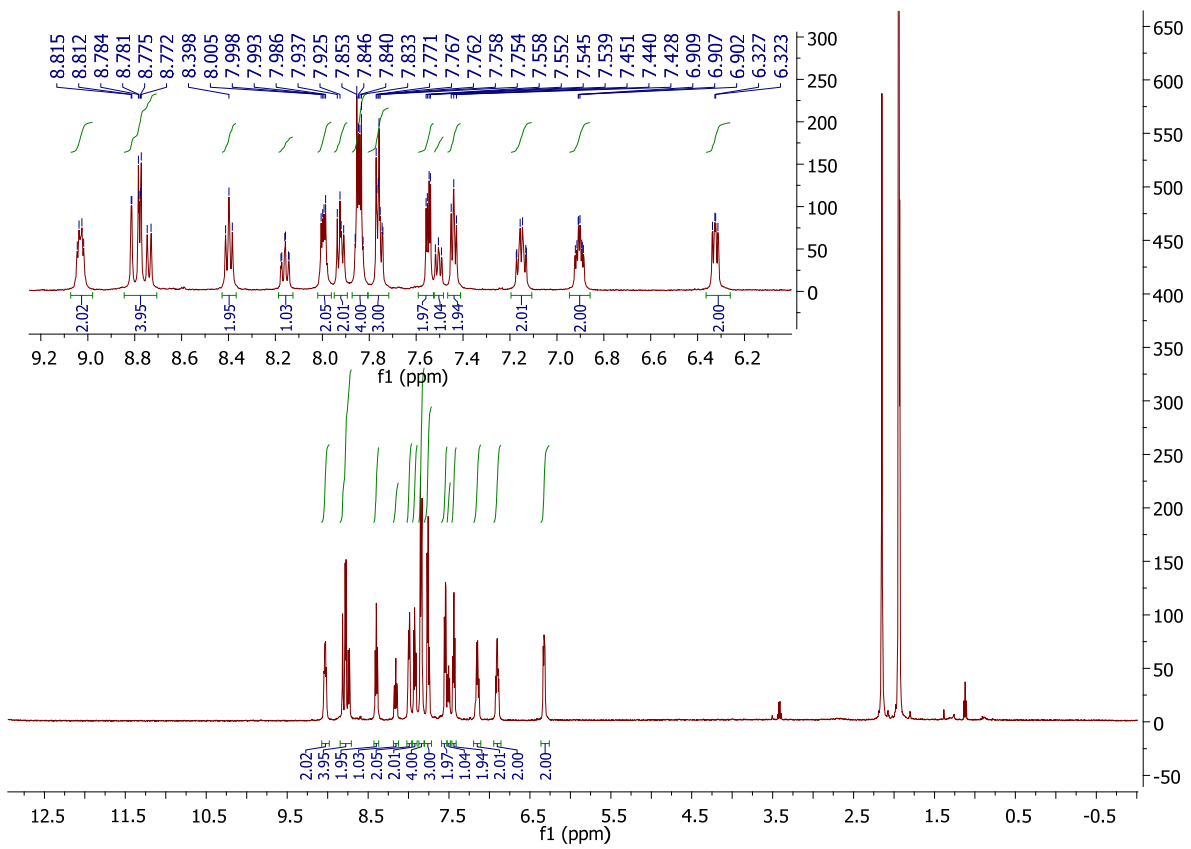


Figure S7 ^1H NMR spectra of Irpiq-2244tpy

Irpiq-2254tpy

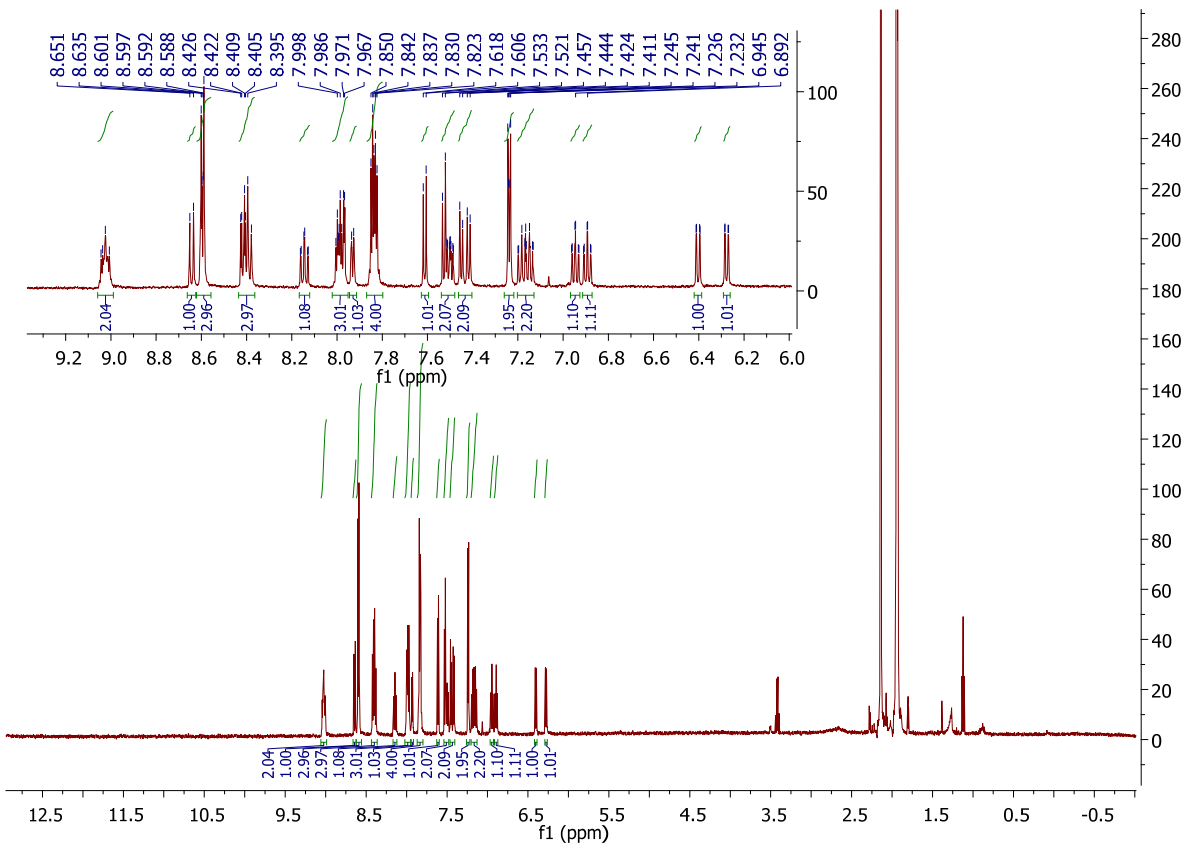


Figure S8 ¹H NMR spectra of Irpiq-2254tpy

Irpiq-bpy

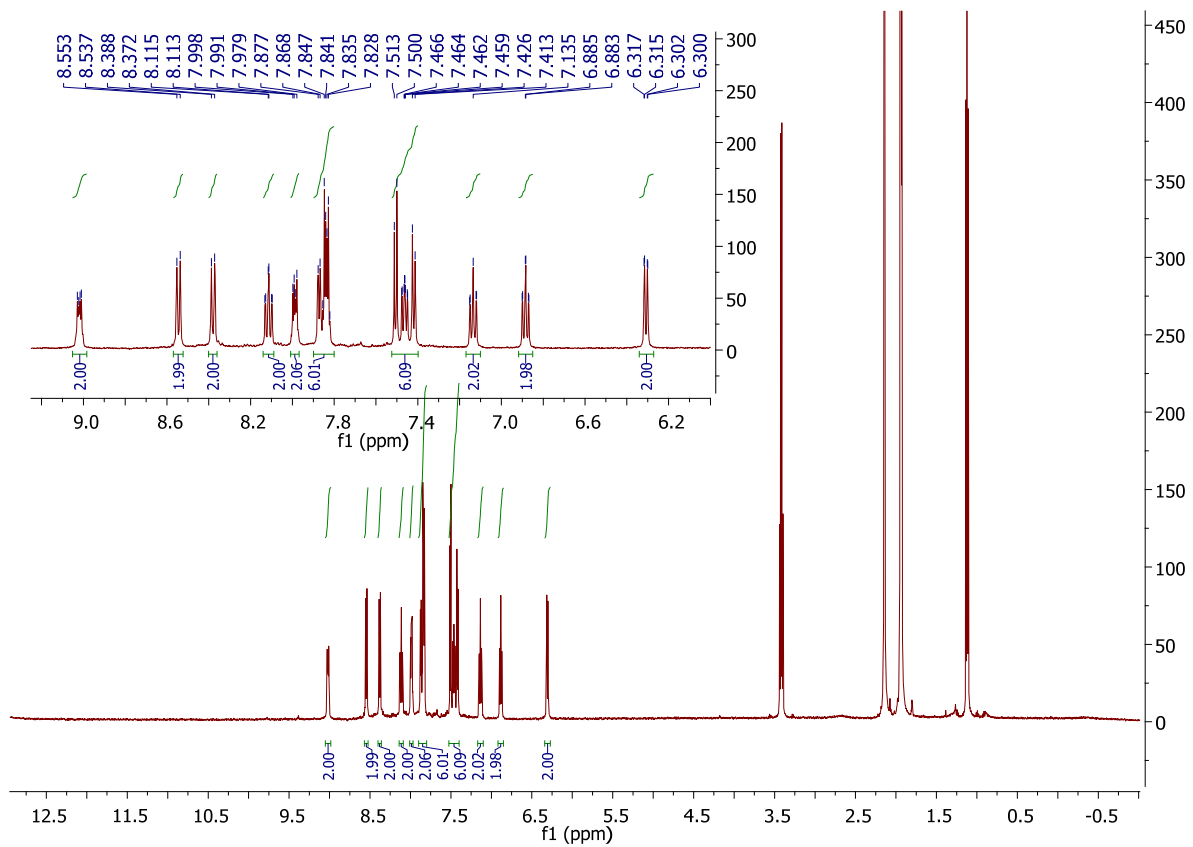


Figure S9 ¹H NMR spectra of Irpiq-bpy

Irppy-2244tpy-Co

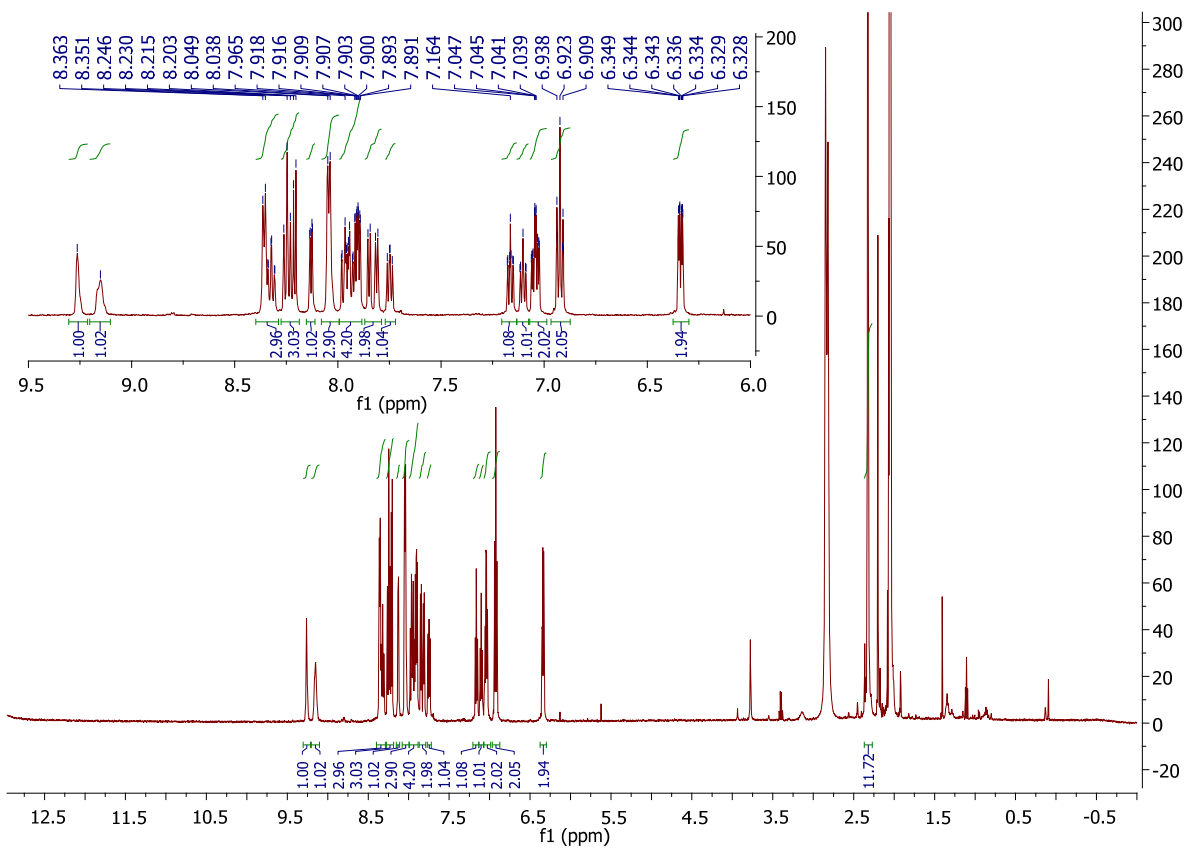


Figure S10 ¹H NMR spectra of Irppy-2244tpy-Co

Irppy-2254tpy-Co

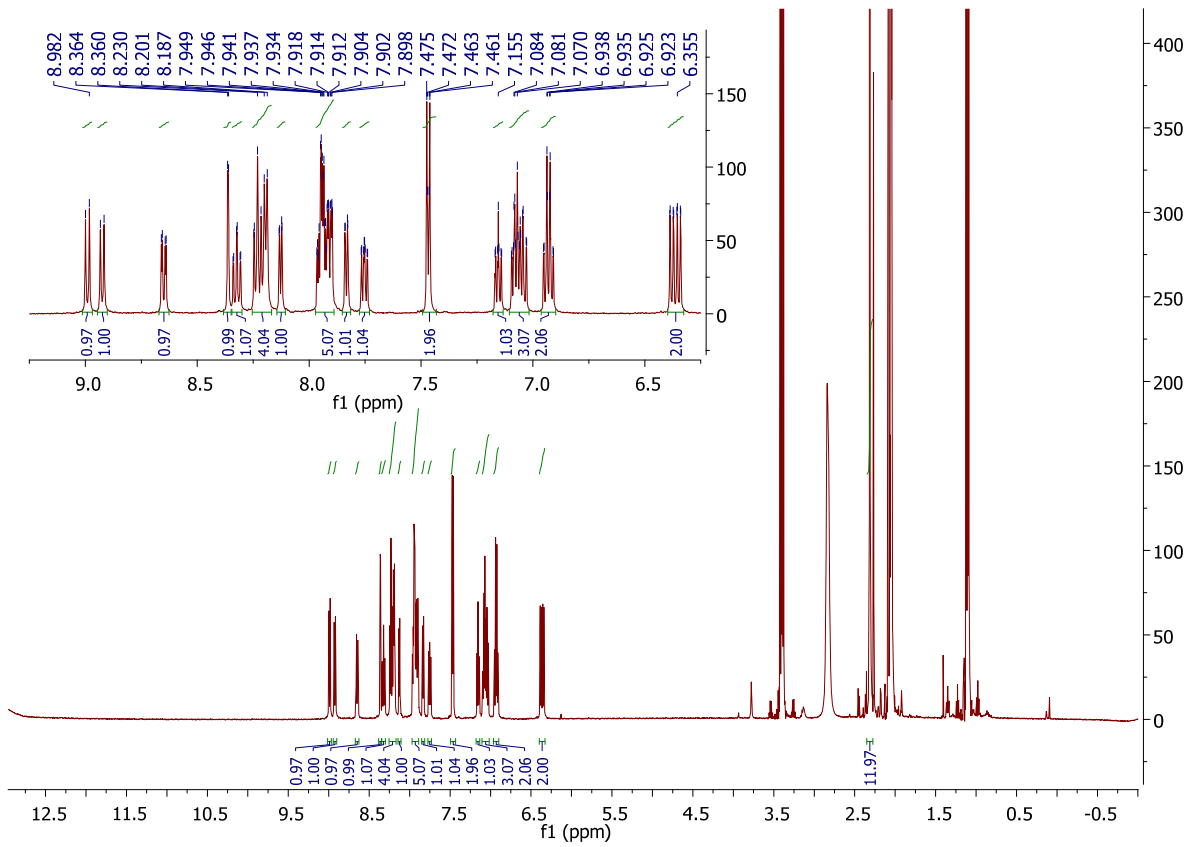


Figure S11 ¹H NMR spectra of Irppy-2254tpy-Co

IrppyF₂-2244tpy-Co

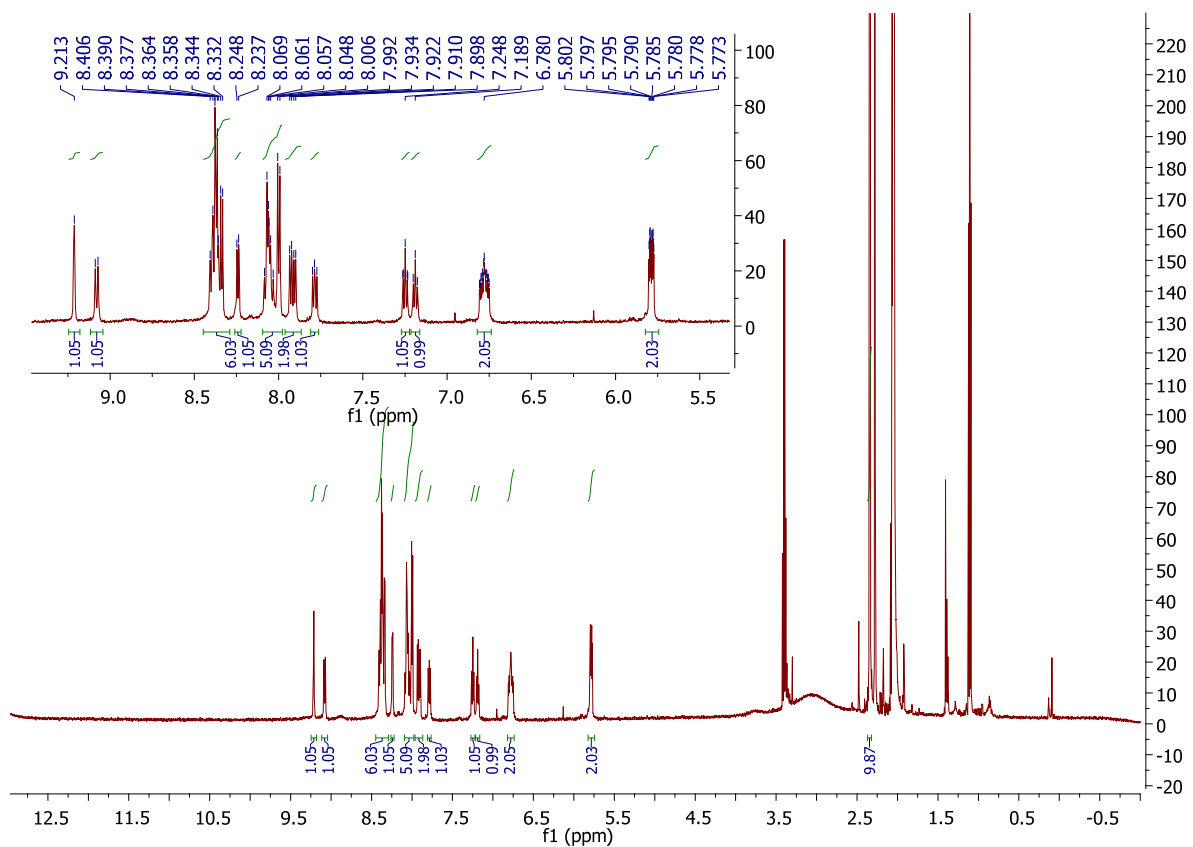


Figure S12 ¹H NMR spectra of IrppyF₂-2244tpy-Co

IrppyF₂-2254tpy-Co

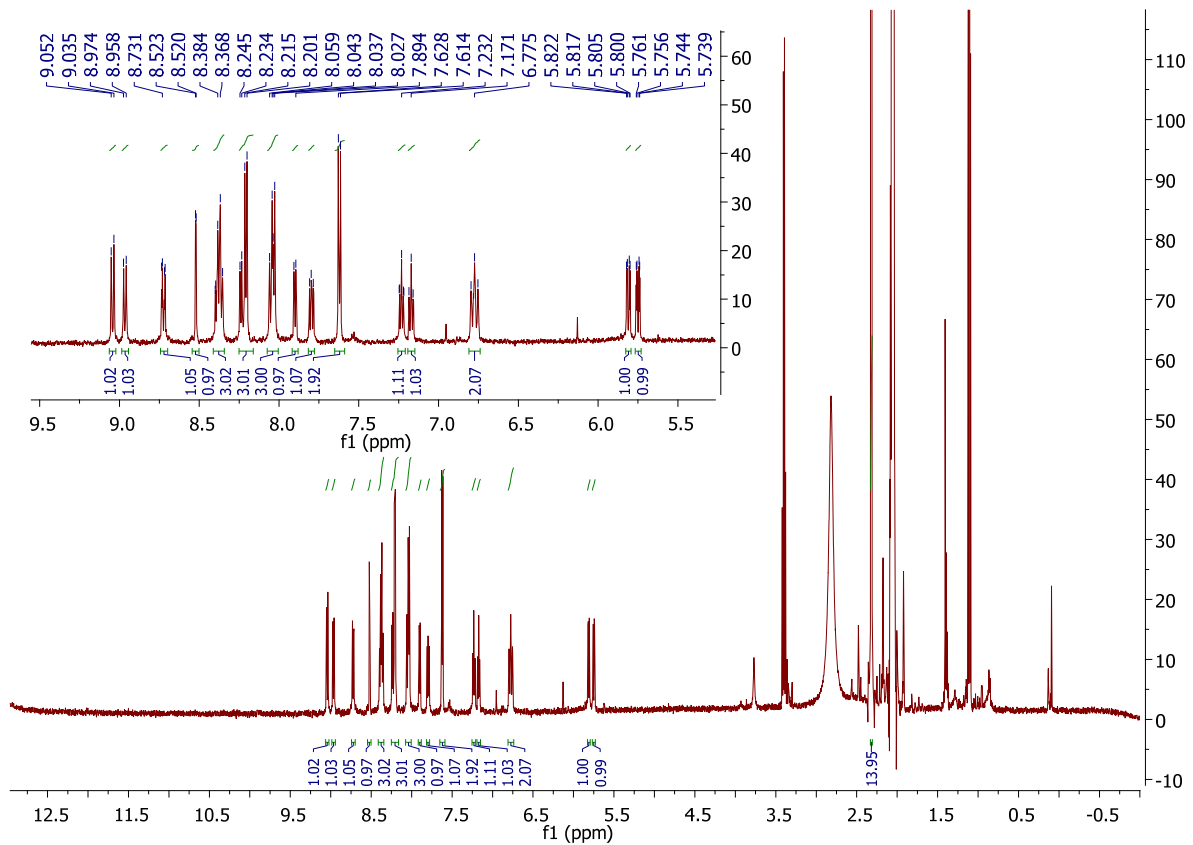


Figure S13 ¹H NMR spectra of IrppyF₂-2254tpy-Co

Irpiq-2244tpy-Co

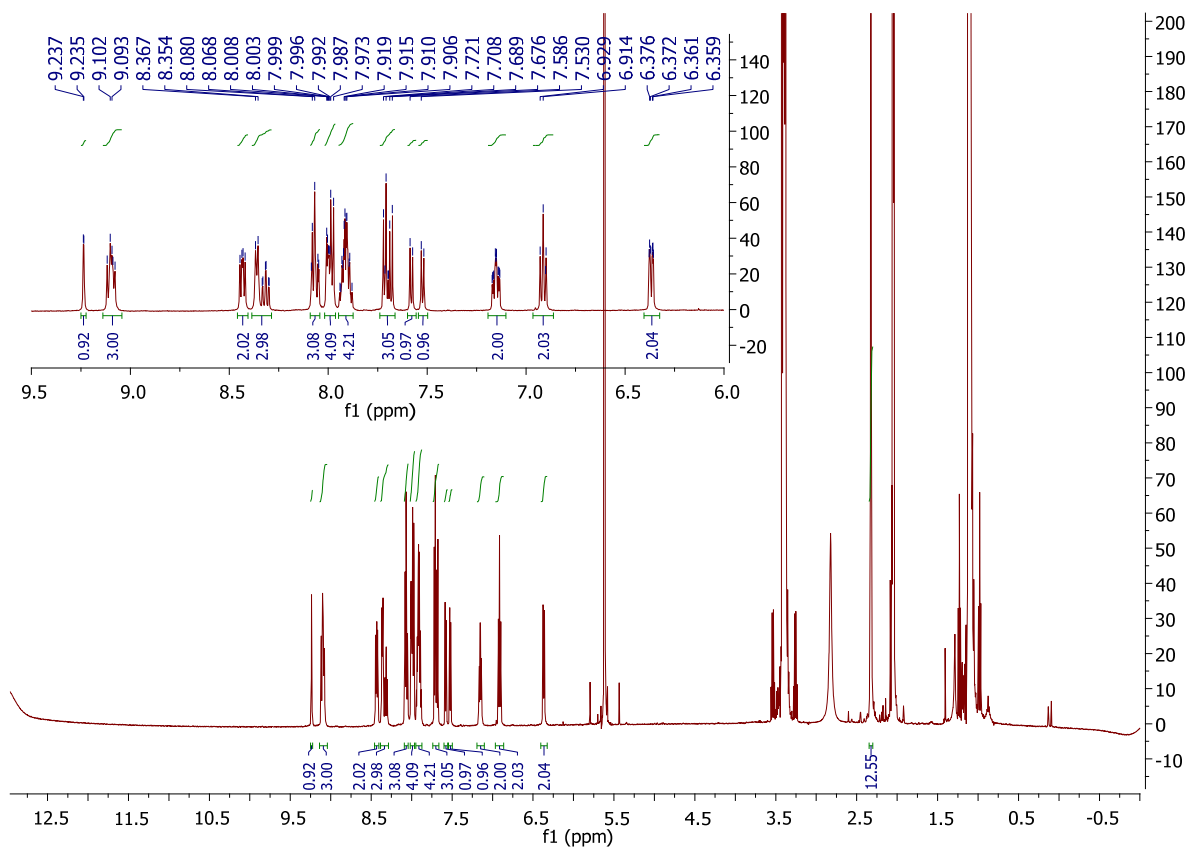


Figure S14 ¹H NMR spectra of Irpiq-2244tpy-Co

Irpiq-2254tpy-Co

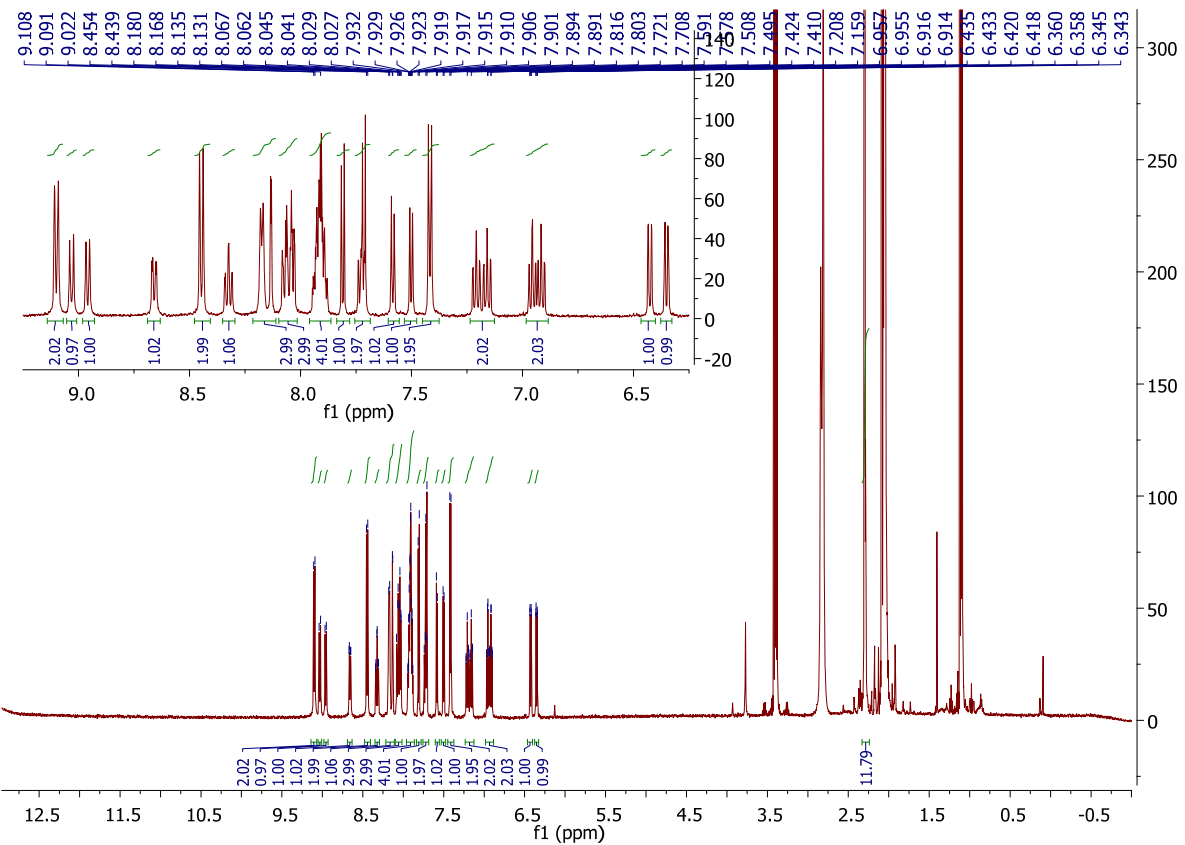


Figure S15 ¹H NMR spectra of Irpiq-2254tpy-Co

Crystallographic study

Crystallographic data for **Irbpy-2254tpy**, **Irbpy-2244tpy** and **Irpiq-2254tpy** were collected at 100 K using a Bruker Venture MetalJet diffractometer equipped with a photon 100 CMOS-based area detector. For data collection, determination of cell parameters, cell refinement, and data reduction *APEX2* and *SAINT* (Bruker, 2007) were used. Absorption and corrections were applied using SADABS and TWINABS (Bruker 2001)⁵. Structure solutions were performed using intrinsic phasing with *SHELXT* (Sheldrick, (2008 and 2015)⁶ and refined on F^2 by fullmatrix least squares using *SHELXL2014* (Sheldrick, 2008 and 2015)^{6b}. *OLEX2* (Dolomanov *et al.*, 2009). The material was prepared for publication using *PLATON* (Spek, 2009)⁷, and *Mercury*⁸.

Irbpy-2254tpy crystalizes as a plate. **Irbpy-2244tpy** grows as needles. **Irbpy-2254tpy** crystallizes as a plate. The space groups are respectively **P2₁/c**, **C₂/c** and **P2₁/c**.

Irbpy-2244tpy : The software Cell Now was used to evaluate the twinning of sets of reflections. Two domains with the same space group are defined with a ratio 35/65. Basis vector orientations for two domains in reciprocal matrix are typical of non-merohedral twining. Both domains are included to match the model, but the outcome is not definitive according to this method. The best iteration is done with the twin4_1.hkl also with the integration of only one domain. The PF₆ are localized on two symmetry elements: one on C₂ axis and the other is disordered around an inversion center. The phosphorous element and two fluorines are on C₂ axis. The occupation factor of two PF₆ localisations is refined using a free variable to 48/52. Disordered acetonitrile solvent molecules were difficult to modelize and the squeeze routine is used, giving a lower the R₁ factor (from 7, 21 % to 7, 10 %). The void volume is 385 Å³ that corresponds to 147 electrons and 6 % of the volume of the cell.

Irppy-2254tpy: The Ir complex and his counter anion PF₆ are well described. The quality of data set permits to modelize a structure without ambiguity. A residual electron density attributed to solvent disorder is treated with the olex mask. The total solvent accessible volume is 197.5 Å³, i.e. 5.8 % of the cell that corresponds at 30.7 electrons. This residual electron density is distributed around 6 volumes of the cell from 39.8 Å³ to 29.5 Å³. The presence of the water molecule could contribute to solvent occupation. The R₁ factor goes from 3.27 % to 3.23 % after the olex-mask process.

Irpiq-2254tpy: Two positions for the PF₆ are evaluated to fit the disorder of the counter-anion PF₆. The R₁ factor before squeeze 5.30 % and after squeeze is 4.19 %. Two voids of 969 Å³ that represents 22 % of the the unit cell are squeezed. The diffuse electron densities accounted for 383 electrons.

The intensity of maximum residual electron density reaches critical values. The reason is related to the bad quality of data set, after omitting reflections with a too important error versus the model. The crystallographic model matches with the data.

Table S1. Crystallographic information for Irpiq-2254tpy-Co (1), Irpiq-2254tpy-Co (2), Irpiq-2254tpy, Irppy-2254tpy and Irppy-2244tpy

Identification	Irpiq-2254tpy	Irppy-2254tpy	Irppy-2244tpy	Irpiq-2254tpy-Co (1)	Irpiq-2254tpy-Co (2)
CCDC Number	1851595	1851560	1851608	1515333	1515335
Empirical formula	C ₄₅ H ₃₁ F ₆ IrN ₅ P	C ₃₇ H ₂₇ F ₆ IrN ₅ P	C ₃₇ H ₂₇ F ₆ IrN ₅ P	C ₅₃ H ₄₅ ClCoF ₆ IrN ₉ O ₄ P	C ₅₃ H ₄₅ ClCoF ₆ IrN ₉ O ₄ P
Formula weight	978.92	878.80	878.80	1303.53	1303.53
Temperature/K	100	100	100	100	100
Crystal system	monoclinic	monoclinic	monoclinic	monoclinic	monoclinic
Space group	C2/c	P2 ₁ /c	C2/c	C2/c	P2 ₁ /n
a/Å	39.0974(12)	8.7575(4)	20.5798 (19)	43.3450(7)	17.1260(10)
b/Å	11.0469(3)	35.7671(18)	24.646 (2)	11.1091(2)	10.4445(6)
c/Å	21.9827(7)	11.0138(6)	14.4517(13)	30.4979(5)	30.4628(19)
α/°	90	90	90	90	90
β/°	110.2910(10)	101.629(2)	108.834(4)	128.3740(10)	91.457(3)
γ/°	90	90	90	90	90
Volume/Å ³	8905.2(5)	3379.0(3)	6937.7(11)	11513.0(4)	5447.2(6)
Z	8	4	8	8	4
ρ _{calcg/cm³}	1.460	1.727	1.683	1.504	1.589
μ/mm ⁻¹	4.407	5.751	5.604	7.954	8.406
F(000)	3856.0	1720.0	3440.0	5184.0	2592.0
Crystal size/mm ³	0.2 × 0.2 × 0.15	0.29 × 0.21 × 0.05	0.21 × 0.1 × 0.09	0.14 × 0.12 × 0.05	0.24 × 0.04 × 0.03
Radiation	GaKα (λ = 1.34139)	GaKα (λ = 1.34139)	GaKα (λ = 1.34139)	CuKα (λ = 1.54178)	CuKα (λ = 1.54178)
2θ range for data collection/°	7.18 to 126.92	4.298 to 126.934	5.03 to 121.596	5.2 to 144.426	5.804 to 144.292
Index ranges	-52 ≤ h ≤ 52, -14 ≤ k ≤ 14, -29 ≤ l ≤ 29	-11 ≤ h ≤ 11, -47 ≤ k ≤ 47, -14 ≤ l ≤ 14	-26 ≤ h ≤ 26, -31 ≤ k ≤ 31, -18 ≤ l ≤ 18	-53 ≤ h ≤ 53, -13 ≤ k ≤ 12, -37 ≤ l ≤ 37	-21 ≤ h ≤ 21, -12 ≤ k ≤ 12, -37 ≤ l ≤ 37
Reflections collected	143630	102448	15701	167315	117808
Independent reflections	11008 [R _{int} = 0.0399, R _{sigma} = 0.0131]	8390 [R _{int} = 0.0559, R _{sigma} = 0.0197]	7954 [R _{int} = 0.0289, R _{sigma} = 0.0363]	11342 [R _{int} = 0.0405, R _{sigma} = 0.0144]	10688 [R _{int} = 0.1045, R _{sigma} = 0.0491]
Data/restraints/parameters	11008/21/540	8390/0/452	7954/353/466	11342/0/712	10688/323/764
Goodness-of-fit on F ²	1.061	1.244	1.066	1.044	1.043
Final R indexes [I>=2σ (I)]	R ₁ = 0.0419, wR ₂ = 0.1089	R ₁ = 0.0323, wR ₂ = 0.0860	R ₁ = 0.0710, wR ₂ = 0.1757	R ₁ = 0.0263, wR ₂ = 0.0670	R ₁ = 0.0554, wR ₂ = 0.1256
Final R indexes [all data]	R ₁ = 0.0422, wR ₂ = 0.1093	R ₁ = 0.0323, wR ₂ = 0.0862	R ₁ = 0.0810, wR ₂ = 0.1835	R ₁ = 0.0277, wR ₂ = 0.0684	R ₁ = 0.0790, wR ₂ = 0.1396
Largest diff. peak/hole / e Å ⁻³	1.87/-1.28	1.48/-1.24	3.32/-1.21	1.84/-0.54	1.72/-1.04

In these archetype complexes, the near octahedral geometry is observed as expected for the reference complexes $\text{Ir}(\text{piq})_2(\text{bpy})^+$ ⁹, $\text{Ir}(\text{ppy})_2(\text{bpy})^{+10}$. The coordination sphere of the Ir-derivatives don't show differences of structural parameters. The length bond of bipyridine $\text{Ir}-\text{N}(\text{bpy})$ 2.14 Å is around 0.08 Å longer than the $\text{Ir}-\text{N}$ cyclometalated ligand around 2.05 Å. The shortest bond around 2.01 Å is the carbanion bond to the Ir that should favorite the σ orbital overlapping. Otherwise, a trans effect of $\text{Ir}\sigma-\text{C}$ could accentuate the longer $\text{Ir}-\text{N}(\text{bpy})$ and promotes the cis-arrangement of the cyclometallated ligand. The bite angle of terpyridine shows a angle of 80° degree and 76 ° for the cyclometallated ligand.

Concerning the difference between the family of 4 and 5 terpyridine derivatives, the angle between the two plans of bipyridine is curiously closed from planarity for the **Irppy-2244tpy** and the twist angle 4,4 bipyridine is the largest as 39°. The electronic delocalization could be favoured on two bipyridine coordinated to the Ir versus 5 isomer where the twist angle 4,5 is smaller that could favor the conjugation of electronic system on the pendant pyridine. Those observations have to be illustrated by more examples of structures because crystal packing induces the stability of particular angle in bonding.

The distance of Ir to nitrogen of pendant pyridine is shorter of around 1 Å in the 5- than the 4-derivative: 8, 1 to 9, 2 Å. The proximity of cobalt catalyst coordinated to the pendant pyridine could influence the electronic communication between both metallic entities.

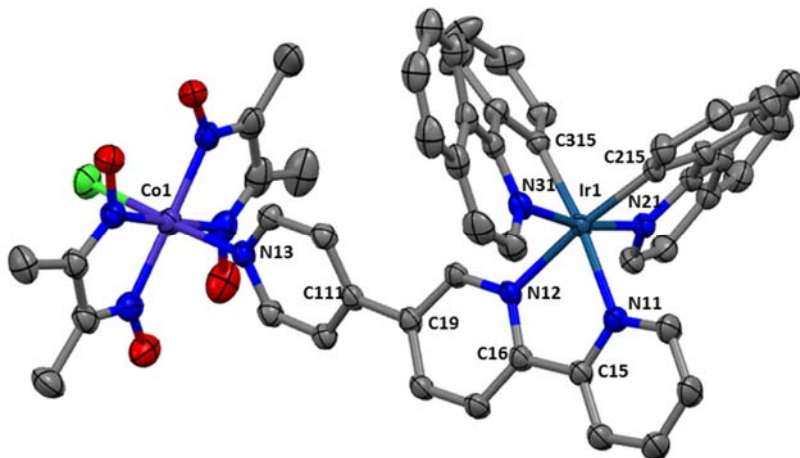


Figure S16. X-ray crystal structure of $\text{Ir}(\text{piq})_2(\text{bpy})\text{Co}$, atoms are represented at the 50 % probability level.

Hydrogen atoms and PF_6^- counteranion are omitted for clarity.

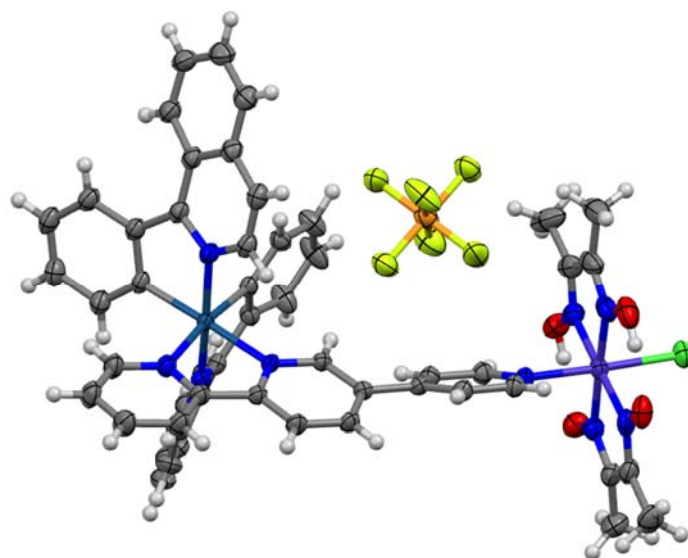


Figure S17. X-ray crystal structure of $\text{Ir}(\text{piq})_2(\text{bpy})\text{Co}$, ellipsoid at 50 % probability level.

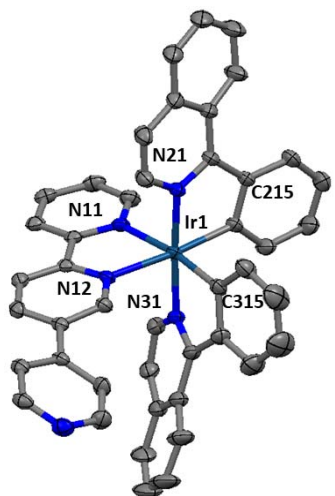


Figure S18. X-ray crystal structure Irpiq-2254tpy, atoms are represented at the 50 % probability level.
Hydrogen atoms and PF₆ counteranion are omitted for clarity.

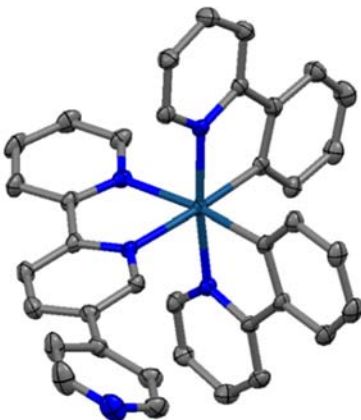


Figure S19. X-ray crystal structure of Irppy-2254tpy, atoms are represented at the 50 % probability level.
Hydrogen atoms and PF₆ counteranion are omitted for clarity.

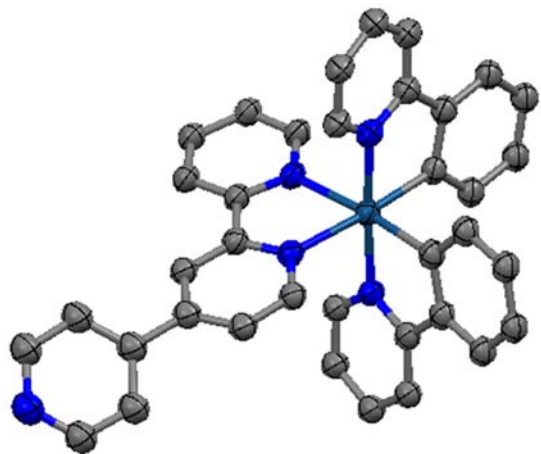


Figure S20. X-ray crystal structure of Irppy-2244tpy, atoms are represented at the 50 % probability level. Hydrogen atoms and PF₆ counteranion are omitted for clarity.

Table S2. Selected angles and bond lengths of crystal structures **Irpiq-2254tpy-Co 1**, **Irpiq-2254tpy-Co 2**, **Irpiq-2254tpy**.

Bond lengths	Irpiq-2254tpy-Co 1	Irpiq-2254tpy-Co 2	Irpiq-2254tpy
Ir(1)–C(315)	2.004 (3)	2.07(2), 1.98(2) ¹	1.998 (3)
Ir(1)–C(215)	2.009 (2)	2.036(7)	2.002 (3)
Ir(1)–N(31)	2.047 (3)	2.033 (15), 2.063(18) ¹	2.043 (3)
Ir(1)–N(21)	2.049 (3)	2.049 (5)	2.049 (3)
Ir(1)–N(11)	2.141 (2)	2.156 (5)	2.129 (3)
Ir(1)–N(12)	2.133 (2)	2.150 (5)	2.142(3)
C(19)–C(111)	1.476 (3)	1.486 (10)	1.486(4)
C(15)–C(16)	1.481 (3)	1.482 (10)	1.480(4)
Co(1)–N(13)	1.966 (2)	1.957 (6)	
Ir-N(13) N terminal pyridine of terpyridine	8,042 (2)	7.954 (2)	8,036 (4)
Angles			
C(215)–Ir(1)–C(315)	87.94 (9)	88.2 (14), 90.6 (18) ¹	88.75 (13)
N(31)–Ir(1)–C(315)	79.91 (9)	78.8 (6), 80.6 (7) ¹	79.77 (13)
N(31)–Ir(1)–C(215)	92.95 (9)	101.8 (7), 97.5 (6) ¹	98.87(12)
N(21)–Ir(1)–C(315)	90.84 (9)	92.0 (5) 95.0 (6) ¹	96.95(13)
N(21)–Ir(1)–C(215)	79.74 (9)	79.1 (2)	79.53(12)
N(12)–Ir(1)–C(315)	97.63 (8)	96.8 (15) 94.5 (18) ¹	95.90(12)
N(12)–Ir(1)–N(31)	90.57 (8)	85.7 (6) 81.0 (7) ¹	83.92(11)
N(12)–Ir(1)–N(21)	97.53 (8)	98.5 (2)	97.91(10)
N(11)–Ir(1)–C(215)	98.26 (9)	99.0 (3)	98.97(12)
N(11)–Ir(1)–N(31)	97.31 (8)	100.1 (4), 94.9 (5) ¹	94.69(11)
N(21)–Ir(1)–N(11)	92.60 (8)	89.4 (2)	88.74(11)
N(12)–Ir(1)–N(11)	76.29 (8)	76.1(2)	76.56(10)
N(21)–Ir(1)–N(31)	168.47 (8)	170.4(4), 175. (5) ¹	176.41(11)
N(12)–Ir(1)–C(215)	173.87 (8)	174.5(2),	174.96(11)
N(11)–Ir(1)–C(315)	173.36 (8)	172.9 (14), 170.2 (16) ¹	171.16(11)
α , average planes angles ($^{\circ}$) of the 5,4' sites or 4,4' sites	31 (1)	27.9 (1)	25.64 (10)
β , average planes angles ($^{\circ}$) of the 2,2' sites	4.7 (1)	7.2 (3)	4.09 (10)

¹ Bond lengths and angles of **Irppy-2244tpy** are selected to compare the same parameter than **Irppy-2254tpy**, **Irpiq-2254tpy**, **Irpiq-2254tpy-Co 1**, **Irpiq-2254tpy-Co 2**. The naming of atoms in Irppy-2244tpy is different than in the table.

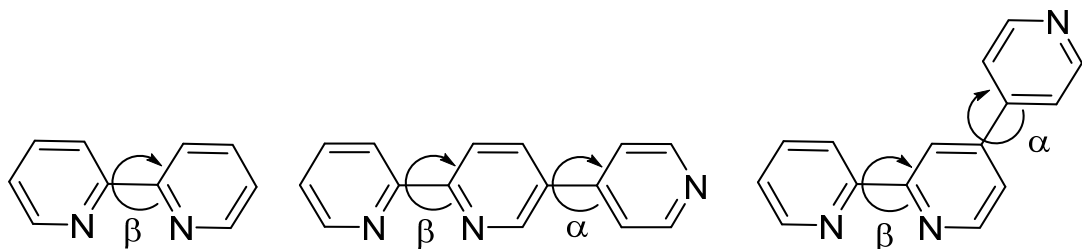


Table S3. Selected angles and bond lengths of crystal structures **Irppy-2254tpy**, **Irppy-2244tpy**, **Ir(ppy)₂(bpy)⁺**.

Bond lengths	Irppy-2254tpy	Irppy-2244tpy ¹	Ir(ppy)2(bpy) ⁺ ²
Ir(1)-C(311)	2.005 (3)	2.028 (8)	2.024 (5)
Ir(1)-C(211)	2.013(3)	2.006 (8)	2.004 (5)
Ir(1)-N(31)	2.028 (8)	2.042 (6)	2.047 (3)
Ir(1)-N(21)	2.047 (3)	2.053 (7)	2.042 (3)
Ir(1)-N(11)	2.135(3)	2.148 (6)	2.136 (3)
Ir(1)-N(12)	2.134(3)	2.142 (6)	2.129 (3)
C(19)-C(111)	1.484(4)	1.486 (10)	
C(15)-C(16)	1.472(4)	1.482 (10)	
Ir-N terminal pyridine of terpyridine	8.124 (3)	9.196 (7)	
Angles			
C(211)-Ir(1)-C(311)	88.53 (11)	87.9(3)	87.90 (17)
N(31)-Ir(1)-C(311)	80.56 (12)	80.3(3)	80.06 (16)
N(31)-Ir(1)-C(211)	95.58 (12)	97.7(3)	95.22 (15)
N(21)-Ir(1)-C(311)	94.46 (12)	95.4(3)	92.98 (16)
N(21)-Ir(1)-C(211)	80.35 (12)	80.6(3)	80.68 (15)
N(12)-Ir(1)-C(311)	95.76 (11)	98.2(3)	99.70 (16)
N(12)-Ir(1)-N(31)	86.68 (10)	82.9(2)	89.17 (13)
N(12)-Ir(1)-N(21)	98.77 (10)	99.3(3)	95.75 (13)
N(11)-Ir(1)-C(211)	96.35 (10)	98.1(3)	96.36 (14)
N(11)-Ir(1)-N(31)	96.36 (10)	97.1(2)	96.75 (13)
N(21)-Ir(1)-N(11)	88.12 (10)	87.3(3)	90.45 (13)
N(12)-Ir(1)-N(11)	76.55 (10)	75.9(2)	76.20 (12)
N(21)-Ir(1)-N(31)	173.66 (10)	175.5(2)	172.09 (13)
N(12)-Ir(1)-C(211)	175.68 (10)	173.9(3)	171.80 (14)
N(11)-Ir(1)-C(311)	171.93 (11)	173.8(3)	174.92 (15)
α, average planes angles (°) of the 5,4' or 4,4' sites	34.43 (13)	39.187 (2)	
β, average planes angles (°) of the 2,2' sites	6.16 (11)	1.902 (2)	3.46 (15)

The geometric details of coordination sphere are compared to those from the X-Ray structure of **Ir(ppy)₂(bpy)PF₆** from reference ¹⁰.

² The coordination sphere data are compared to the reference X-Ray structure of **Ir(ppy)₂(bpy)PF₆** from reference ¹⁰.

Cyclic voltammetry

1) Ir(III) photosensitizers

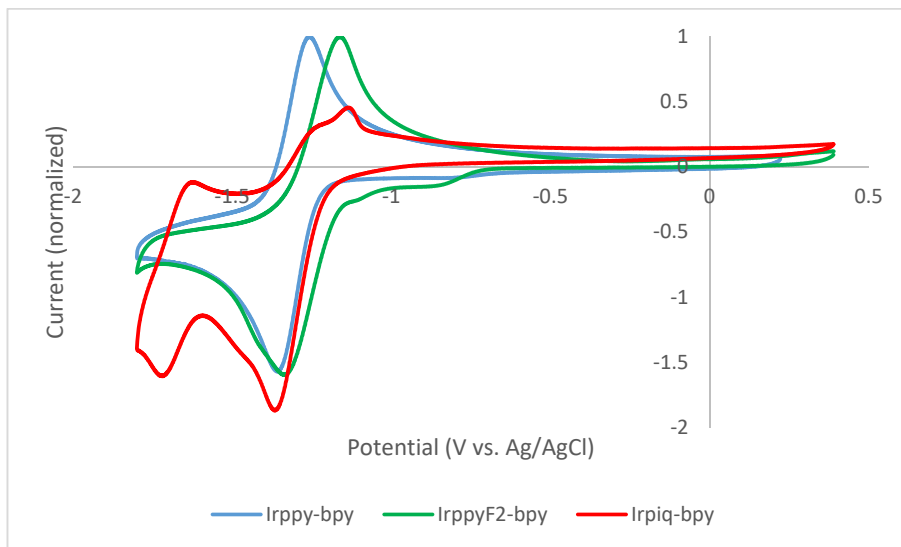


Figure S21. Reduction voltammograms of Irppy-bpy, IrppyF₂-bpy and Irpiq-bpy (10^{-5} M) in acetonitrile with Bu_4NClO_4 0.1 M as supporting electrolyte.

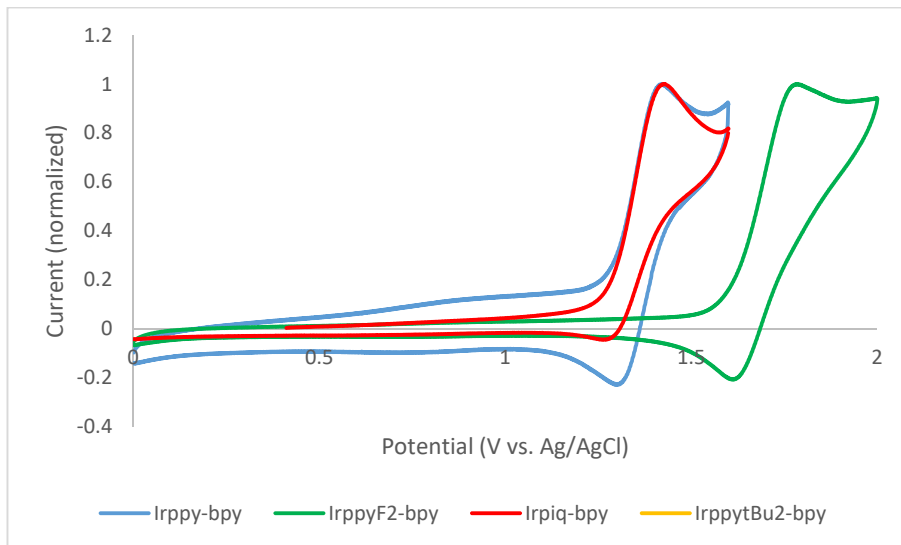


Figure S22. Oxidation voltammograms of Irppy-bpy, IrppyF₂-bpy and Irpiq-bpy (10^{-5} M) in acetonitrile with Bu_4NClO_4 0.1 M as supporting electrolyte.

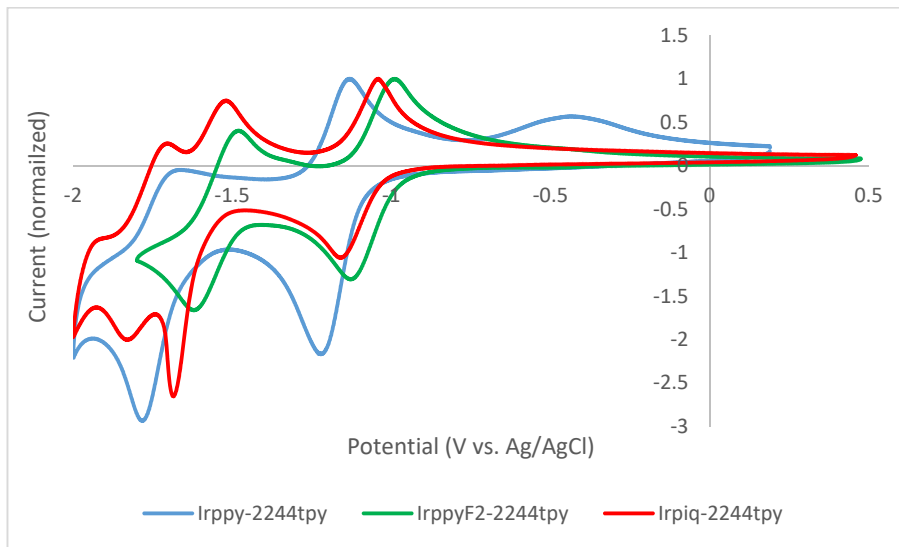


Figure S23. Reduction voltammograms of Irppy-2244tpy, IrppyF₂-2244tpy and Irpiq-2244tpy (10^{-5} M) in acetonitrile with Bu_4NClO_4 0.1 M as supporting electrolyte.

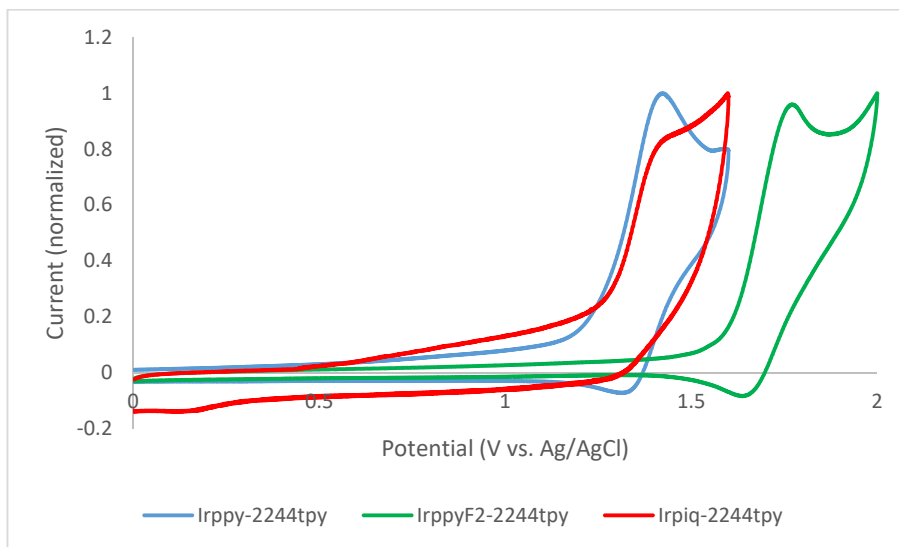


Figure S24. Oxidation voltammograms of Irppy-2244tpy, IrppyF₂-2244tpy and Irpiq-2244tpy (10^{-5} M) in acetonitrile with Bu_4NClO_4 0.1 M as supporting electrolyte.

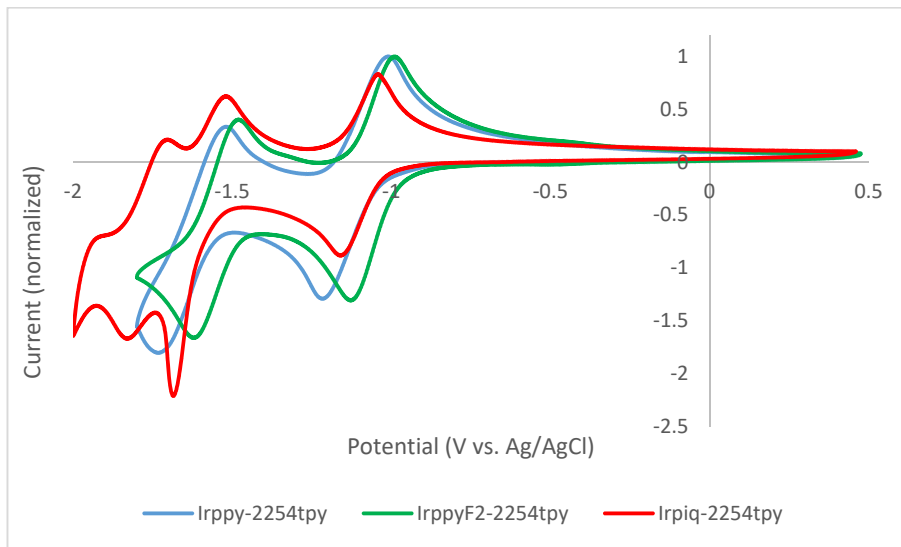


Figure S25. Reduction voltammograms of Irppy-2254tpy, IrppyF₂-2254tpy and Irpiq-2254tpy (10^{-5} M) in acetonitrile with Bu_4NClO_4 0.1 M as supporting electrolyte.

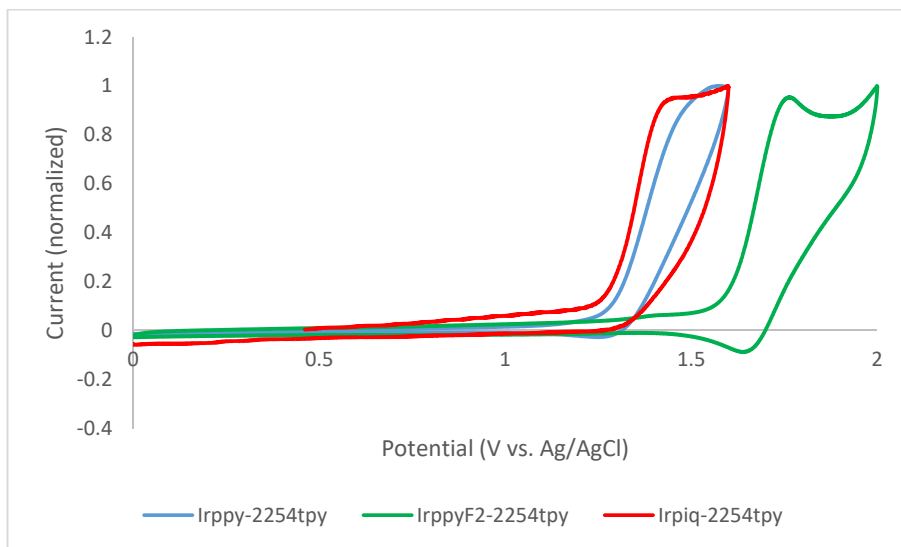


Figure S26. Oxidation voltammograms of Irppy-2254tpy, IrppyF₂-2254tpy and Irpiq-2254tpy (10^{-5} M) in acetonitrile with Bu_4NClO_4 0.1 M as supporting electrolyte.

2) Ir(III)-Co(III) dyads

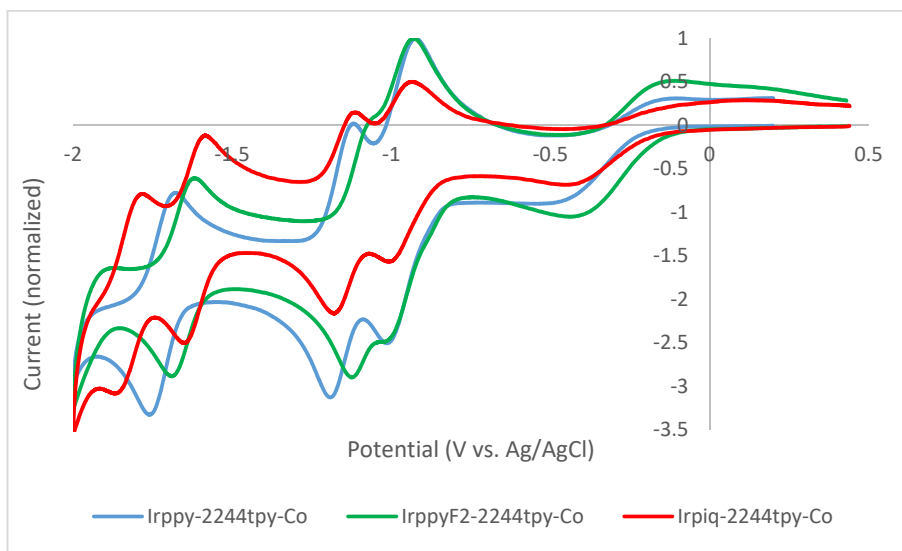


Figure S27. Reduction voltammograms of Irppy-2244tpy-Co, IrppyF₂-2244tpy-Co and Irpiq-2244tpy-Co (10^{-5} M) in acetonitrile with Bu₄NClO₄ 0.1 M as supporting electrolyte.

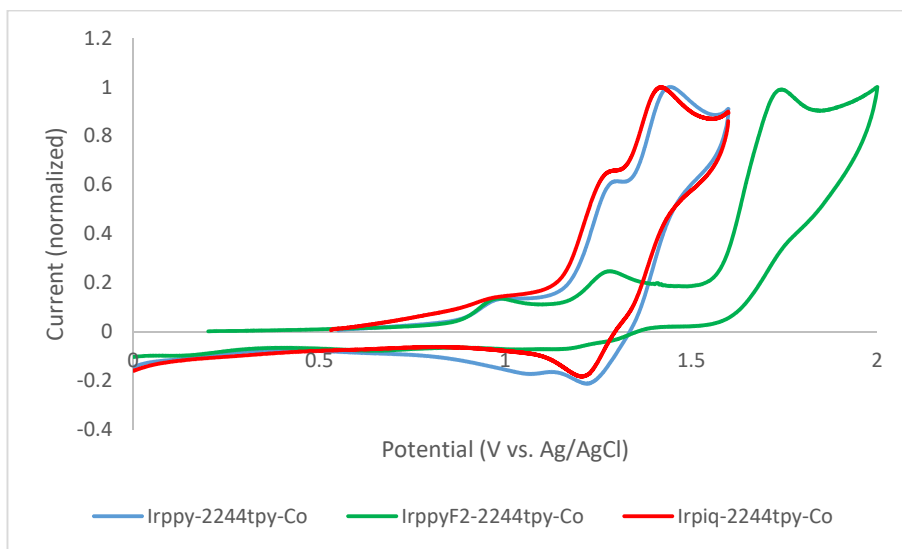


Figure S28. Oxidation voltammograms of Irppy-2244tpy-Co, IrppyF₂-2244tpy-Co and Irpiq-2244tpy-Co (10^{-5} M) in acetonitrile with Bu₄NClO₄ 0.1 M as supporting electrolyte.

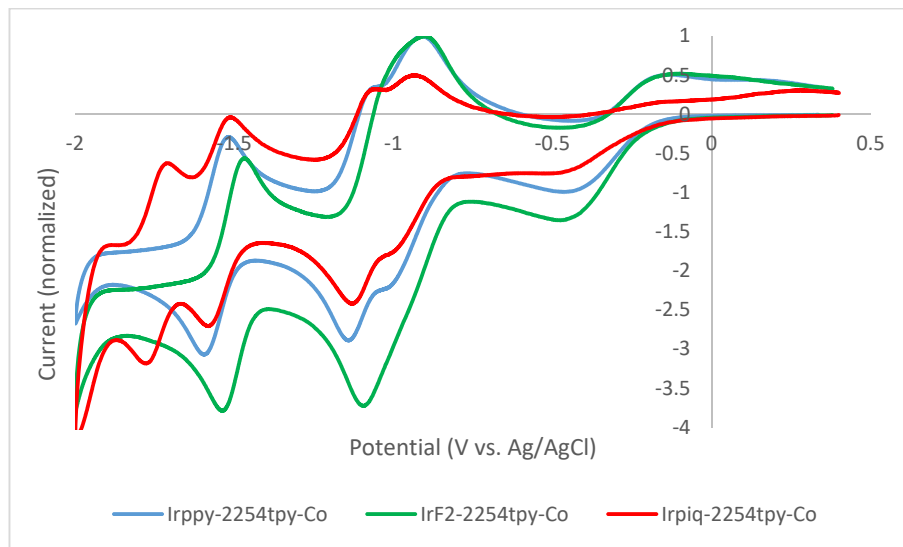


Figure S29. Reduction voltammograms of Irppy-2254tpy-Co, IrppyF₂-2254tpy-Co and Irpiq-2254tpy-Co (10^{-5} M) in acetonitrile with Bu_4NClO_4 0.1 M as supporting electrolyte.

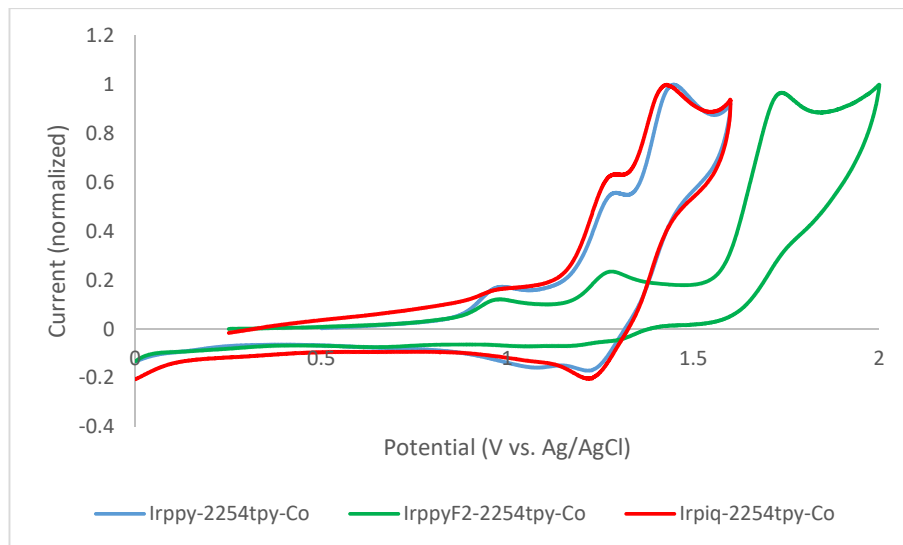


Figure S30. Oxidation voltammograms of Irppy-2254tpy-Co, IrppyF₂-2254tpy-Co and Irpiq-2254tpy-Co (10^{-5} M) in acetonitrile with Bu_4NClO_4 0.1 M as supporting electrolyte.

Absorption and emission spectra of Ir(III) photosensitzers

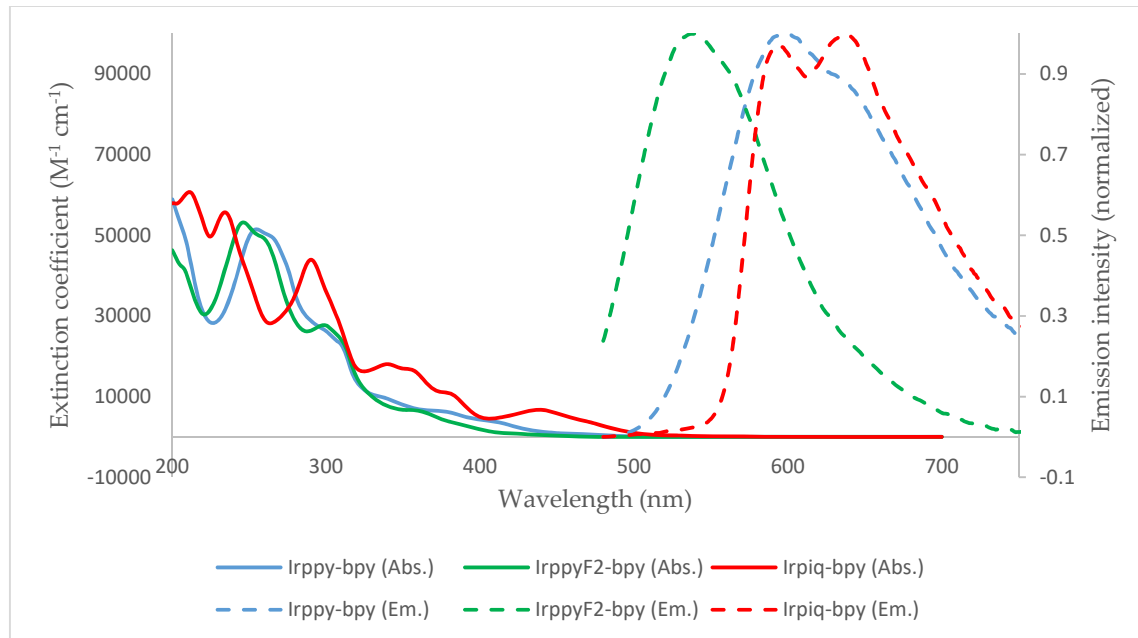


Figure S31. Absorption and emission spectra (excitation at $\lambda = 405 \text{ nm}$) of Irppy-bpy, IrppyF₂-bpy and Irpiq-bpy in acetonitrile at room temperature.

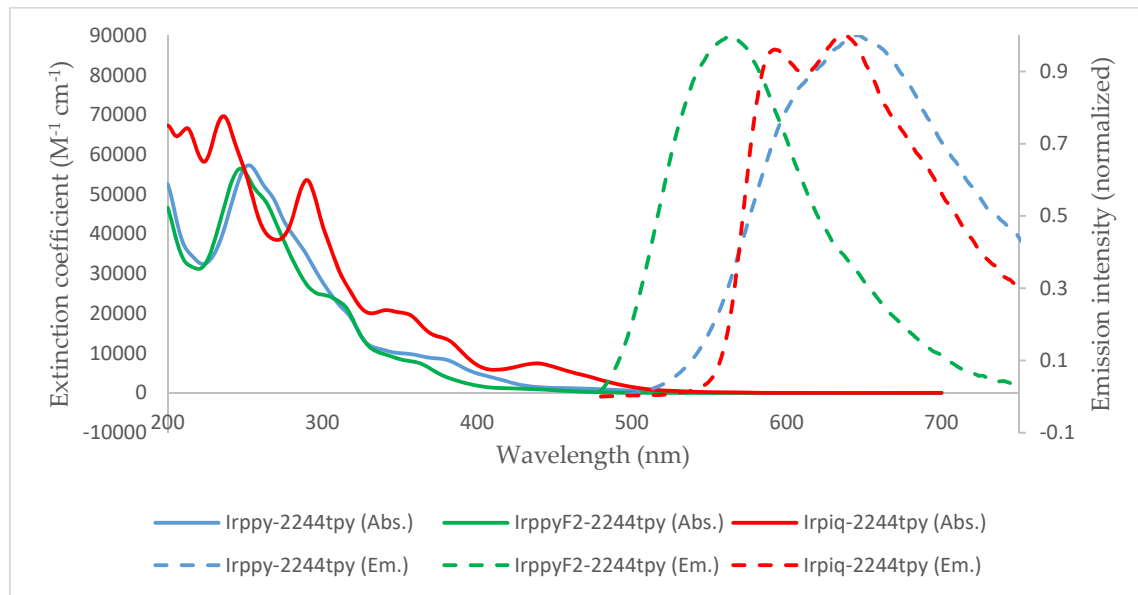


Figure S32. Absorption and emission spectra (excitation at $\lambda = 405 \text{ nm}$) of Irppy-2244tpy, IrppyF₂-2244tpy and Irpiq-2244tpy in acetonitrile at room temperature.

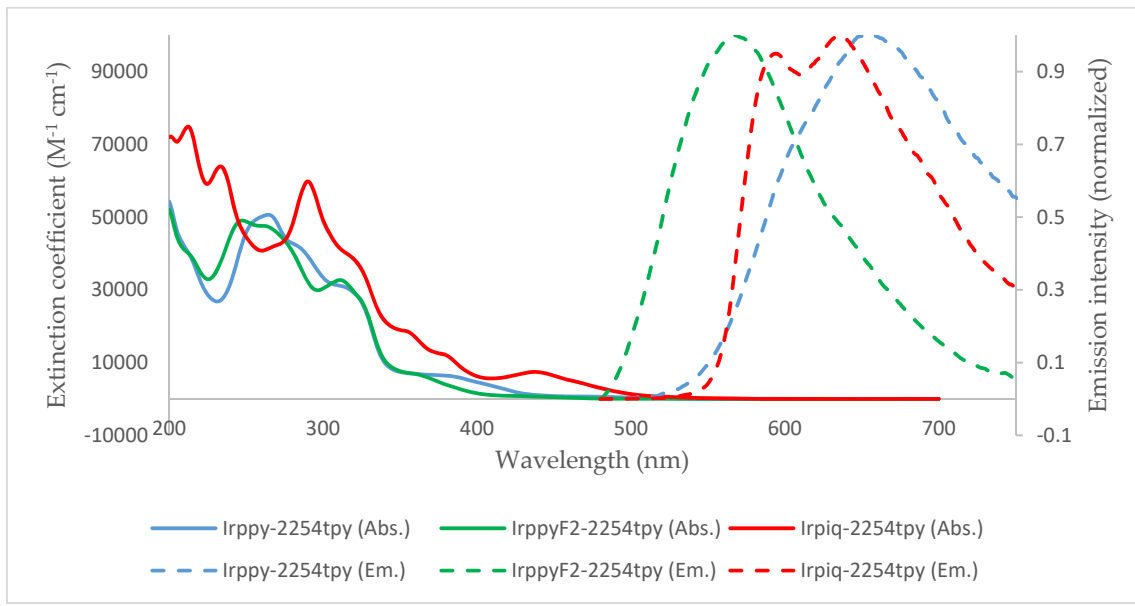


Figure S33. Absorption and emission spectra (excitation at $\lambda = 405 \text{ nm}$) of Irppy-2254tpy, IrppyF₂-2254tpy and Irpiq-2254tpy in acetonitrile at room temperature.

Table S4. Spectroscopic data of Ir(III) Photosensitizers^a

Complex	λ_{abs} [nm] (ϵ [$\times 10^2$ M ⁻¹ cm ⁻¹])	$\lambda_{\text{em},298k}$ [nm]	τ^b [μs]	Φ^c (Ar)	k_r^d [$\times 10^3$ s ⁻¹]	$\lambda_{\text{em},77k}$ [nm] ^e
Irppy-2244tpy	256 (562), 318 (191), 383 (80), 418 (31), 468 (11)	646	0.266	0.0228	85.7	543
Irppy-2254tpy	255 (489), 270 (484), 289 (398), 321 (287), 382 (64), 467 (7)	654	0.128	0.0103	80.5	554
Irppy-bpy	257 (512), 267 (487), 310 (227), 339 (96), 376 (64), 412 (36), 467 (7)	599	0.267	0.0215	80.5	514
IrppyF ₂ -2244tpy	247 (565), 262 (489), 308 (236), 340 (97), 358 (79), 427 (11), 447 (8)	564	1.192	0.1182	99.2	502
IrppyF ₂ -2254tpy	249 (490), 263 (475), 311 (327), 324 (275), 358 (70), 428 (8), 449 (5)	567	1.272	0.1183	93.0	485, 520
IrppyF ₂ -bpy	247 (531), 262 (481), 298 (277), 310 (241), 360 (65), 423 (8), 449 (4)	539	1.274	0.0758	59.5	455, 483
Irpiq-2244tpy	214 (662), 236 (696), 343 (208), 357 (195), 380 (136), 439 (74), 527 (5), 560 (2)	592, 636	1.528 (12%) 3.049 (88%)	0.0125	4.4	579, 626
Irpiq-2254tpy	212 (749), 234 (639), 291 (596), 322 (374), 357 (180), 381 (118), 438 (74), 527 (5), 565 (2)	593, 636	1.619 (43%) 2.372 (57%)	0.0130	6.3	578, 625
Irpiq-bpy	212 (606), 234 (557), 290 (440), 338 (180), 354 (168), 379 (109), 439 (67), 527 (4), 564 (1)	593, 638	1.059 (39%) 1.638 (61%)	0.0110	7.8	580, 627

^aMeasurements in degassed acetonitrile at 298K. ^b Lifetime under N₂ atmosphere. ^c Quantum yield measured by using [Ru(bpy)₃]²⁺ as a reference, $\Phi_{\text{ref}} = 0.028$ in water under air. ^d Radiative rate constant determined under an inert atmosphere at 298K ($k_r = \Phi/\tau$). ^e in degassed EtOH:MeOH / 4:1

Table S5. Excited states oxidation and reduction potentials of Ir(III) photosensitizers

Complex	$\lambda_{\text{max em}}$ [nm] ^a	E_{ox}^*	E_{red}^*
		(V vs. Ag/AgCl)	(V vs. Ag/AgCl)
Irppy-2244tpy	646	-0.54	0.74
Irppy-2254tpy	654	-0.52	0.78
Irppy-bpy	599	-0.69	0.76
IrppyF ₂ -2244tpy	564	-0.47	1.02
IrppyF ₂ -2254tpy	567	-0.46	1.12
IrppyF ₂ -bpy	539	-0.58	1.04
Irpiq-2244tpy	592	-0.67	0.93
Irpiq-2254tpy	593	-0.65	0.99
Irpiq-bpy	593	-0.72	0.78

^aEmission maximum for the most hypsochromic band if multiband spectrum

Absorption spectra of Ir(III)-Co(III) dyads

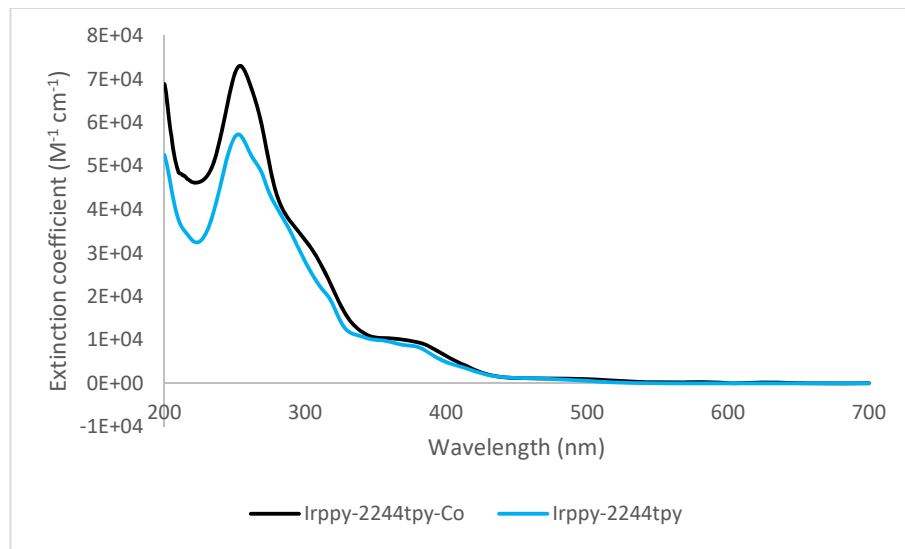


Figure S34. Absorption spectra of Irppy-2244tpy-Co and Irppy-2244tpy in acetonitrile at room temperature.

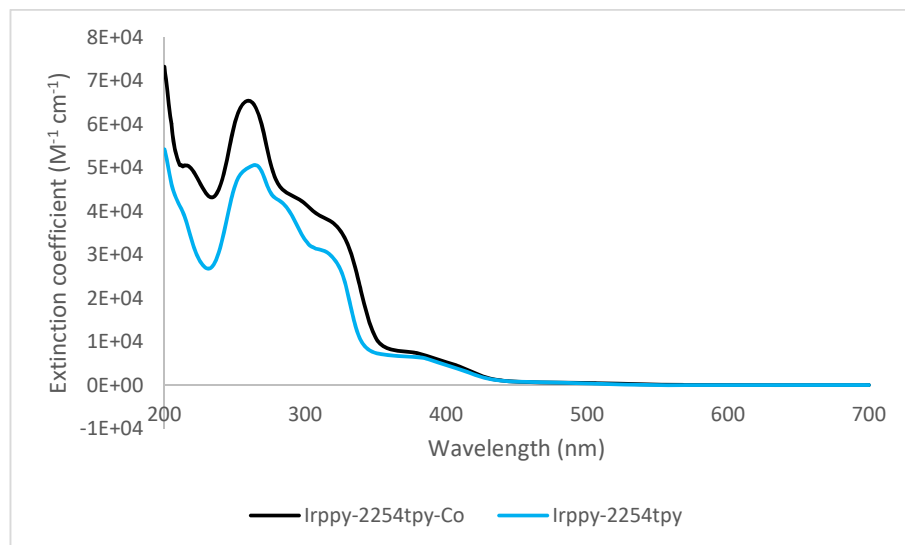


Figure S35. Absorption spectra of Irppy-2254tpy-Co and Irppy-2254tpy in acetonitrile at room temperature.

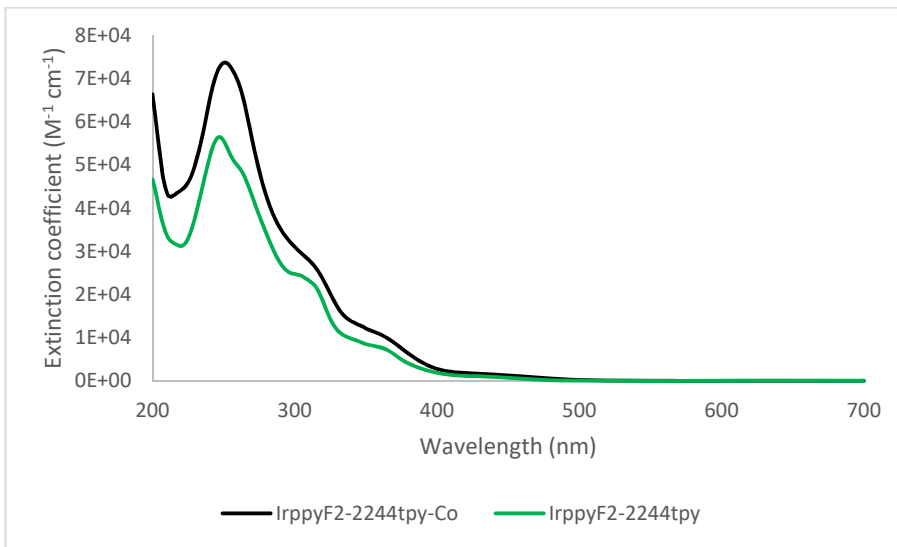


Figure S36. Absorption spectra of IrppyF₂-2244tpy-Co and IrppyF₂-2244tpy in acetonitrile at room temperature.

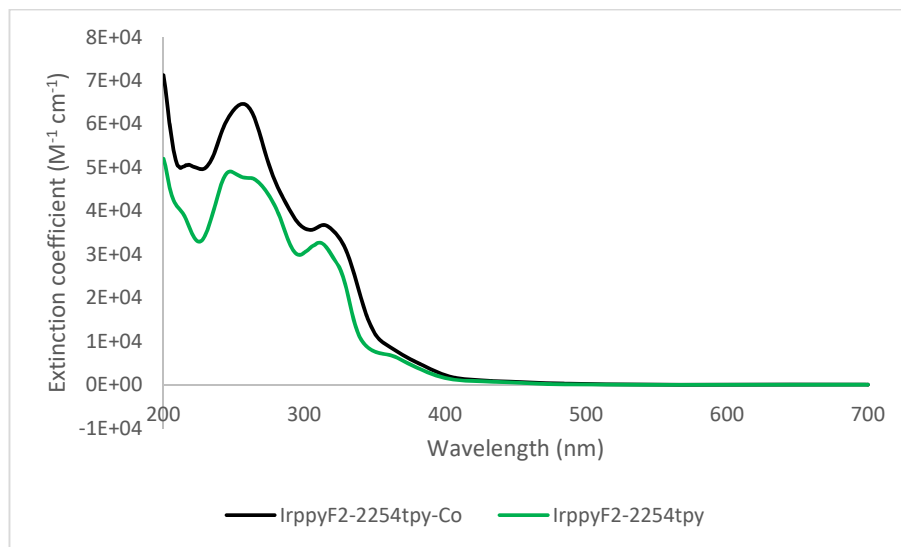


Figure S37. Absorption spectra of IrppyF₂-2254tpy-Co and IrppyF₂-2254tpy in acetonitrile at room temperature.

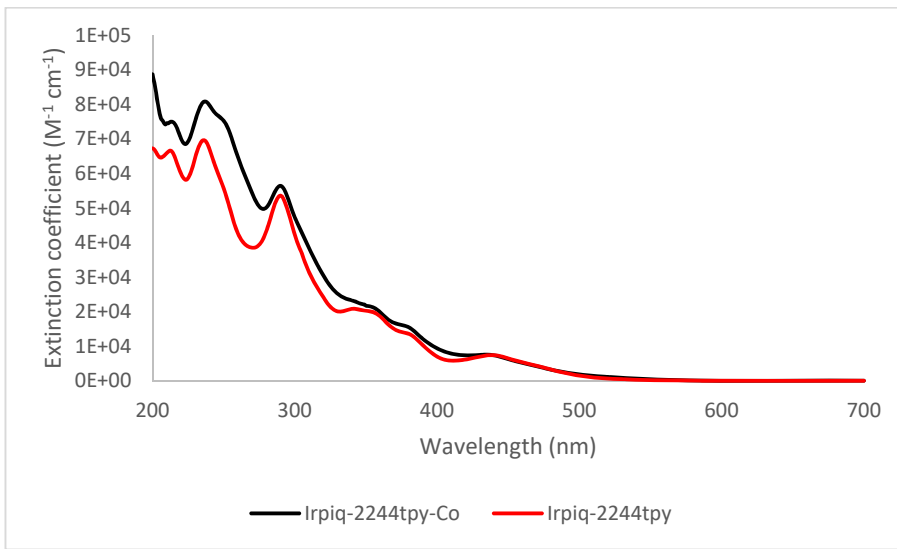


Figure S38. Absorption spectra of Irpiq-2244tpy-Co and Irpiq-2244tpy in acetonitrile at room temperature.

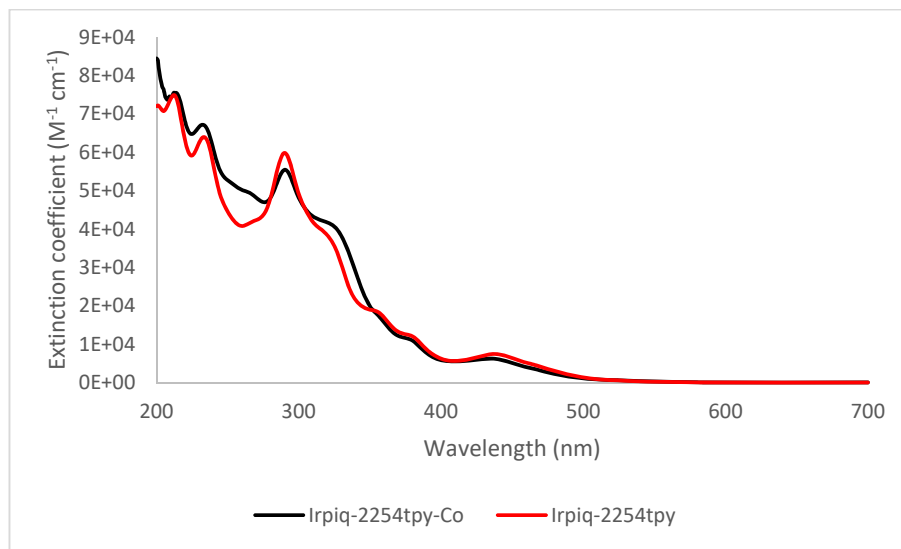


Figure S39. Absorption spectra of Irpiq-2254tpy-Co and Irpiq-2254tpy in acetonitrile at room temperature.

Acid titrations data

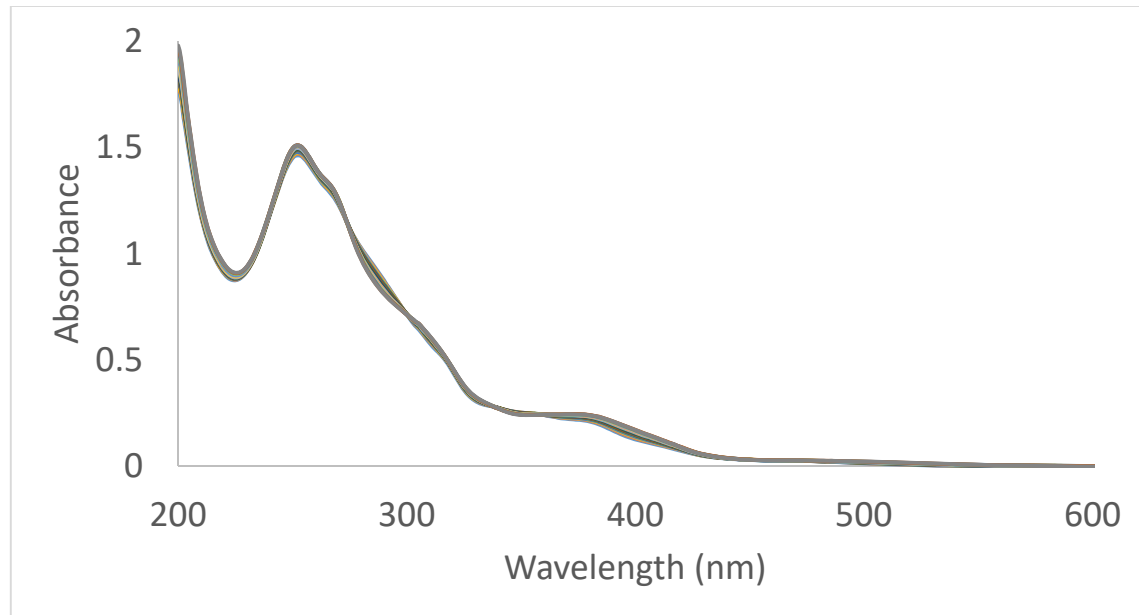


Figure S40. Absorption spectral changes for a 2.5×10^{-5} mol.L⁻¹ solution of Irppy-2244tpy in acetonitrile for increasing concentrations of trifluoroacetic acid.

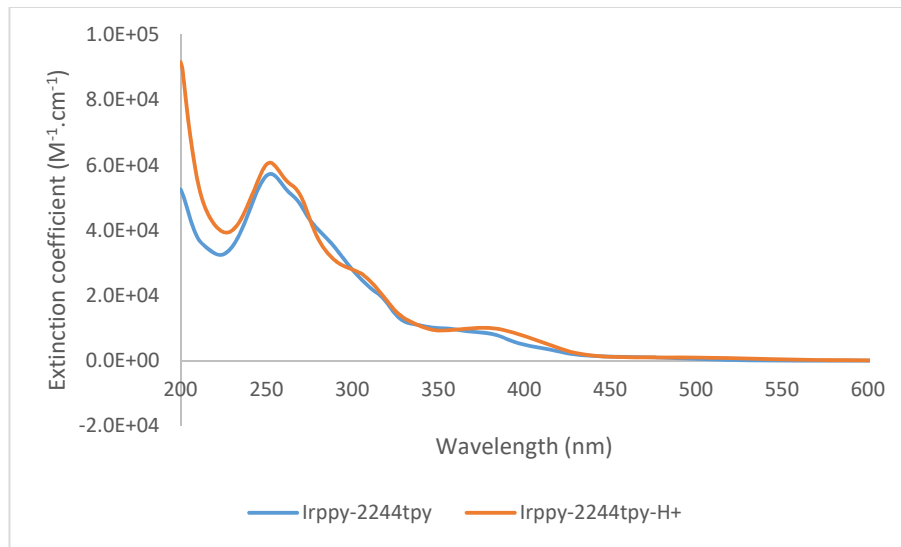


Figure S41. Absorption spectra for neutral (blue) and protonated (orange) Irppy-2244tpy photosensitizer

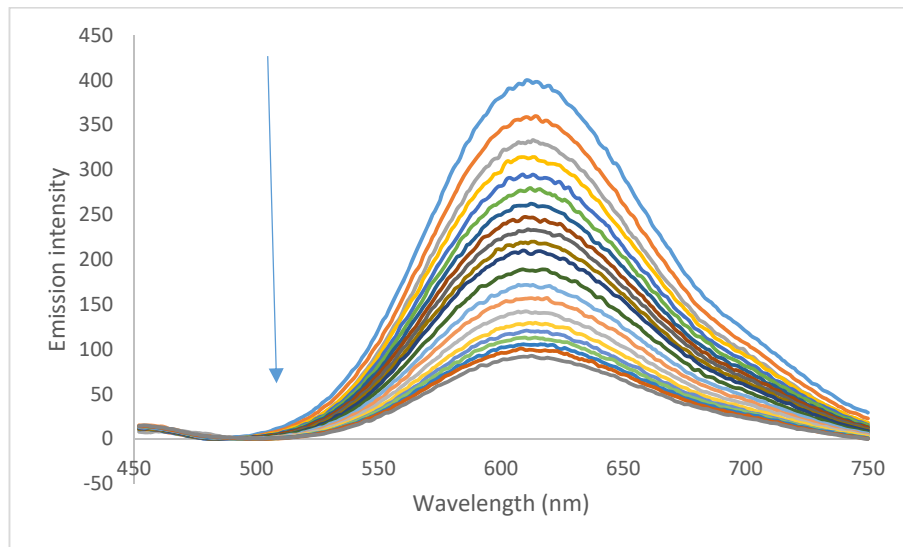


Figure S42. Emission spectral changes for a 2.5×10^{-5} mol.L $^{-1}$ solution of Irppy-2244tpy in acetonitrile for increasing concentrations of trifluoroacetic acid.

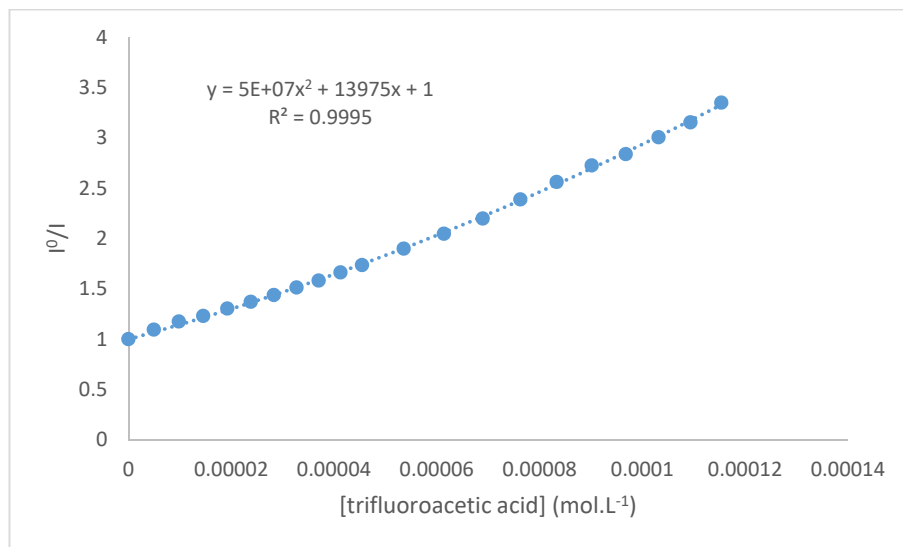


Figure S43. Stern-Volmer plots of the luminescence quenching of Irppy-2244tpy upon the addition of trifluoroacetic acid.

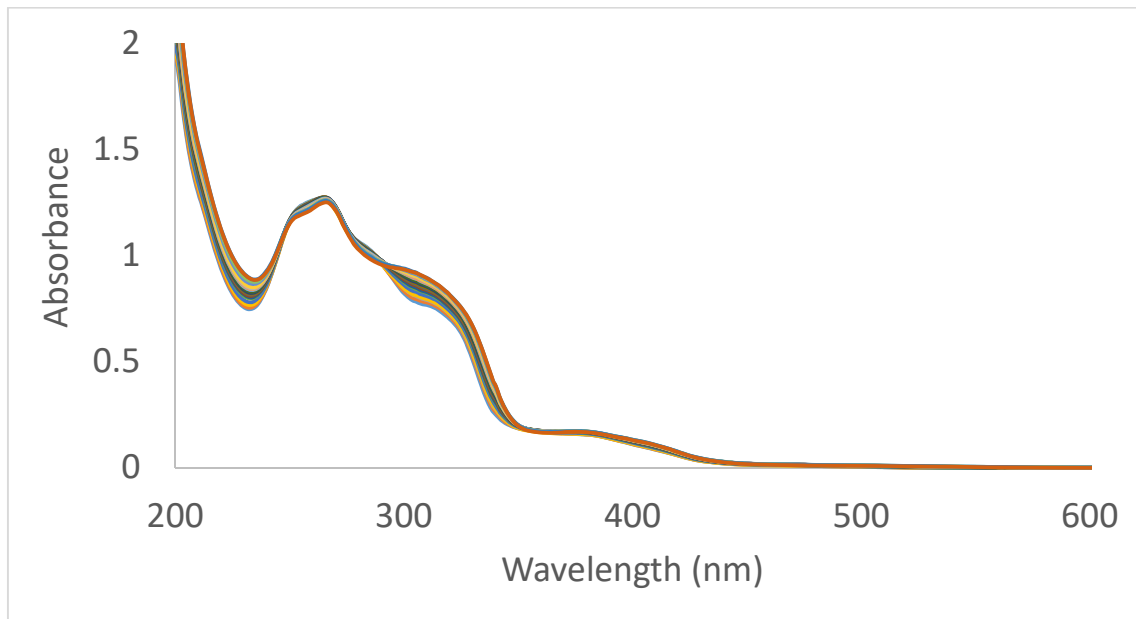


Figure S44. Absorption spectral changes for a 2.5×10^{-5} mol.L⁻¹ solution of Irppy-2254tpy in acetonitrile for increasing concentrations of trifluoroacetic acid.

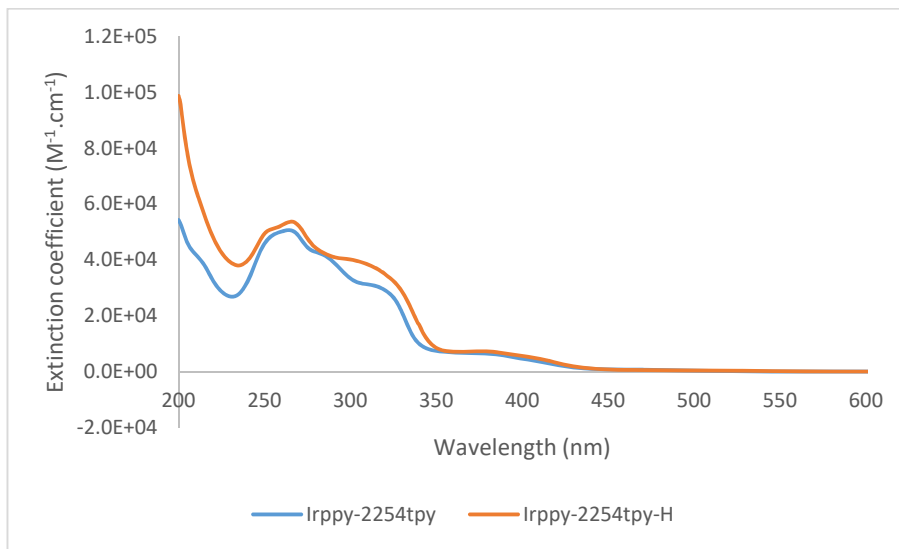


Figure S45. Absorption spectra for neutral (blue) and protonated (orange) Irppy-2254tpy photosensitizer

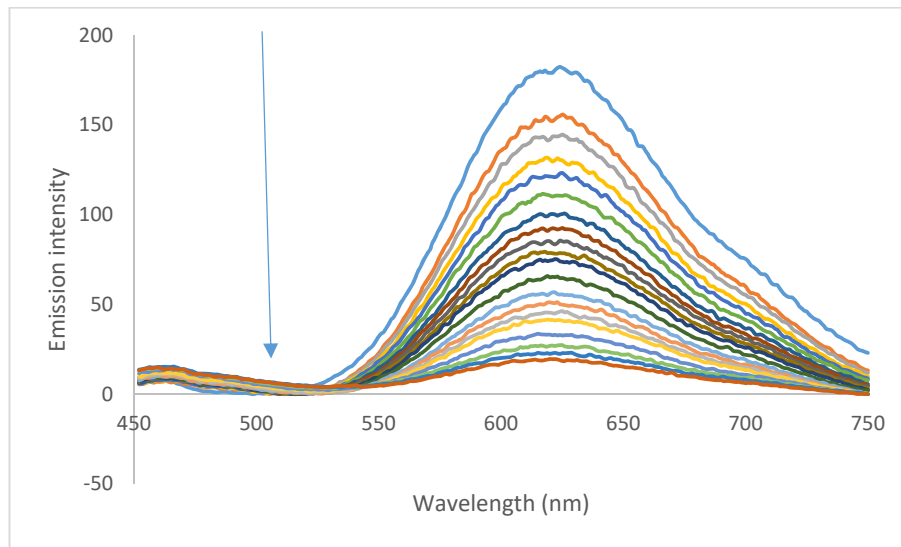


Figure S46. Emission spectral changes for a 2.5×10^{-5} mol.L $^{-1}$ solution of Irppy-2254tpy in acetonitrile for increasing concentrations of trifluoroacetic acid.

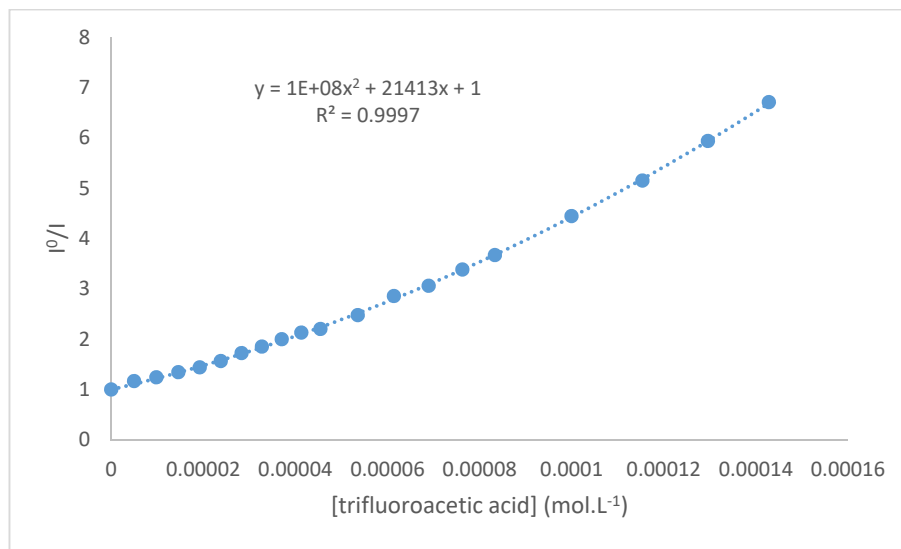


Figure S47. Stern-Volmer plots of the luminescence quenching of Irppy-2254tpy upon the addition of trifluoroacetic acid.

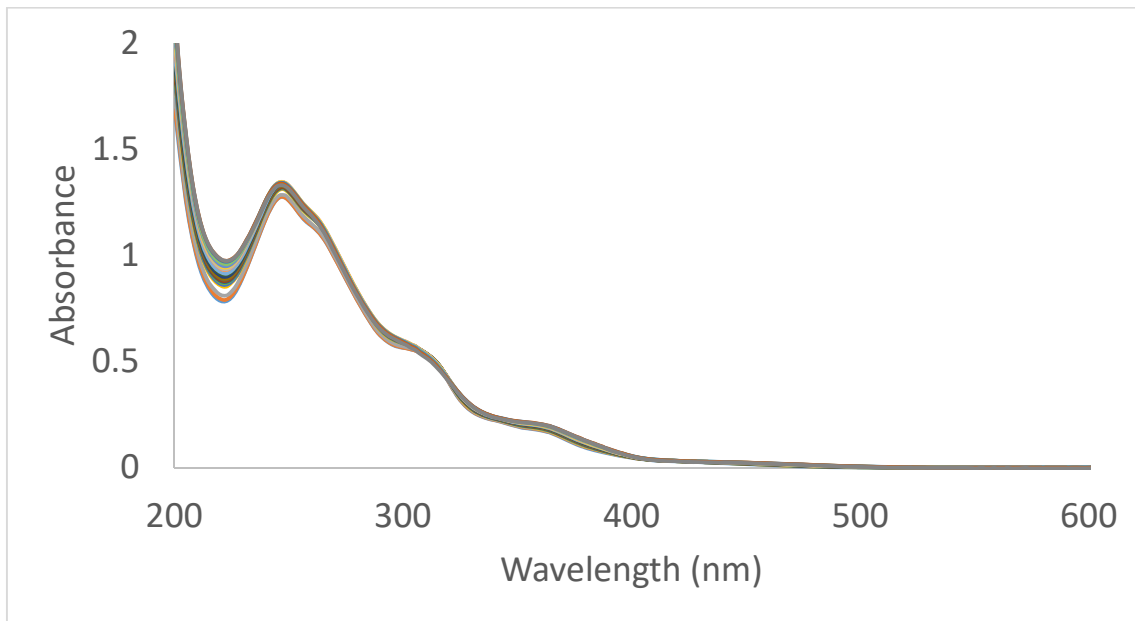


Figure S48. Absorption spectral changes for a 2.5×10^{-5} mol.L⁻¹ solution of IrppyF₂-2244tpy in acetonitrile for increasing concentrations of trifluoroacetic acid.

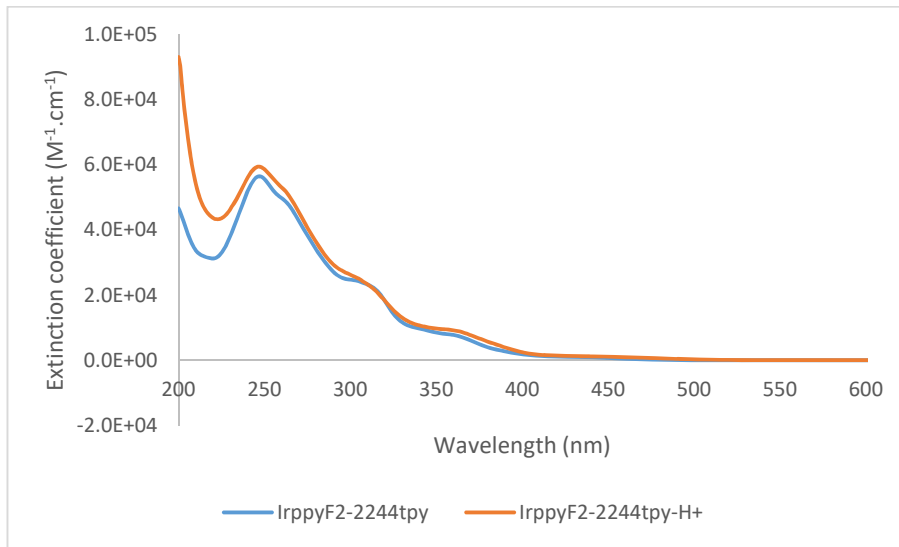


Figure S49. Absorption spectra for neutral (blue) and protonated (orange) IrppyF₂-2244tpy photosensitizer.

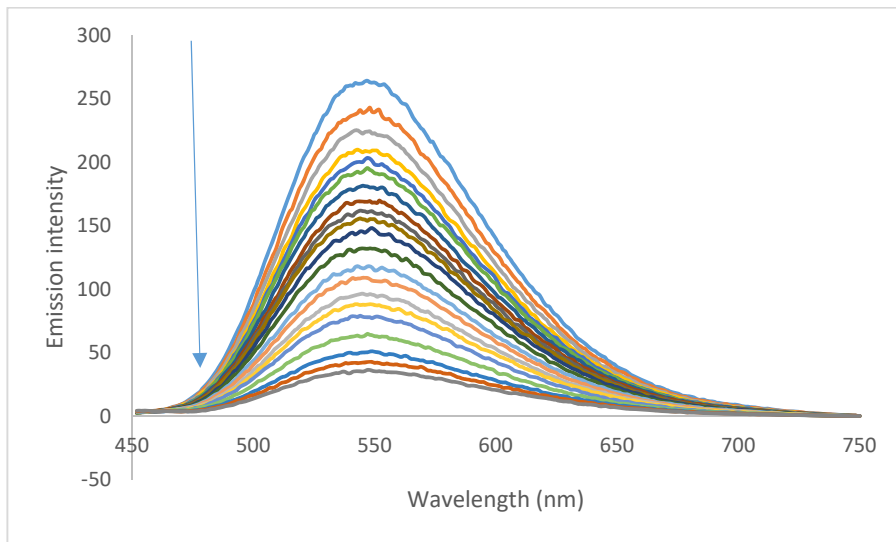


Figure S50. Emission spectral changes for a 2.5×10^{-5} mol. L^{-1} solution of IrppyF₂-2244tpy in acetonitrile for increasing concentrations of trifluoroacetic acid.

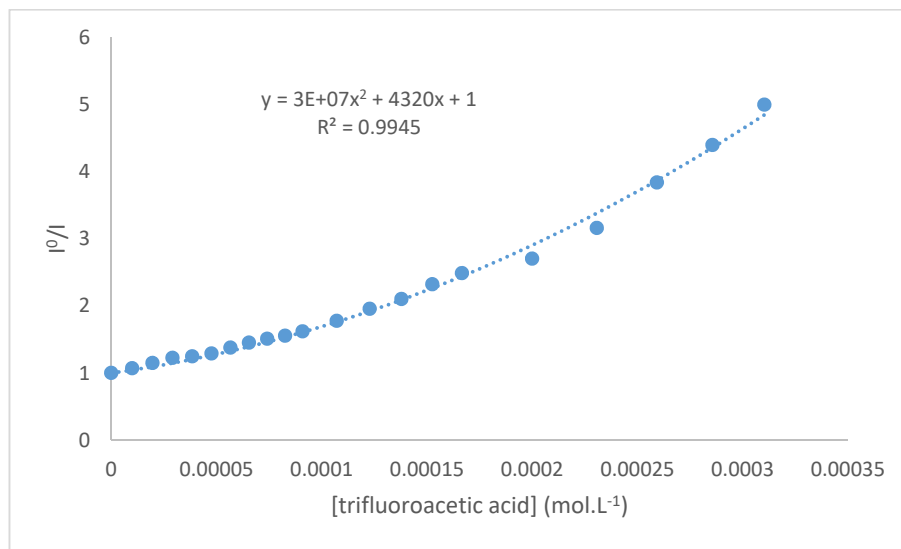


Figure S51. Stern-Volmer plots of the luminescence quenching of IrppyF₂-2244tpy upon the addition of trifluoroacetic acid.

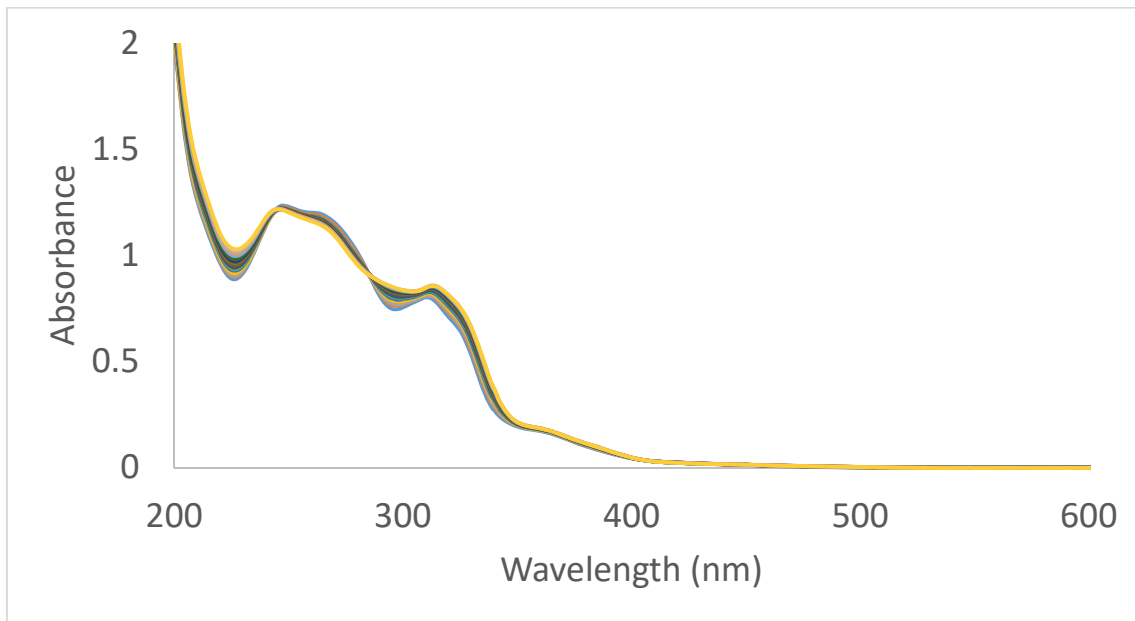


Figure S52. Absorption spectral changes for a 2.5×10^{-5} mol.L⁻¹ solution of IrppyF₂-2254tpy in acetonitrile for increasing concentrations of trifluoroacetic acid.

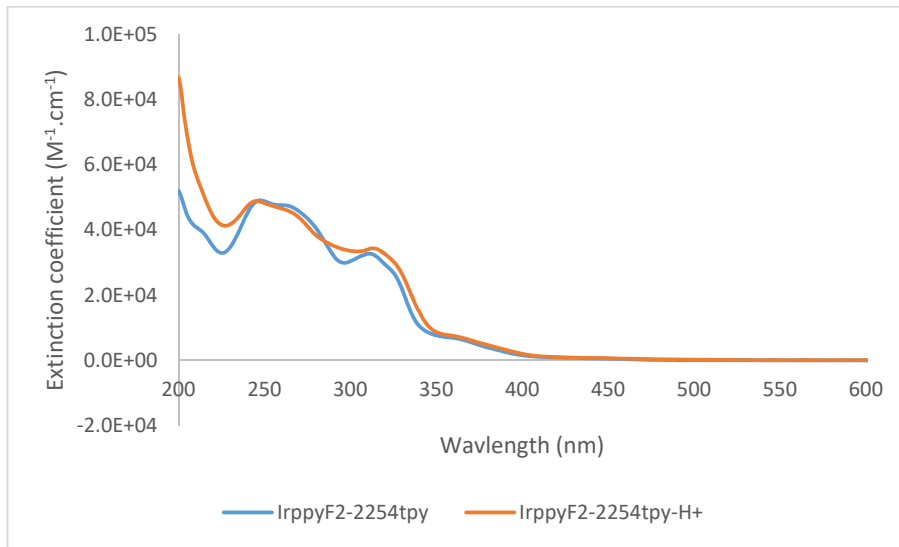


Figure S53. Absorption spectra for neutral (blue) and protonated (orange) IrppyF₂-2254tpy photosensitizer.

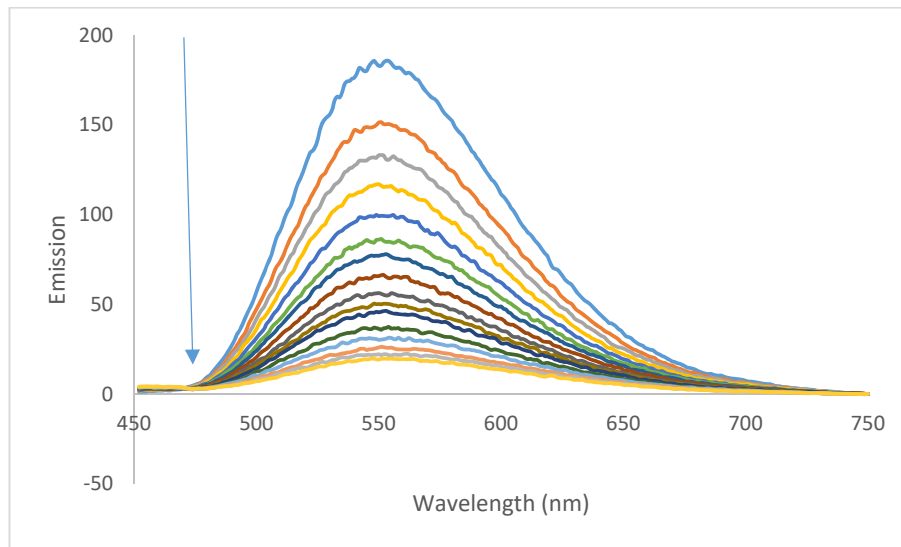


Figure S54. Emission spectral changes for a 2.5×10^{-5} mol. L⁻¹ solution of IrppyF₂-2254tpy in acetonitrile for increasing concentrations of trifluoroacetic acid.

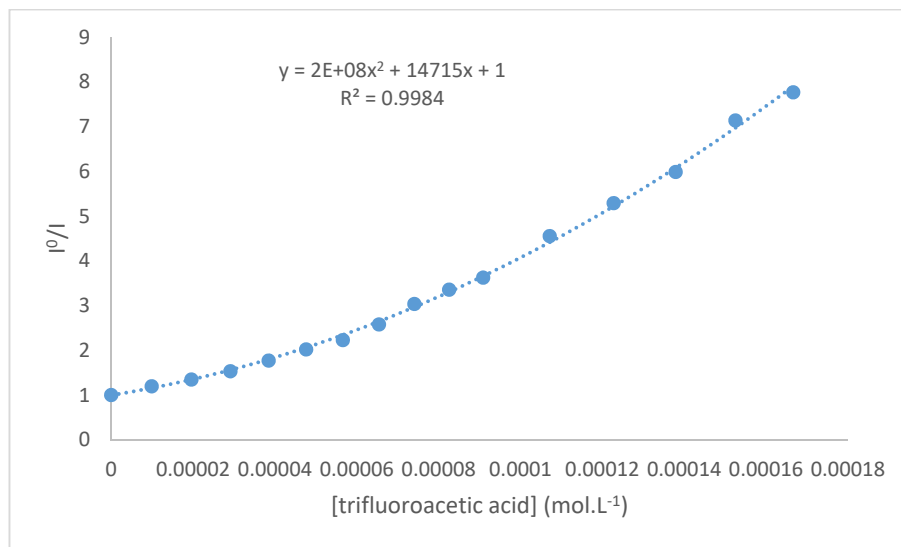


Figure S55. Stern-Volmer plots of the luminescence quenching of IrppyF₂-2254tpy upon the addition of trifluoroacetic acid.

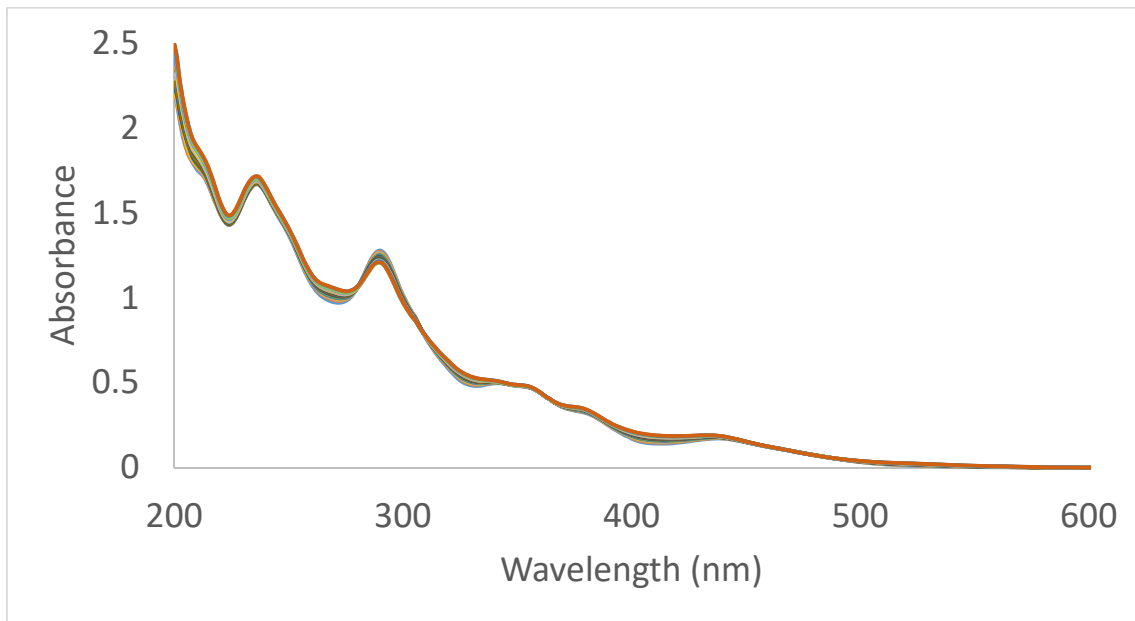


Figure S56. Absorption spectral changes for a 2.5×10^{-5} mol.L⁻¹ solution of Irpiq-2244tpy in acetonitrile for increasing concentrations of trifluoroacetic acid.

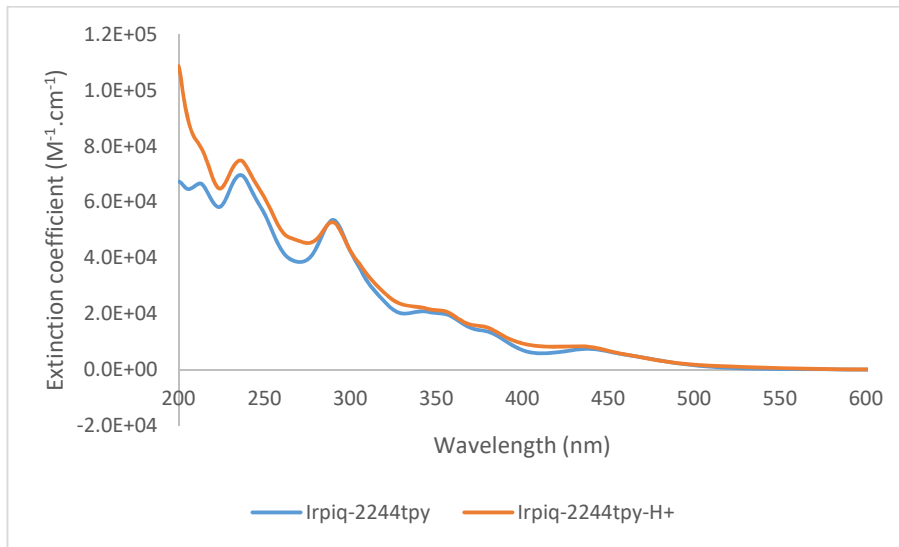


Figure S57. Absorption spectra for neutral (blue) and protonated (orange) Irpiq-2244tpy photosensitizer.

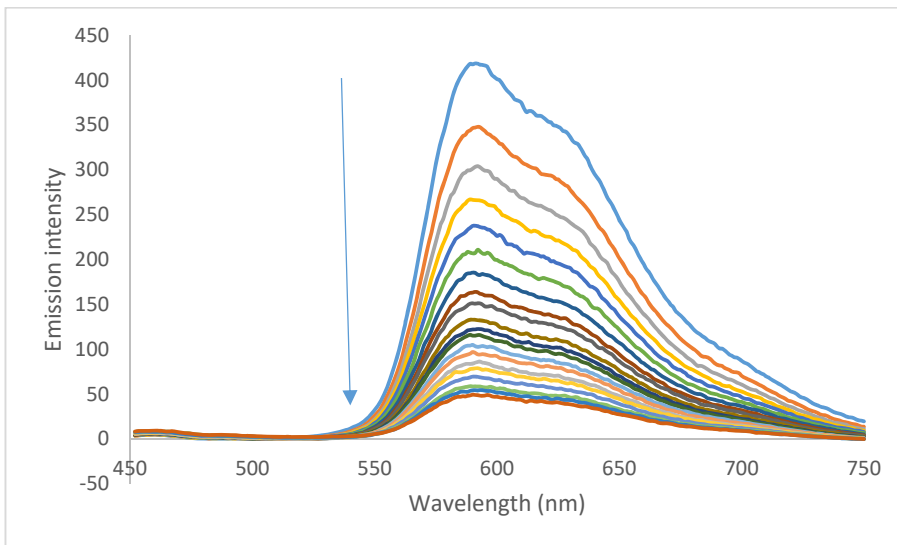


Figure S58. Emission spectral changes for a 2.5×10^{-5} mol.L $^{-1}$ solution of Irpiq-2244tpy in acetonitrile for increasing concentrations of trifluoroacetic acid.

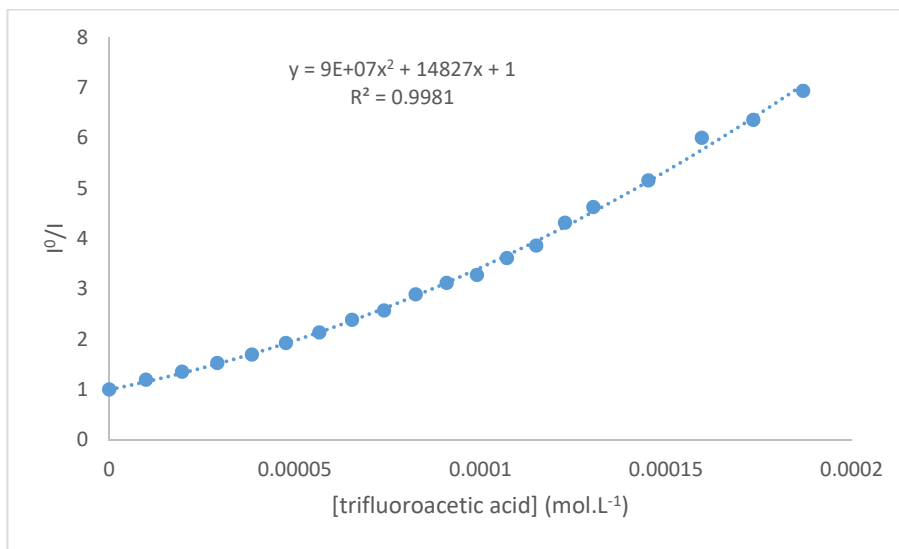


Figure S59. Stern-Volmer plots of the luminescence quenching of Irpiq-2244tpy upon the addition of trifluoroacetic acid.

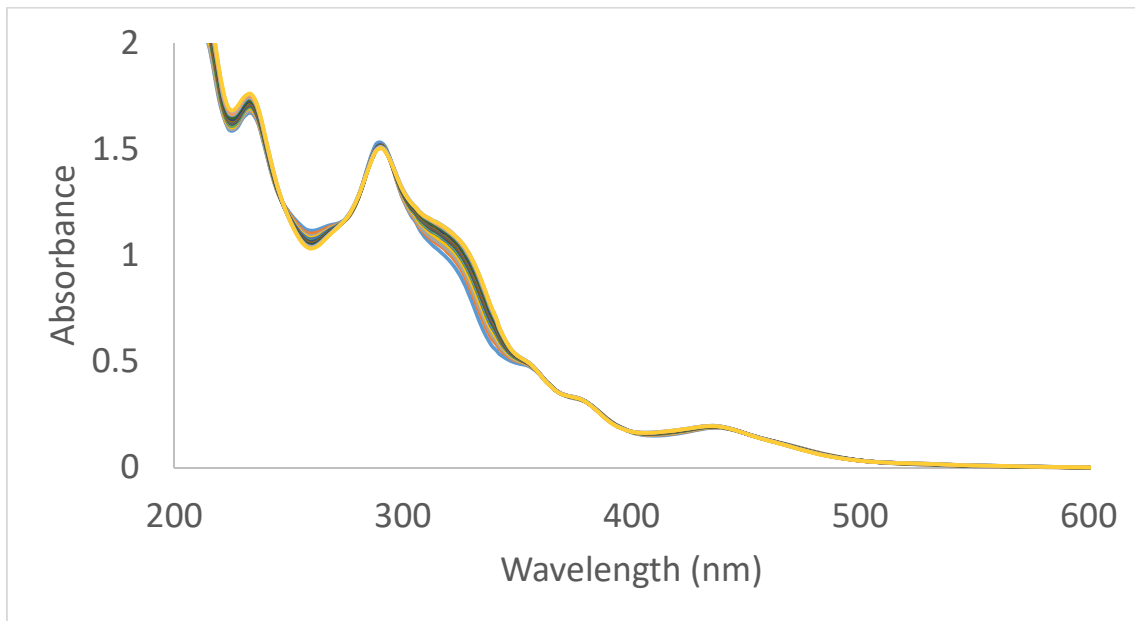


Figure S60. Absorption spectral changes for a 2.5×10^{-5} mol.L⁻¹ solution of Irpiq-2254tpy in acetonitrile for increasing concentrations of trifluoroacetic acid.

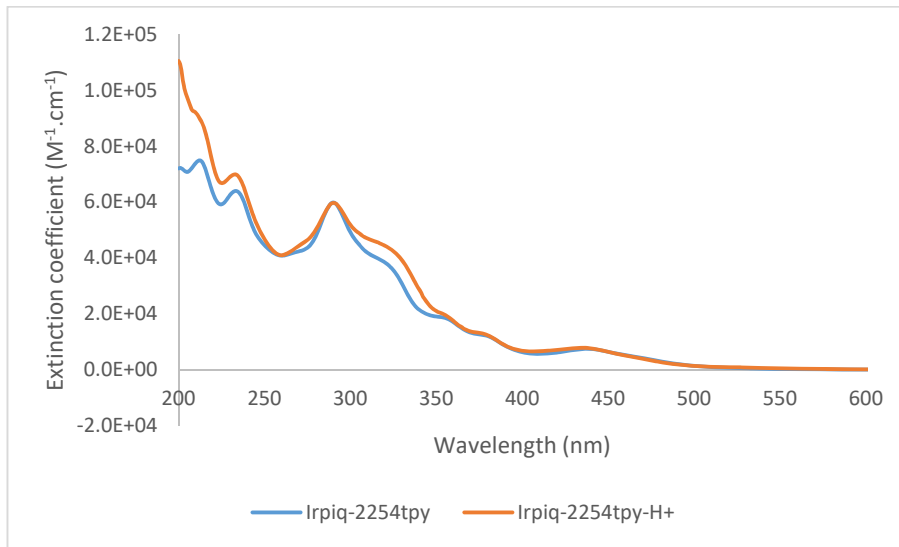


Figure S61. Absorption spectra for neutral (blue) and protonated (orange) Irpiq-2254tpy photosensitizer.

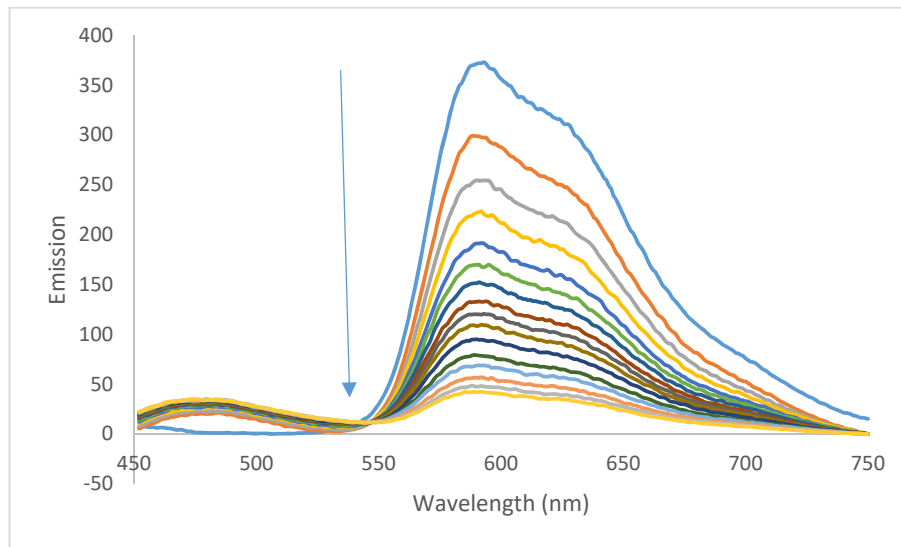


Figure S62. Emission spectral changes for a 2.5×10^{-5} mol.L⁻¹ solution of Irpiq-2254tpy in acetonitrile for increasing concentrations of trifluoroacetic acid.

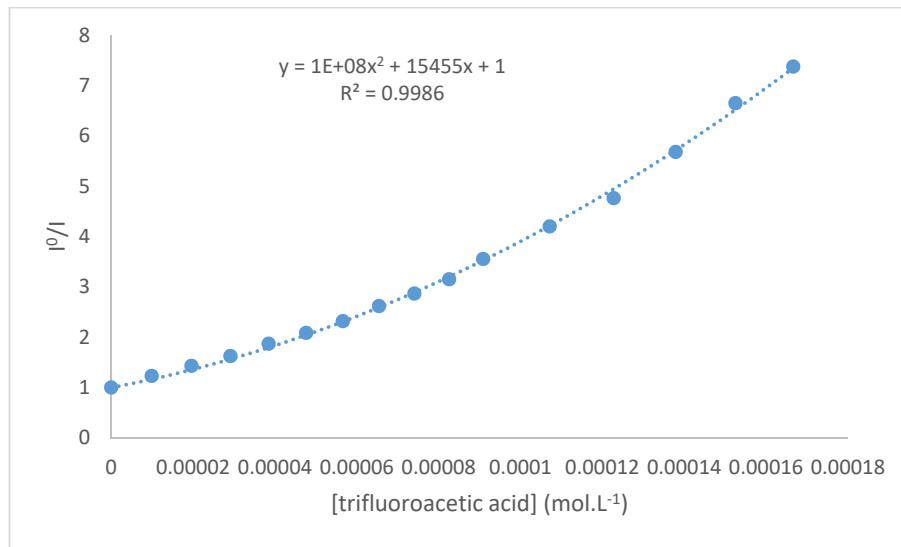


Figure S63. Stern-Volmer plots of the luminescence quenching of Irpiq-2254tpy upon the addition of trifluoroacetic acid.

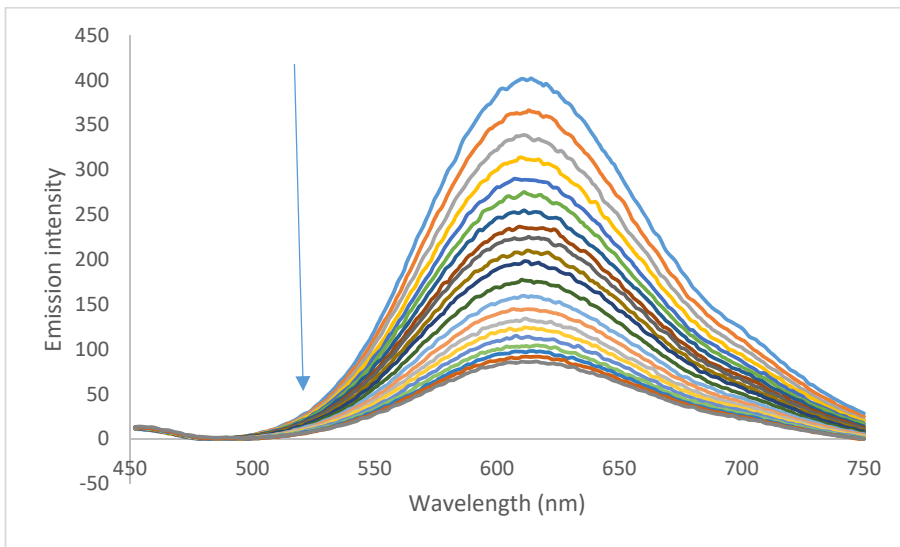


Figure S64. Emission spectral changes for a 2.5×10^{-5} mol.L⁻¹ solution of Irppy-2244tpy in acetonitrile for increasing concentrations of acetic acid.

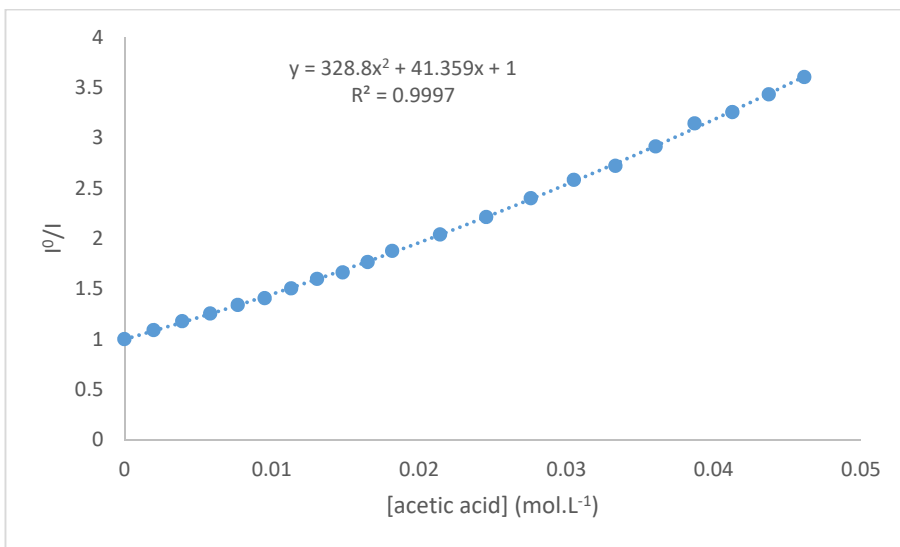


Figure S65. Stern-Volmer plots of the luminescence quenching of Irppy-2244tpy upon the addition of acetic acid.

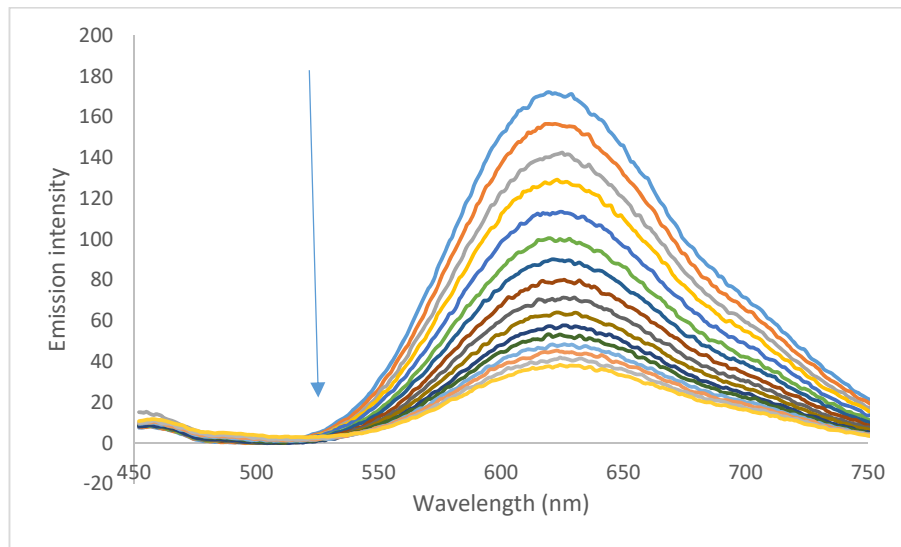


Figure S66. Emission spectral changes for a 2.5×10^{-5} mol.L $^{-1}$ solution of Irppy-2254tpy in acetonitrile for increasing concentrations of acetic acid.

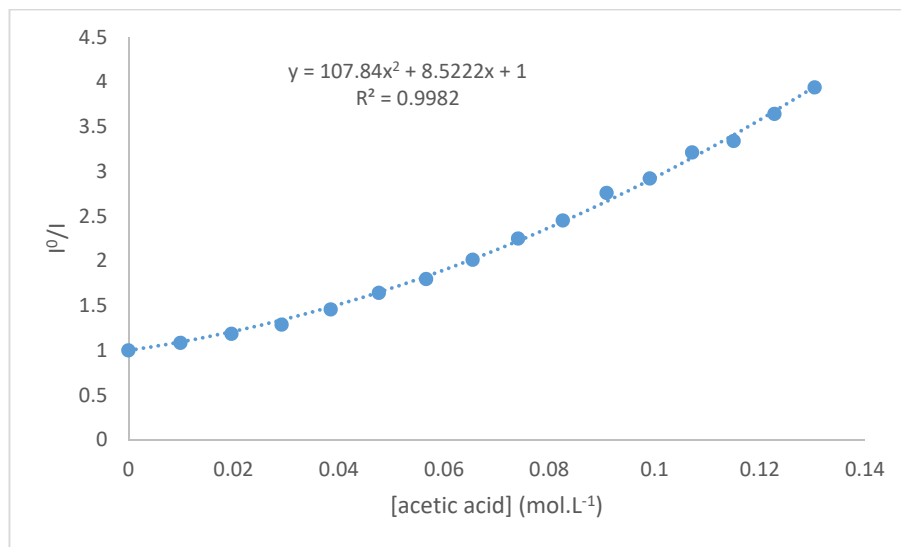


Figure S67. Stern-Volmer plots of the luminescence quenching of Irppy-2254tpy upon the addition of acetic acid.

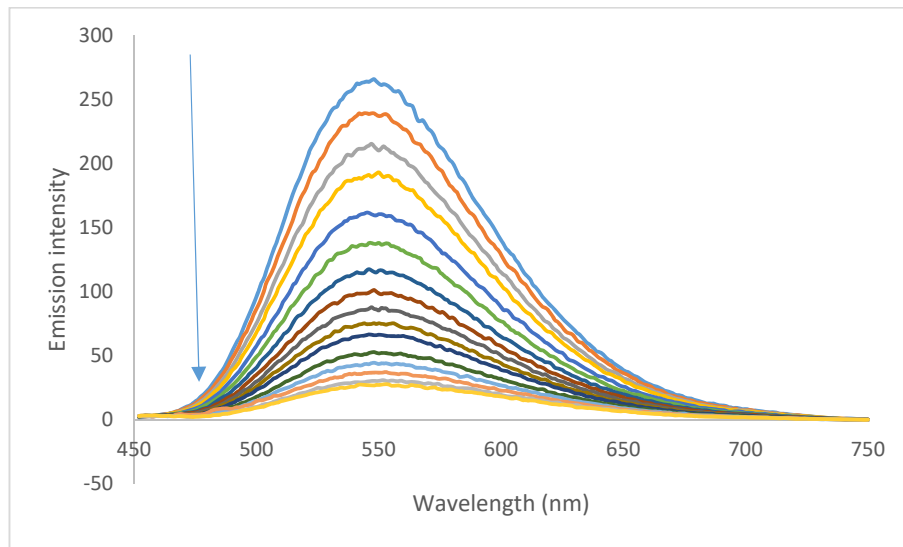


Figure S68. Emission spectral changes for a 2.5×10^{-5} mol.L⁻¹ solution of IrppyF₂-2244tpy in acetonitrile for increasing concentrations of acetic acid.

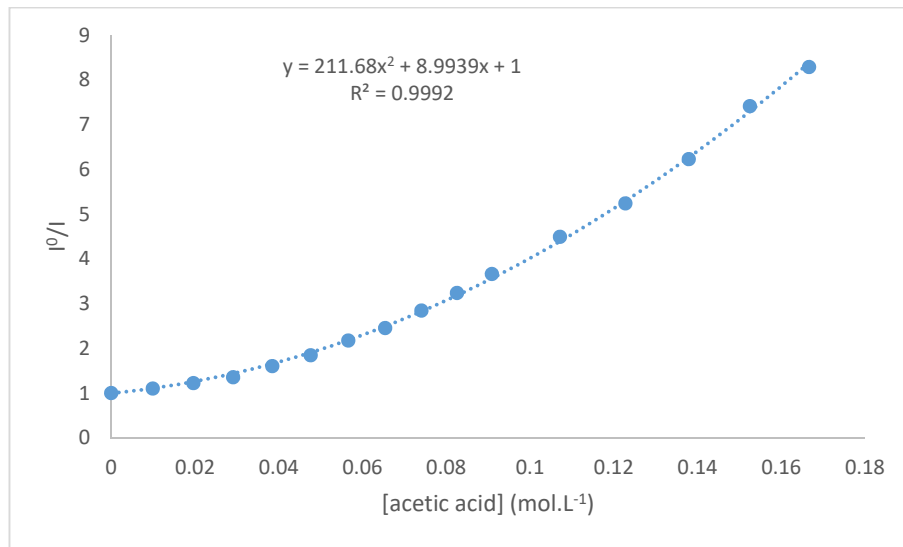


Figure S69. Stern-Volmer plots of the luminescence quenching of IrppyF₂-2244tpy upon the addition of acetic acid.

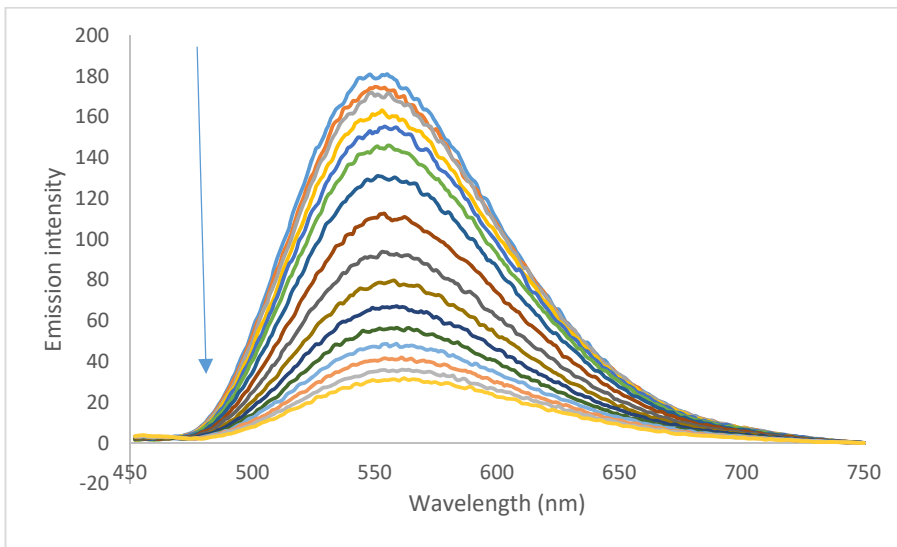


Figure S70. Emission spectral changes for a 2.5×10^{-5} mol.L $^{-1}$ solution of IrppyF₂-2254tpy in acetonitrile for increasing concentrations of acetic acid.

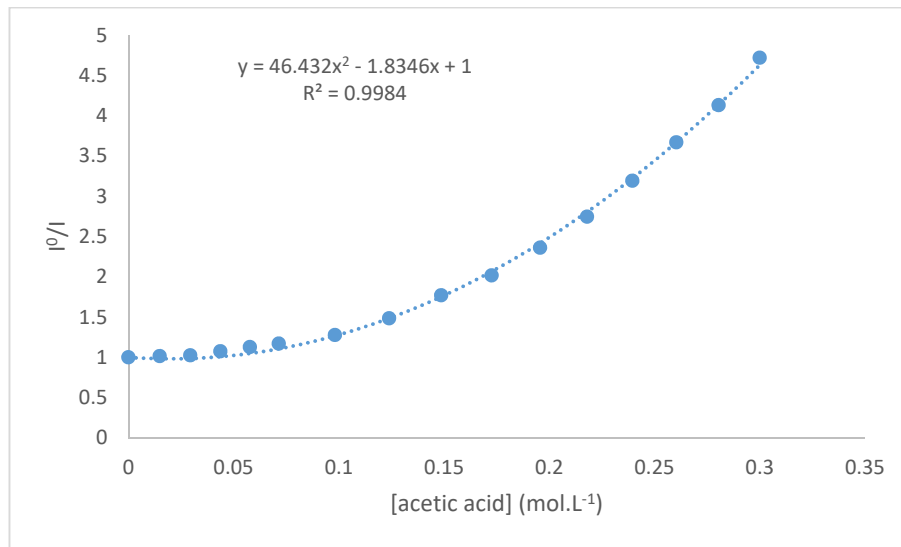


Figure S71. Stern-Volmer plots of the luminescence quenching of IrppyF₂-2254tpy upon the addition of acetic acid.

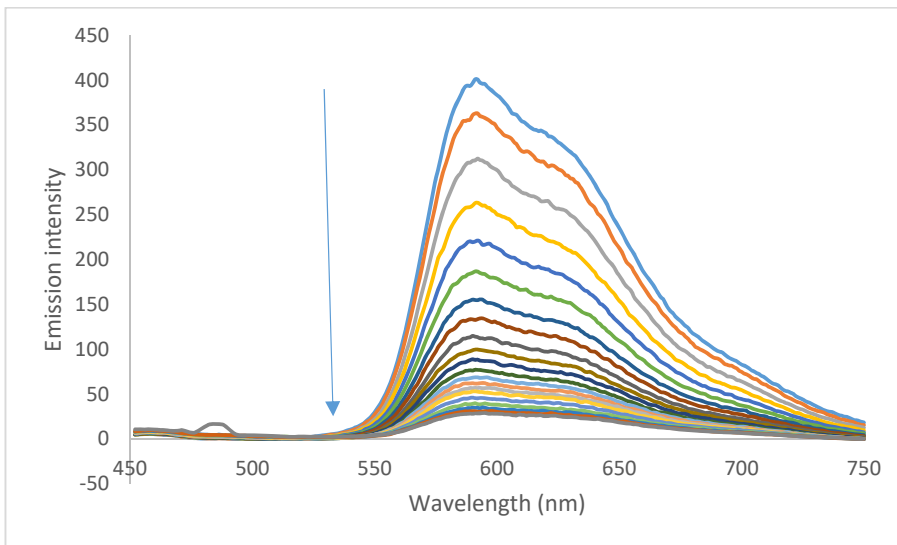


Figure S72. Emission spectral changes for a 2.5×10^{-5} mol·L⁻¹ solution of Irpiq-2244tpy in acetonitrile for increasing concentrations of acetic acid.

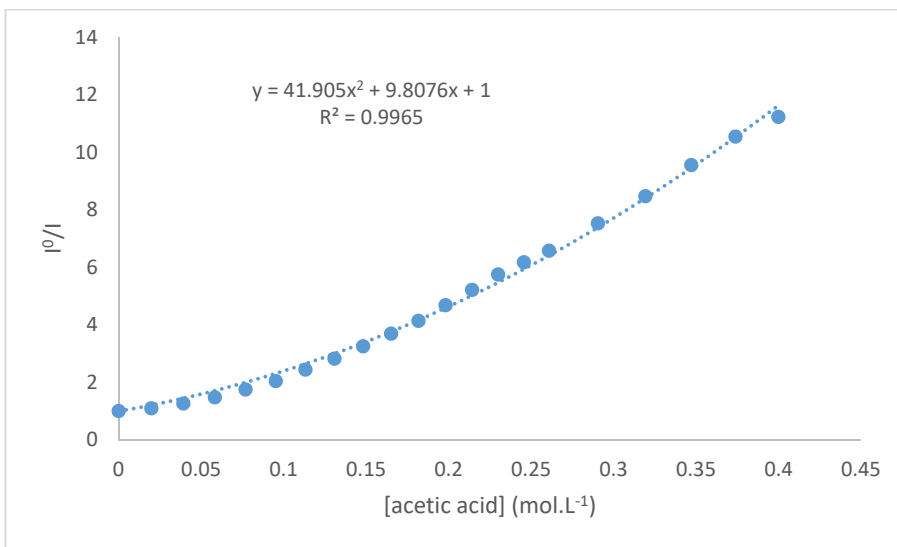


Figure S73. Stern-Volmer plots of the luminescence quenching of Irpiq-2244tpy upon the addition of acetic acid.

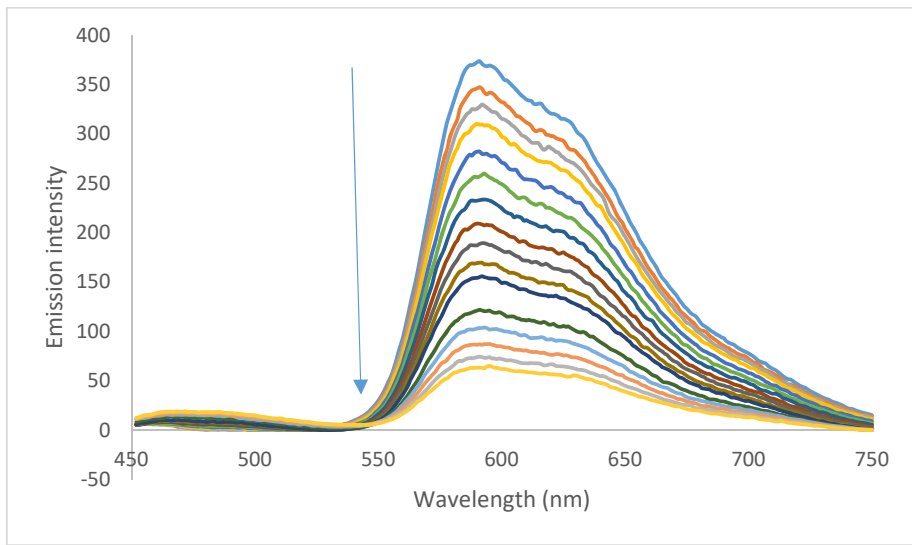


Figure S74. Emission spectral changes for a 2.5×10^{-5} mol.L $^{-1}$ solution of Irpiq-2254tpy in acetonitrile for increasing concentrations of acetic acid.

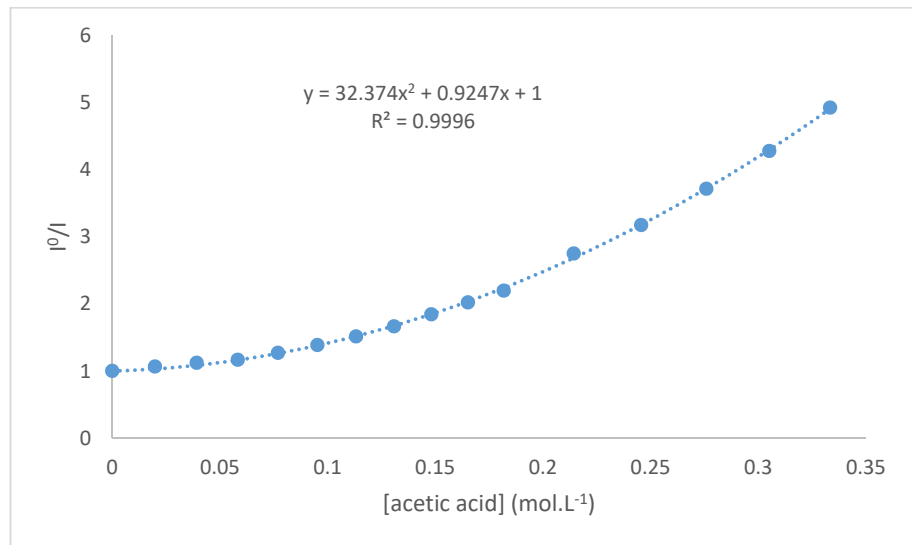


Figure S75. Stern-Volmer plots of the luminescence quenching of Irpiq-2254tpy upon the addition of acetic acid.

Theoretical model

All Ir compounds were studied by DFT and TD-DFT using Gaussian9 Revision E.01.¹¹ We used B3LYP¹² and two basis set (6-31G*¹³ for C, H, and N / VDZ (valence double ζ) with the SBKJC effective core potential¹⁴ basis set for Ir). Geometry optimizations were conducted without symmetry constraints, followed by frequency calculations to confirm that energy minima had been reached. The energy, oscillator strength, and related MO contributions for the 100 lowest singlet–singlet and 10 lowest singlet–triplet excitations were obtained from the TD-DFT/singlets and the TD-DFT/triplets output files, respectively, for the S0-optimized geometry. GaussView5.0, GaussSum3.0¹⁵ and Chem3DPro4.43¹⁶ were used for data analysis, visualization and surface plots. All calculations were performed in MeCN solution by use of the polarized continuum (PCM) solvation model.¹⁷

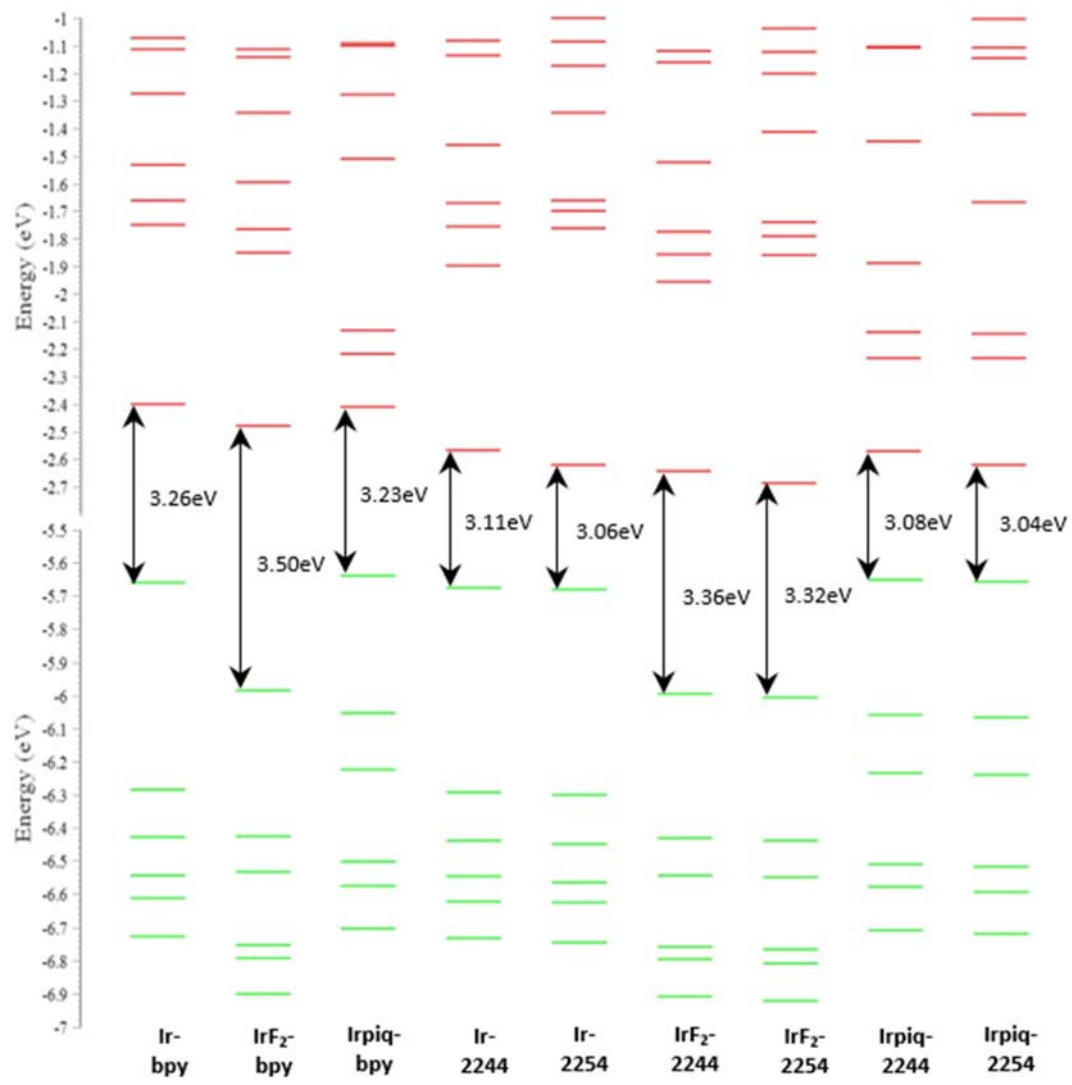


Figure S76. Molecular orbitals diagram of the different cyclometalated iridium complexes studied (green : HOMOs, red : LUMOs)

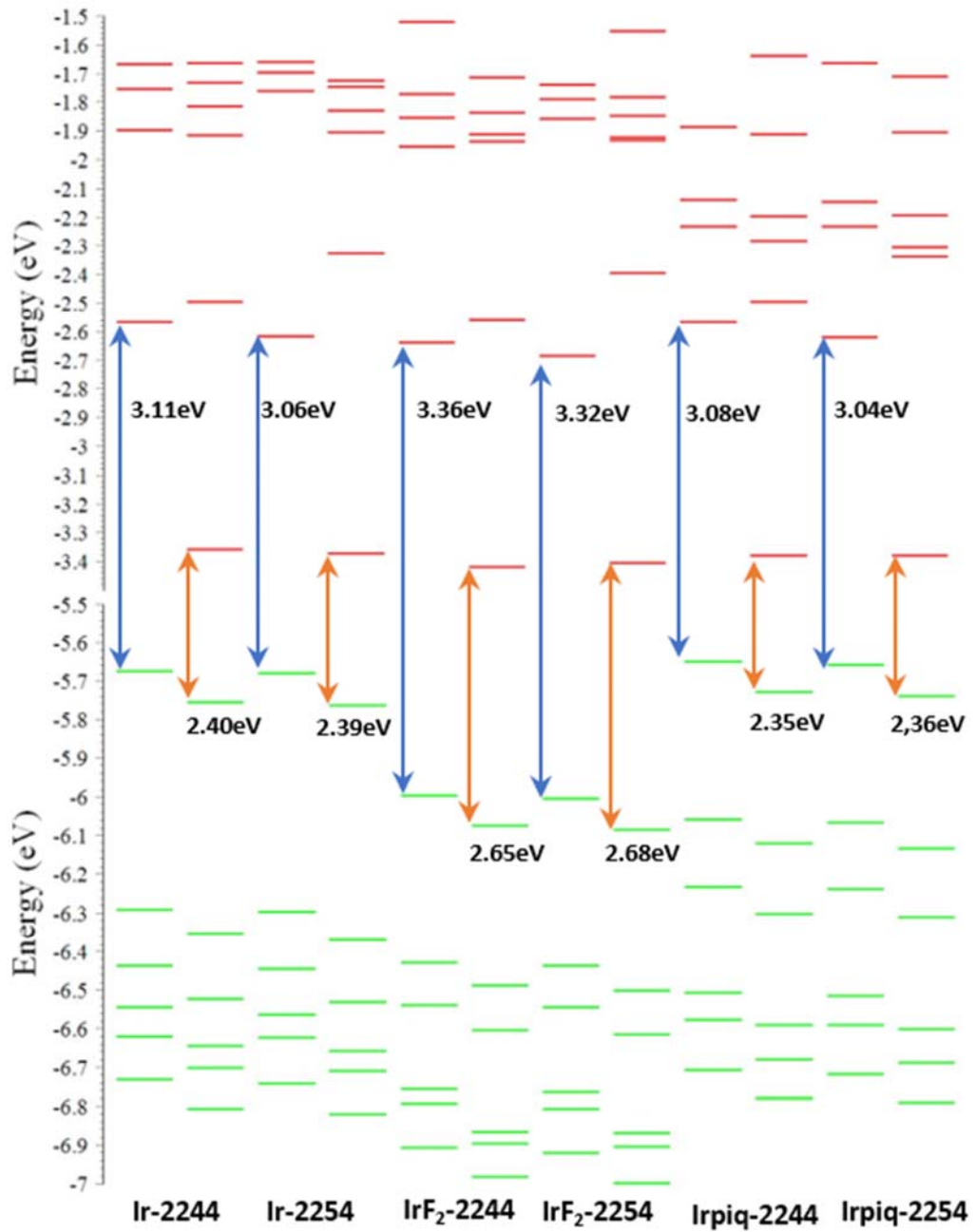


Figure S77. Effect of the protonation on the orbitals of the different cyclometalated iridium complexes studied (green : HOMOs, red : LUMOs / left with blue arrow : free form, right with orange arrow : protonated form)

Table S6. Contributions to MOs for Irppy-bpy (isovalue : 0.03 e. \AA^{-3})

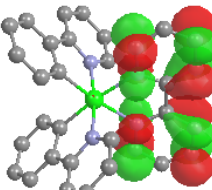
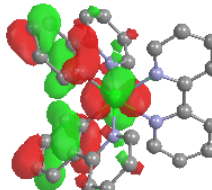
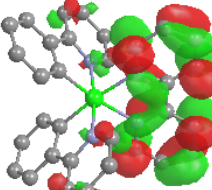
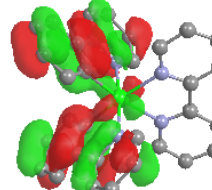
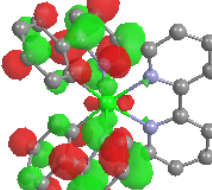
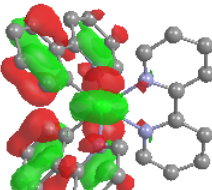
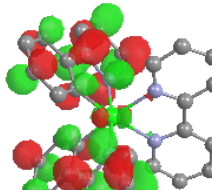
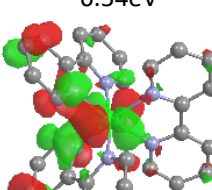
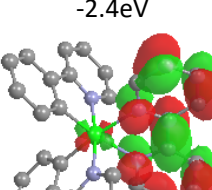
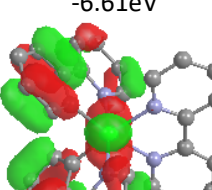
Orbital	Contributions	Orbital	Contributions
LUMO+4 -1.27eV 	Ir : 1% ppy : 2% bpy : 97%	HOMO -5.66eV 	Ir : 40% ppy : 58% bpy : 2%
LUMO+3 -1.53eV 	Ir : 1% ppy : 15% bpy : 83%	HOMO-1 -6.28eV 	Ir : 8% ppy : 91% bpy : 1%
LUMO+2 -1.66eV 	Ir : 4% ppy : 94% bpy : 2%	HOMO-2 -6.43eV 	Ir : 48% ppy : 49% bpy : 4%
LUMO+1 -1.75eV 	Ir : 2% ppy : 95% bpy : 1%	HOMO-3 -6.54eV 	Ir : 48% ppy : 45% bpy : 7%
LUMO -2.4eV 	Ir : 2% ppy : 1% bpy : 97%	HOMO-4 -6.61eV 	Ir : 30% ppy : 67% bpy : 3%

Table S7. Contributions to MOs for IrppyF₂-bpy (isovalue : 0.03 e. \AA^{-3})

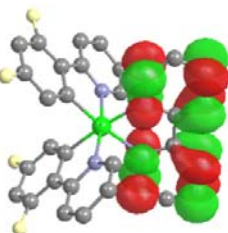
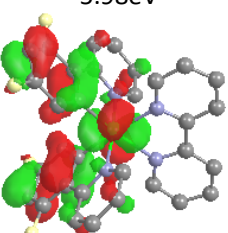
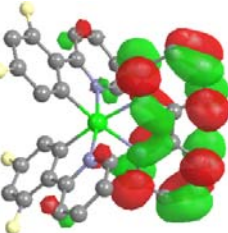
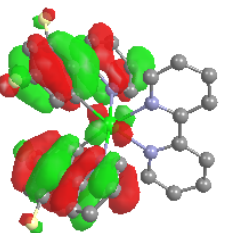
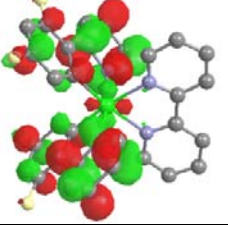
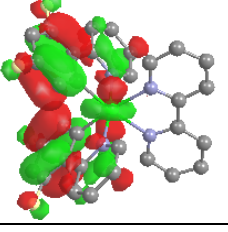
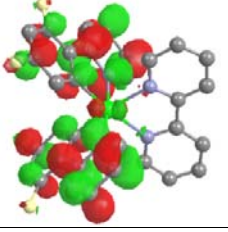
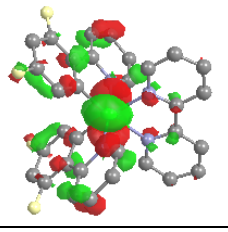
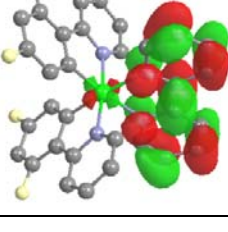
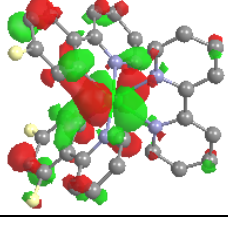
Orbital	Contributions	Orbital	Contributions
LUMO+4 -1.34eV 	Ir : 0% F ₂ ppy : 2% bpy : 98%	HOMO -5.98eV 	Ir : 38% F ₂ ppy : 60% bpy : 2%
LUMO+3 -1.59eV 	Ir : 2% F ₂ ppy : 13% bpy : 85%	HOMO-1 -6.42eV 	Ir : 6% F ₂ ppy : 93% bpy : 1%
LUMO+2 -1.77eV 	Ir : 4% F ₂ ppy : 94% bpy : 2%	HOMO-2 -6.53eV 	Ir : 15% F ₂ ppy : 84% bpy : 1%
LUMO+1 -1.85eV 	Ir : 4% F ₂ ppy : 95% bpy : 1%	HOMO-3 -6.75eV 	Ir : 62% F ₂ ppy : 31% bpy : 7%
LUMO -2.48eV 	Ir : 2% F ₂ ppy : 1% bpy : 97%	HOMO-4 -6.79eV 	Ir : 51% F ₂ ppy : 41% bpy : 8%

Table S8. Contributions to MOs for Irpiq-bpy (isovalue : 0.03 e. \AA^{-3})

Orbital	Contributions	Orbital	Contributions
LUMO+4 -1.28eV 	Ir : 1% piq : 2% bpy : 97%	HOMO -5.64eV 	Ir : 37% piq : 62% bpy : 2%
LUMO+3 -1.51eV 	Ir : 2% piq : 10% bpy : 88%	HOMO-1 -6.05eV 	Ir : 10% piq : 89% bpy : 1%
LUMO+2 -2.13eV 	Ir : 3% piq : 96% bpy : 1%	HOMO-2 -6.22eV 	Ir : 27% piq : 72% bpy : 1%
LUMO+1 -2.22eV 	Ir : 4% piq : 91% bpy : 5%	HOMO-3 -6.5eV 	Ir : 36% piq : 59% bpy : 5%
LUMO -2.41eV 	Ir : 2% piq : 5% bpy : 93%	HOMO-4 -6.58eV 	Ir : 50% piq : 45% bpy : 5%

Table S9. Contributions to MOs for Irppy-2244tpy (isovalue : 0.03 e. \AA^{-3})

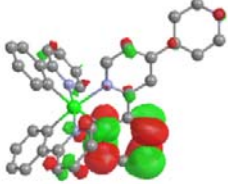
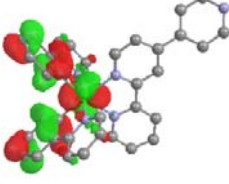
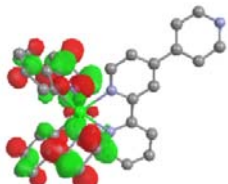
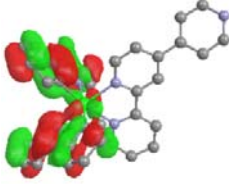
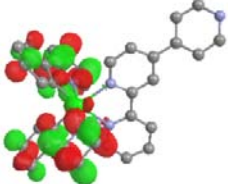
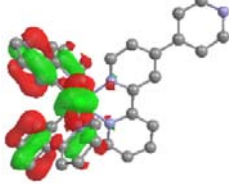
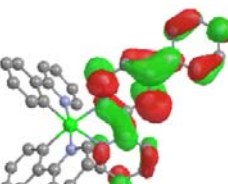
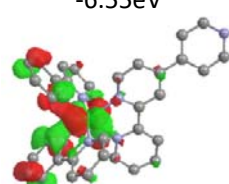
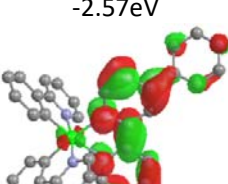
Orbital	Contributions	Orbital	Contributions
LUMO+4 -1.46eV 	Ir : 1% ppy : 13% 2244tpy : 86%	HOMO -5.68eV 	Ir : 39% ppy : 59% 2244tpy : 2%
LUMO+3 -1.67eV 	Ir : 4% ppy : 94% 2244tpy : 3%	HOMO-1 -6.29eV 	Ir : 8% ppy : 91% 2244tpy : 1%
LUMO+2 -1.76eV 	Ir : 4% ppy : 95% 2244tpy : 1%	HOMO-2 -6.44eV 	Ir : 47% ppy : 49% 2244tpy : 4%
LUMO+1 -1.9eV 	Ir : 2% ppy : 1% 2244tpy : 97%	HOMO-3 -6.55eV 	Ir : 47% ppy : 45% 2244tpy : 8%
LUMO -2.57eV 	Ir : 2% ppy : 1% 2244tpy : 97%	HOMO-4 -6.62eV 	Ir : 30% ppy : 66% 2244tpy : 4%

Table S10. Contributions to MOs for Irppy-2254tpy (isovalue : 0.03 e. \AA^{-3})

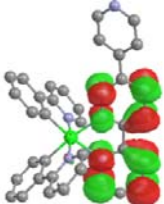
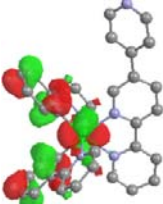
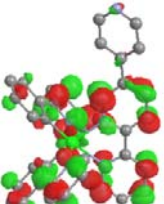
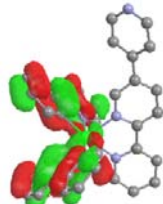
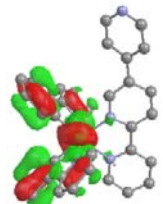
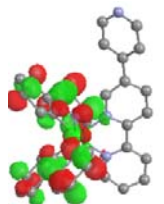
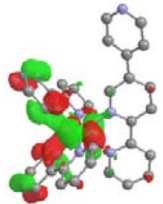
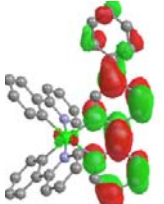
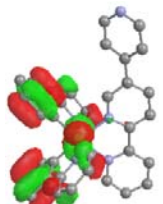
Orbital	Contributions	Orbital	Contribution
LUMO+4 -1.34eV 	Ir : 1% ppy : 3% 2254tpy : 96%	HOMO -5.68eV 	Ir : 39% ppy : 59% 2254tpy : 2%
LUMO+3 -1.66eV 	Ir : 3% ppy : 58% 2254tpy : 39%	HOMO-1 -6.3eV 	Ir : 8% ppy : 91% 2254tpy : 1%
LUMO+2 -1.7eV 	Ir : 3% ppy : 44% 2254tpy : 53%	HOMO-2 -6.45eV 	Ir : 46% ppy : 50% 2254tpy : 4%
LUMO+1 -1.76eV 	Ir : 4% ppy : 93% 2254tpy : 3%	HOMO-3 -6.56eV 	Ir : 46% ppy : 47% 2254tpy : 7%
LUMO -2.62eV 	Ir : 2% ppy : 1% 2254tpy : 98%	HOMO-4 -6.63eV 	Ir : 30% ppy : 65% 2254tpy : 5%

Table S11. Contributions to MOs for IrppyF₂-2244tpy (isovalue : 0.03 e. \AA^{-3})

Orbital	Contributions	Orbital	Contribution
LUMO+4 -1.52eV 	Ir : 1% F ₂ ppy : 10% 2244tpy : 88%	HOMO -6.00eV 	Ir : 38% F ₂ ppy : 60% 2244tpy : 2%
LUMO+3 -1.77eV 	Ir : 4% F ₂ ppy : 94% 2244tpy : 2%	HOMO-1 -6.43eV 	Ir : 6% F ₂ ppy : 93% 2244tpy : 1%
LUMO+2 -1.86eV 	Ir : 4% F ₂ ppy : 95% 2244tpy : 1%	HOMO-2 -6.54eV 	Ir : 15% F ₂ ppy : 84% 2244tpy : 1%
LUMO+1 -1.96eV 	Ir : 1% F ₂ ppy : 3% 2244tpy : 97%	HOMO-3 -6.76eV 	Ir : 60% F ₂ ppy : 31% 2244tpy : 9%
LUMO -2.64eV 	Ir : 2% F ₂ ppy : 1% 2244tpy : 97%	HOMO-4 -6.8eV 	Ir : 52% F ₂ ppy : 39% 2244tpy : 9%

Table S12.: Contributions to MOs for IrppyF₂-2254tpy (isovalue : 0.03 e. \AA^{-3})

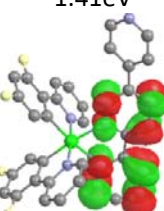
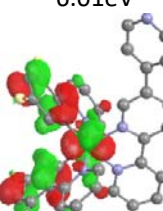
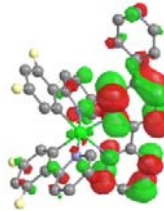
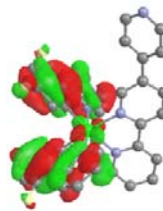
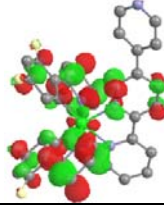
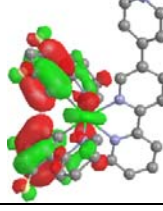
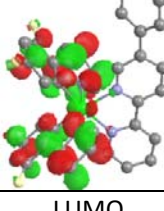
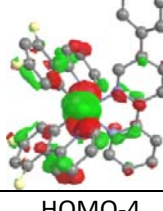
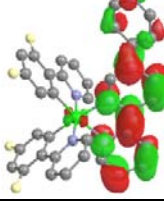
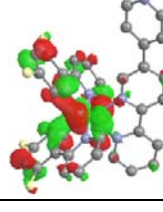
Orbital	Contributions	Orbital	Contribution
LUMO+4 -1.41eV 	Ir : 1% F ₂ ppy : 3% 2254tpy : 97%	HOMO -6.01eV 	Ir : 38% F ₂ ppy : 60% 2254tpy : 2%
LUMO+3 -1.74eV 	Ir : 2% F ₂ ppy : 20% 2254tpy : 78%	HOMO-1 -6.44eV 	Ir : 6% F ₂ ppy : 93% 2254tpy : 1%
LUMO+2 -1.79eV 	Ir : 4% F ₂ ppy : 80% 2254tpy : 16%	HOMO-2 -6.55eV 	Ir : 15% F ₂ ppy : 84% 2254tpy : 1%
LUMO+1 -1.86eV 	Ir : 4% F ₂ ppy : 95% 2254tpy : 1%	HOMO-3 -6.77eV 	Ir : 60% F ₂ ppy : 29% 2254tpy : 10%
LUMO -2.69eV 	Ir : 2% F ₂ ppy : 1% 2254tpy : 98%	HOMO-4 -6.81eV 	Ir : 48% F ₂ ppy : 45% 2254tpy : 8%

Table S13. Contributions to MOs for Irpiq-2244tpy (isovalue : 0.03 e. \AA^{-3})

Orbital	Contributions	Orbital	Contribution
LUMO+4 -1.45eV 	Ir : 1% piq : 9% 2244tpy : 90%	HOMO -5.65eV 	Ir : 36% piq : 62% 2244tpy : 2%
LUMO+3 -1.89eV 	Ir : 1% piq : 3% 2244tpy : 97%	HOMO-1 -6.06eV 	Ir : 10% piq : 89% 2244tpy : 1%
LUMO+2 -2.14eV 	Ir : 3% piq : 95% 2244tpy : 1%	HOMO-2 -6.23eV 	Ir : 26% piq : 72% 2244tpy : 2%
LUMO+1 -2.23eV 	Ir : 4% piq : 94% 2244tpy : 2%	HOMO-3 -6.51eV 	Ir : 36% piq : 59% 2244tpy : 6%
LUMO -2.57eV 	Ir : 2% piq : 2% 2244tpy : 96%	HOMO-4 -6.58eV 	Ir : 49% piq : 44% 2244tpy : 6%

Table S14. Contributions to MOs for Irpiq-2254tpy (isovalue : 0.03 e. \AA^{-3})

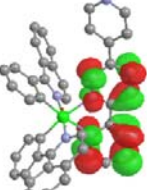
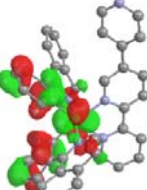
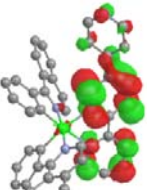
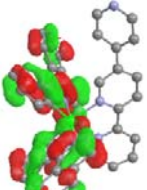
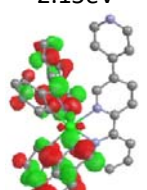
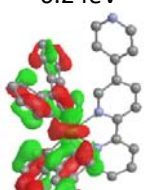
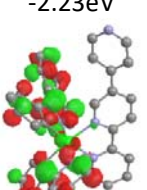
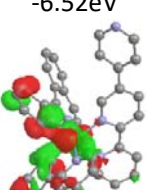
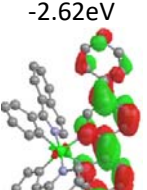
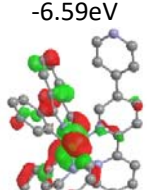
Orbital	Contributions	Orbital	Contribution
LUMO+4 -1.35eV 	Ir : 1% piq : 3% 2254tpy : 96%	HOMO -5.66eV 	Ir : 36% piq : 62% 2254tpy : 2%
LUMO+3 -1.67eV 	Ir : 2% piq : 5% 2254tpy : 93%	HOMO-1 -6.07eV 	Ir : 10% piq : 89% 2254tpy : 1%
LUMO+2 -2.15eV 	Ir : 3% piq : 85% 2254tpy : 11%	HOMO-2 -6.24eV 	Ir : 26% piq : 72% 2254tpy : 2%
LUMO+1 -2.23eV 	Ir : 4% piq : 94% 2254tpy : 2%	HOMO-3 -6.52eV 	Ir : 35% piq : 59% 2254tpy : 5%
LUMO -2.62eV 	Ir : 2% piq : 2% 2254tpy : 97%	HOMO-4 -6.59eV 	Ir : 50% piq : 44% 2254tpy : 6%

Table S15. Contributions to MOs for the protonated form of Irppy-2244tpy (isovalue : 0.03 e. \AA^{-3})

Orbital	Contributions	Orbital	Contribution
LUMO+4 -1.73eV 	Ir : 4% ppy : 94% H-2244tpy : 2%	HOMO -5.76eV 	Ir : 39% ppy : 59% H-2244tpy : 2%
LUMO+3 -1.82eV 	Ir : 4% ppy : 94% H-2244tpy : 2%	HOMO-1 -6.36eV 	Ir : 6% ppy : 93% H-2244tpy : 1%
LUMO+2 -1.92eV 	Ir : 0% ppy : 2% H-2244tpy : 98%	HOMO-2 -6.52eV 	Ir : 36% ppy : 61% H-2244tpy : 3%
LUMO+1 -2.5eV 	Ir : 1% ppy : 3% H-2244tpy : 96%	HOMO-3 -6.65eV 	Ir : 39% ppy : 55% H-2244tpy : 6%
LUMO -3.36eV 	Ir : 2% ppy : 14% H-2244tpy : 85%	HOMO-4 -6.7eV 	Ir : 41% ppy : 55% H-2244tpy : 4%

Table S16. Contributions to MOs for the protonated form of Irppy-2254tpy (isovalue : 0.03 e. \AA^{-3})

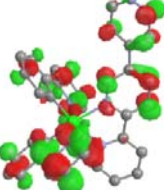
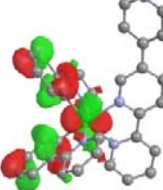
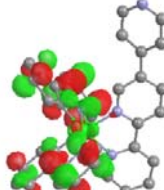
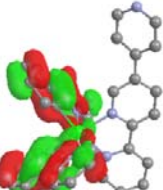
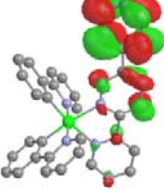
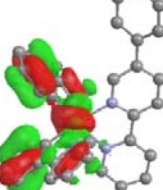
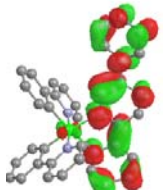
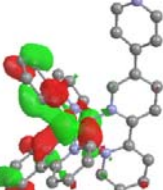
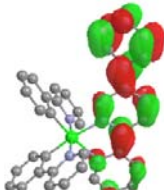
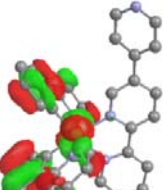
Orbital	Contributions	Orbital	Contribution
LUMO+4 -1.75eV 	Ir : 3% ppy : 69% H-2254tpy : 28%	HOMO -5.76eV 	Ir : 39% ppy : 59% H-2254tpy : 2%
LUMO+3 -1.83eV 	Ir : 4% ppy : 92% H-2254tpy : 4%	HOMO-1 -6.37eV 	Ir : 7% ppy : 92% H-2254tpy : 1%
LUMO+2 -1.91eV 	Ir : 0% ppy : 4% H-2254tpy : 96%	HOMO-2 -6.53eV 	Ir : 38% ppy : 59% H-2254tpy : 3%
LUMO+1 -2.33eV 	Ir : 2% ppy : 6% H-2254tpy : 91%	HOMO-3 -6.66eV 	Ir : 41% ppy : 53% H-2254tpy : 6%
LUMO -3.37eV 	Ir : 1% ppy : 12% H-2254tpy : 87%	HOMO-4 -6.71eV 	Ir : 40% ppy : 57% H-2254tpy : 3%

Table S17. Contributions to MOs for the protonated form of IrppyF₂-2244tpy (isovalue : 0.03 e. \AA^{-3})

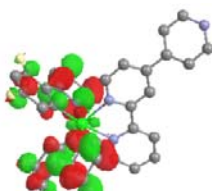
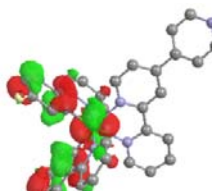
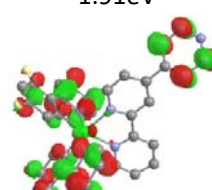
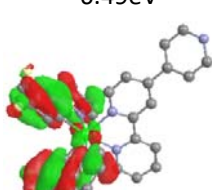
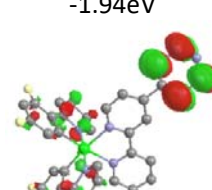
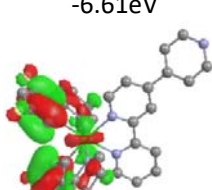
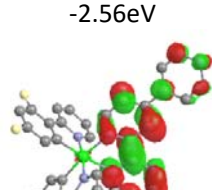
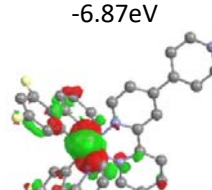
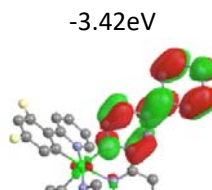
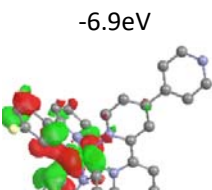
Orbital	Contributions	Orbital	Contribution
LUMO+4 -1.84eV 	Ir : 4% F ₂ ppy : 94% H-2244tpy : 2%	HOMO -6.07eV 	Ir : 37% F ₂ ppy : 61% H-2244tpy : 2%
LUMO+3 -1.91eV 	Ir : 3% F ₂ ppy : 72% H-2244tpy : 25%	HOMO-1 -6.49eV 	Ir : 5% F ₂ ppy : 94% H-2244tpy : 1%
LUMO+2 -1.94eV 	Ir : 1% F ₂ ppy : 24% H-2244tpy : 75%	HOMO-2 -6.61eV 	Ir : 12% F ₂ ppy : 87% H-2244tpy : 1%
LUMO+1 -2.56eV 	Ir : 1% F ₂ ppy : 3% H-2244tpy : 96%	HOMO-3 -6.87eV 	Ir : 66% F ₂ ppy : 28% H-2244tpy : 6%
LUMO -3.42eV 	Ir : 2% F ₂ ppy : 13% H-2244tpy : 85%	HOMO-4 -6.9eV 	Ir : 37% F ₂ ppy : 57% H-2244tpy : 6%

Table S18. Contributions to MOs for the protonated form of IrppyF₂-2254tpy (isovalue : 0.03 e. \AA^{-3})

Orbital	Contributions	Orbital	Contribution
LUMO+4 -1.85eV 	Ir : 4% F ₂ ppy : 91% H-2254tpy : 6%	HOMO -6.09eV 	Ir : 37% F ₂ ppy : 61% H-2254tpy : 2%
LUMO+3 -1.92eV 	Ir : 3% F ₂ ppy : 64% H-2254tpy : 33%	HOMO-1 -6.5eV 	Ir : 5% F ₂ ppy : 94% H-2254tpy : 1%
LUMO+2 -1.94eV 	Ir : 2% F ₂ ppy : 34% H-2254tpy : 64%	HOMO-2 -6.62eV 	Ir : 12% F ₂ ppy : 87% H-2254tpy : 1%
LUMO+1 -2.39eV 	Ir : 2% F ₂ ppy : 6% H-2254tpy : 91%	HOMO-3 -6.87eV 	Ir : 65% F ₂ ppy : 29% H-2254tpy : 6%
LUMO -3.41eV 	Ir : 1% F ₂ ppy : 12% H-2254tpy : 88%	HOMO-4 -6.91eV 	Ir : 40% F ₂ ppy : 54% H-2254tpy : 6%

Table S19. Contributions to MOs for the protonated form of Irpiq-2244tpy (isovalue : 0.03 e. \AA^{-3})

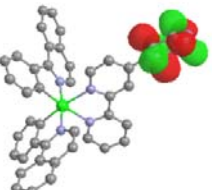
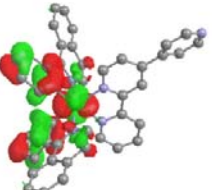
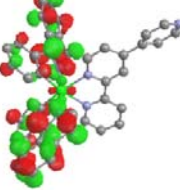
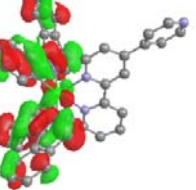
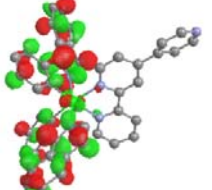
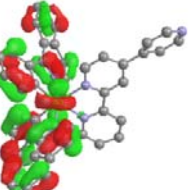
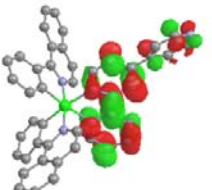
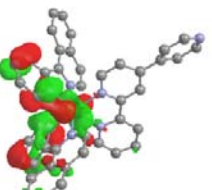
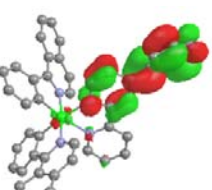
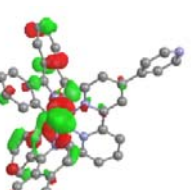
Orbital	Contributions	Orbital	Contribution
LUMO+4 -1.91eV 	Ir : 0% piq : 0% H-2244tpy : 100%	HOMO -5.73eV 	Ir : 35% piq : 63% H-2244tpy : 2%
LUMO+3 -2.2eV 	Ir : 3% piq : 1% H-2244tpy : 96%	HOMO-1 -6.12eV 	Ir : 8% piq : 91% H-2244tpy : 1%
LUMO+2 -2.28eV 	Ir : 4% piq : 92% H-2244tpy : 4%	HOMO-2 -6.3eV 	Ir : 23% piq : 76% H-2244tpy : 2%
LUMO+1 -2.5eV 	Ir : 1% piq : 4% H-2244tpy : 95%	HOMO-3 -6.59eV 	Ir : 31% piq : 64% H-2244tpy : 5%
LUMO -3.38eV 	Ir : 2% piq : 0% H-2244tpy : 98%	HOMO-4 -6.68eV 	Ir : 52% piq : 43% H-2244tpy : 5%

Table S20.: Contributions to MOs for the protonated form of Irpiq-2254tpy (isovalue : 0.03 e. \AA^{-3})

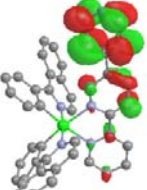
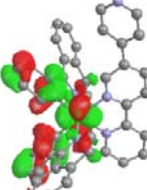
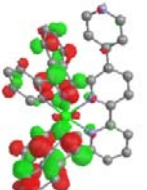
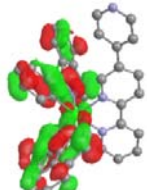
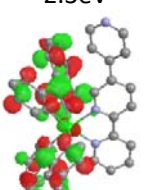
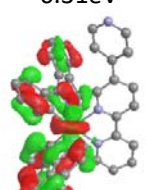
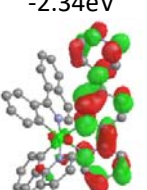
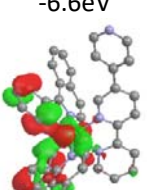
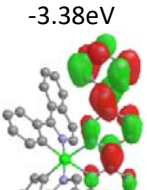
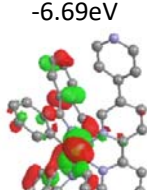
Orbital	Contributions	Orbital	Contribution
LUMO+4 -1.91eV 	Ir : 0% piq : 2% H-2254tpy : 98%	HOMO -5.74eV 	Ir : 36% piq : 63% H-2254tpy : 2%
LUMO+3 -2.2eV 	Ir : 3% piq : 89% H-2254tpy : 8%	HOMO-1 -6.13eV 	Ir : 8% piq : 91% H-2254tpy : 1%
LUMO+2 -2.3eV 	Ir : 4% piq : 95% H-2254tpy : 1%	HOMO-2 -6.31eV 	Ir : 24% piq : 75% H-2254tpy : 2%
LUMO+1 -2.34eV 	Ir : 3% piq : 13% H-2254tpy : 85%	HOMO-3 -6.6eV 	Ir : 33% piq : 62% H-2254tpy : 5%
LUMO -3.38eV 	Ir : 1% piq : 12% H-2254tpy : 87%	HOMO-4 -6.69eV 	Ir : 51% piq : 44% H-2254tpy : 4%

Table S21. Singlet-singlet transitions above 300nm and 10 first singlet-triplet transitions predicted for Irppy-bpy in MeCN with their oscillator strength and major orbitals contributions

S ₀ to S _x	Energy (cm ⁻¹)	Wavelength (nm)	Osc. Strength	Major contributions	Attribution
1	20730,06	482,39	0,0001	HOMO->LUMO (99%)	MLCT
2	25465,34	392,69	0,0598	HOMO->L+1 (97%)	MLCT/LC (C^N)
3	26310,61	380,07	0,0004	H-4->LUMO (17%), H-2->LUMO (82%)	MLCT
4	26354,17	379,45	0,0017	HOMO->L+2 (91%)	MLCT/LC (C^N)
5	26830,03	372,72	0,0293	H-1->LUMO (87%)	MLCT
6	28154,40	355,18	0,0031	HOMO->L+3 (98%)	MLCT
7	28174,56	354,93	0,0573	H-3->LUMO (84%)	MLCT
8	29465,85	339,38	0,0001	H-4->LUMO (82%), H-2->LUMO (17%)	MLCT
9	30128,84	331,91	0,0087	HOMO->L+4 (96%)	MLCT
10	30632,94	326,45	0,007	H-5->LUMO (91%)	MLCT
11	31177,36	320,75	0,0018	H-2->L+1 (28%), HOMO->L+5 (56%)	MLCT/LC (C^N)
12	31272,53	319,77	0,0434	H-2->L+1 (42%), HOMO->L+5 (40%)	MLCT/LC (C^N)
13	31362,06	318,86	0,014	H-3->L+1 (15%), H-1->L+1 (62%)	MLCT/LC (C^N)
14	31508,05	317,38	0,0009	HOMO->L+6 (85%)	MLCT/LC (C^N)
15	32052,47	311,99	0,0561	H-3->L+2 (10%), H-2->L+1 (10%), H-1->L+2 (70%)	MLCT/LC (C^N)
16	32208,94	310,47	0,0127	H-3->L+1 (18%), H-2->L+2 (49%), H-1->L+1 (21%)	MLCT/LC (C^N)
17	33188,10	301,31	0,0007	H-3->L+1 (55%), H-2->L+2 (21%)	MLCT/LC (C^N)
18	33365,54	299,71	0,09	H-3->L+2 (61%), H-2->L+3 (13%), H-1->L+2 (13%)	MLCT/LC (C^N)
S ₀ to T _x	Energy (cm ⁻¹)	Wavelength (nm)	Osc. Strength	Major contributions	Attribution
1	20492,93	487,97	0	HOMO->LUMO (97%)	MLCT
2	22381,89	446,79	0	H-1->L+2 (18%), HOMO->L+1 (64%)	MLCT/LC (C^N)
3	22742,42	439,71	0	H-1->L+1 (27%), HOMO->L+2 (51%)	MLCT/LC (C^N)
4	23953,86	417,47	0	H-6->LUMO (37%), H-4->LUMO (16%), H-2->LUMO (31%)	MLCT
5	25208,86	396,69	0	H-5->LUMO (11%), H-3->LUMO (48%), H-1->LUMO (33%)	MLCT
6	26017,03	384,36	0	H-2->L+1 (22%), H-1->L+2 (14%), HOMO->L+1 (29%)	MLCT/LC (C^N)
7	26083,16	383,39	0	H-2->L+2 (15%), H-1->L+1 (13%), HOMO->L+2 (40%)	MLCT/LC (C^N)
8	26769,54	373,56	0	H-6->LUMO (41%), H-2->LUMO (49%)	MLCT / LC (N^N)
9	27423,66	364,65	0	H-3->LUMO (33%), H-1->LUMO (62%)	MLCT
10	27500,28	363,63	0	HOMO->L+3 (74%), HOMO->L+5 (11%)	MLCT - MLCT/LC (C^N)

Table S22. Singlet-singlet transitions above 300nm and 10 first singlet-triplet transitions predicted for IrppyF₂-bpy in MeCN with their oscillator strength and major orbitals contributions

S ₀ to S _x	Energy (cm ⁻¹)	Wavelength (nm)	Osc. Strength	Major contributions	Attribution
1	22731,93	439,91	0,0002	HOMO->LUMO (98%)	MLCT
2	27191,37	367,76	0,0542	HOMO->L+1 (94%)	MLCT/LC (C^N)
3	27381,72	365,21	0,0018	H-3->LUMO (45%), H-2->LUMO (52%)	MLCT
4	27431,72	364,54	0,0213	H-1->LUMO (93%)	ILCT
5	28121,33	355,60	0,0006	HOMO->L+2 (93%)	MLCT/LC (C^N)
6	29100,48	343,64	0,0002	H-3->LUMO (52%), H-2->LUMO (47%)	MLCT
7	29410,20	340,02	0,0753	H-4->LUMO (85%)	MLCT
8	30292,57	330,11	0,0025	HOMO->L+3 (98%)	MLCT
9	31424,17	318,23	0,0054	H-5->LUMO (89%)	MLCT
10	32050,86	312,00	0,0353	H-4->L+1 (10%), H-1->L+1 (66%), HOMO->L+4 (14%)	MLCT - LC (C^N)
11	32073,44	311,78	0,0291	H-3->L+1 (33%), H-2->L+1 (47%), H-1->L+2 (11%)	MLCT/LC (C^N)
12	32222,66	310,34	0,0001	H-1->L+1 (10%), HOMO->L+4 (82%)	MLCT
13	32702,56	305,79	0,0863	H-2->L+1 (13%), H-1->L+2 (68%)	MLCT/LC (C^N)
14	33146,97	301,69	0,0394	H-3->L+2 (26%), H-2->L+2 (46%), H-1->L+1 (12%)	MLCT/LC (C^N)
S ₀ to T _x	Energy (cm ⁻¹)	Wavelength (nm)	Osc. Strength	Major contributions	Attribution
1	22441,57	445,60	0	HOMO->LUMO (93%)	MLCT
2	23439,28	426,63	0	H-2->L+1 (12%), H-1->L+2 (25%), HOMO->L+1 (48%)	MLCT/LC (C^N)
3	23642,53	422,97	0	H-2->L+2 (12%), H-1->L+1 (35%), HOMO->L+2 (37%)	MLCT/LC (C^N)
4	24303,90	411,46	0	H-6->LUMO (47%), H-3->LUMO (27%)	MLCT - LC (N^N)
5	26154,14	382,35	0	H-5->LUMO (10%), H-4->LUMO (41%), H-1->LUMO (41%)	MLCT
6	27197,82	367,68	0	H-2->L+1 (24%), H-1->L+2 (11%), HOMO->L+1 (43%)	MLCT/LC (C^N)
7	27411,56	364,81	0	H-6->LUMO (27%), H-3->LUMO (21%), H-2->LUMO (49%)	MLCT - LC (N^N)
8	27414,79	364,77	0	H-2->L+2 (16%), HOMO->L+2 (52%)	MLCT/LC (C^N)
9	28268,12	353,76	0	H-4->LUMO (36%), H-1->LUMO (55%)	MLCT
10	29082,74	343,85	0	H-3->LUMO (24%), H-2->LUMO (29%), HOMO->L+3 (15%)	MLCT

Table S23.Singlet-singlet transitions above 300nm and 10 first singlet-triplet transitions predicted for Irpiq-bpy in MeCN with their oscillator strength and major orbitals contributions

S ₀ to S _x	Energy (cm ⁻¹)	Wavelength (nm)	Osc. Strength	Major contributions	Attribution
1	20614,72	485,09	0,0023	HOMO->LUMO (97%)	MLLCT
2	21960,86	455,36	0,0968	HOMO->L+1 (96%)	MLCT/LC (C^N)
3	22972,28	435,31	0,0009	HOMO->L+2 (97%)	MLCT/LC (C^N)
4	24966,89	400,53	0,0293	H-1->LUMO (96%)	MLLCT
5	25502,44	392,12	0,0007	H-4->LUMO (11%), H-2->LUMO (83%)	MLLCT
6	26640,49	375,37	0,0197	H-1->L+1 (88%)	MLCT/LC (C^N)
7	27001,83	370,35	0,042	H-2->L+1 (44%), H-1->L+2 (36%)	MLCT/LC (C^N)
8	27618,84	362,07	0,0861	H-2->L+1 (33%), H-1->L+2 (54%)	MLCT/LC (C^N)
9	27856,78	358,98	0,0674	H-3->LUMO (79%)	MLLCT
10	28217,31	354,39	0,0069	H-4->LUMO (21%), HOMO->L+3 (63%)	MLLCT
11	28289,09	353,49	0,0262	H-2->L+2 (54%), HOMO->L+3 (16%)	MLCT/LC (C^N)
12	28397,17	352,15	0,0033	H-4->LUMO (61%), HOMO->L+3 (18%)	MLLCT
13	29440,04	339,67	0,0172	H-3->L+1 (68%)	MLCT/LC (C^N)
14	29753,79	336,09	0,1394	H-3->L+2 (83%)	MLCT/LC (C^N)
15	29898,97	334,46	0,1481	H-4->L+1 (53%), H-2->L+1 (12%), HOMO->L+4 (20%)	MLCT (C^N) - MLLCT
16	30073,19	332,52	0,0581	H-4->L+1 (21%), HOMO->L+4 (61%)	MLCT (C^N) - MLLCT
17	30168,36	331,47	0,0004	H-5->LUMO (75%)	MLLCT
18	30582,12	326,99	0,0506	H-4->L+2 (62%)	MLCT/LC (C^N)
19	31152,36	321,00	0,0106	H-5->L+1 (67%)	MLCT/LC (C^N)
20	31543,54	317,02	0,0472	H-5->L+2 (23%), HOMO->L+5 (16%), HOMO->L+6 (46%)	MLCT/LC (C^N)
21	31825,83	314,21	0,0011	H-5->L+1 (10%), HOMO->L+5 (72%), HOMO->L+6 (10%)	MLCT/LC (C^N)
22	31950,04	312,99	0,0581	H-5->L+2 (57%), HOMO->L+6 (34%)	MLCT/LC (C^N)
23	32331,54	309,30	0,0084	H-1->L+3 (92%)	MLLCT
24	33095,35	302,16	0,0459	H-2->L+3 (78%)	MLLCT
S ₀ to T _x	Energy (cm ⁻¹)	Wavelength (nm)	Osc. Strength	Major contributions	Attribution
1	18120,05	551,87	0	H-2->L+1 (14%), H-1->L+2 (31%), HOMO->L+1 (42%)	MLCT/LC (C^N)
2	18297,49	546,52	0	H-2->L+2 (16%), H-1->L+1 (39%), HOMO->L+2 (33%)	MLCT/LC (C^N)
3	20397,76	490,25	0	HOMO->LUMO (91%)	MLLCT
4	21777,78	459,18	0	H-2->L+1 (24%), H-1->L+2 (14%), HOMO->L+1 (45%)	MLCT/LC (C^N)
5	22261,71	449,20	0	H-2->L+2 (18%), H-1->L+1 (10%), HOMO->L+2 (57%)	MLCT/LC (C^N)
6	23847,39	419,33	0	H-8->LUMO (30%), H-4->LUMO (21%), H-2->LUMO (27%)	MLLCT - LC (N^N)
7	24133,72	414,36	0	H-3->LUMO (14%), H-1->LUMO (68%)	MLLCT
8	26012,19	384,44	0	H-8->LUMO (32%), H-2->LUMO (51%)	MLLCT - LC (N^N)
9	26091,23	383,27	0	H-4->L+1 (12%), H-2->L+1 (17%), H-2->L+2 (10%), H-1->L+1 (11%), H-1->L+2 (14%)	MLCT/LC (C^N)
10	26295,29	380,30	0	H-4->L+1 (14%), H-2->L+1 (13%), H-2->L+2 (12%), H-1->L+1 (11%)	MLCT/LC (C^N)

Table S24. Singlet-singlet transitions above 300nm and 10 first singlet-triplet transitions predicted for Irppy-2244tpy in MeCN with their oscillator strength and major orbitals contributions

S ₀ to S _x	Energy (cm ⁻¹)	Wavelength (nm)	Osc. Strength	Major contributions	Attribution
1	19725,90	506,95	0,0007	HOMO->LUMO (99%)	MLCT
2	25341,13	394,62	0,0042	H-4->LUMO (16%), H-2->LUMO (80%)	MLCT
3	25541,97	391,51	0,0596	HOMO->L+2 (95%)	MLCT/LC (C^N)
4	25688,76	389,28	0,0426	H-1->LUMO (83%)	ILCT
5	25948,47	385,38	0,0032	HOMO->L+1 (83%)	MLCT
6	26478,38	377,67	0,0022	HOMO->L+3 (83%)	MLCT/LC (C^N)
7	27186,53	367,83	0,1014	H-3->LUMO (79%)	MLCT
8	28324,58	353,05	0,0006	H-4->LUMO (81%), H-2->LUMO (16%)	MLCT
9	28869,81	346,38	0,0085	HOMO->L+4 (96%)	MLCT
10	29481,98	339,19	0,0121	H-5->LUMO (92%)	MLCT
11	31153,97	320,99	0,0024	HOMO->L+5 (81%)	MLCT/LC (C^N)
12	31269,31	319,80	0,034	H-2->L+2 (42%), H-1->L+1 (13%), HOMO->L+5 (15%)	MLCT/LC (C^N)
13	31387,07	318,60	0,0353	H-3->L+2 (12%), H-1->L+2 (53%)	MLCT/LC (C^N)
14	31436,27	318,10	0,0187	H-2->L+2 (11%), H-1->L+1 (53%), HOMO->L+6 (18%)	MLCT - MLCT/LC (C^N)
15	31576,61	316,69	0,0026	H-1->L+1 (13%), HOMO->L+6 (73%)	MLCT/LC (C^N)
16	31807,28	314,39	0,0163	H-4->L+1 (10%), H-2->L+1 (69%)	MLCT
17	32108,93	311,44	0,0427	H-1->L+3 (64%)	MLCT/LC (C^N)
18	32230,72	310,26	0,0177	H-3->L+2 (16%), H-2->L+3 (45%), H-1->L+2 (17%)	MLCT/LC (C^N)
19	32759,82	305,25	0,0114	H-3->L+1 (70%), H-1->L+1 (10%)	MLCT
20	33184,07	301,35	0,0108	H-3->L+2 (51%), H-2->L+3 (20%)	MLCT/LC (C^N)
21	33304,25	300,26	0,0517	H-7->LUMO (30%), H-6->LUMO (42%)	LC (N^N)
S ₀ to T _x	Energy (cm ⁻¹)	Wavelength (nm)	Osc. Strength	Major contributions	Attribution
1	19488,77	513,12	0	HOMO->LUMO (97%)	MLCT
2	22418,99	446,05	0	H-1->L+3 (18%), HOMO->L+2 (62%)	MLCT/LC (C^N)
3	22760,16	439,36	0	H-1->L+2 (27%), HOMO->L+3 (50%)	MLCT/LC (C^N)
4	23104,56	432,82	0	H-6->LUMO (13%), H-4->LUMO (15%), H-2->LUMO (35%)	MLCT - LC (N^N)
5	24215,18	412,96	0	H-3->LUMO (41%), H-1->LUMO (29%)	MLCT
6	25771,83	388,02	0	HOMO->L+1 (72%)	MLCT
7	26047,68	383,91	0	H-2->L+2 (20%), H-1->L+3 (12%), HOMO->L+2 (27%)	MLCT/LC (C^N)
8	26133,17	382,66	0	H-6->LUMO (21%), H-2->LUMO (27%), HOMO->L+3 (12%)	MLCT - LC (N^N)
9	26173,50	382,07	0	H-6->LUMO (10%), H-2->LUMO (14%), HOMO->L+1 (14%), HOMO->L+3 (19%)	MLCT - LC (N^N)
10	26312,23	380,05	0	H-3->LUMO (26%), H-1->LUMO (51%)	MLCT

Table S25. Singlet-singlet transitions above 300nm and 10 first singlet-triplet transitions predicted for Irppy-2254tpy in MeCN with their oscillator strength and major orbitals contributions

S ₀ to S _x	Energy (cm ⁻¹)	Wavelength (nm)	Osc. Strength	Major contributions	Attribution
1	19464,58	513,75	0,0001	HOMO->LUMO (99%)	MLLCT
2	25128,20	397,96	0,0012	H-4->LUMO (16%), H-2->LUMO (82%)	MLLCT
3	25370,98	394,15	0,0218	H-1->LUMO (92%)	ILCT
4	25530,67	391,69	0,0595	HOMO->L+1 (96%)	MLCT/LC (C ^N)
5	26366,26	379,27	0,0024	HOMO->L+2 (60%), HOMO->L+3 (29%)	MLLCT - MLCT/LC (C ^N)
6	26867,94	372,19	0,0491	H-3->LUMO (79%)	MLLCT
7	27095,39	369,07	0,0034	HOMO->L+2 (28%), HOMO->L+3 (67%)	MLCT (N ^N)
8	27981,79	357,38	0,0026	H-4->LUMO (81%), H-2->LUMO (16%)	MLLCT
9	29150,49	343,05	0,0074	H-5->LUMO (92%)	MLLCT
10	29734,44	336,31	0,0041	HOMO->L+4 (97%)	MLLCT
11	31001,53	322,56	0,01	HOMO->L+5 (88%)	MLLCT - MLCT/LC (C ^N)
12	31296,73	319,52	0,035	H-4->L+1 (11%), H-2->L+1 (64%)	MLCT/LC (C ^N)
13	31445,14	318,01	0,0162	H-3->L+1 (11%), H-1->L+1 (59%)	MLCT/LC (C ^N)
14	31570,15	316,75	0,0011	HOMO->L+6 (85%)	MLCT/LC (C ^N)
15	31939,56	313,09	0,2185	H-6->LUMO (58%), H-2->L+2 (10%)	MLLCT - MLCT/LC (C ^N) - LC (N ^N)
16	32095,22	311,57	0,2048	H-6->LUMO (10%), H-2->L+2 (11%), H-1->L+2 (36%), H-1->L+3 (19%)	MLLCT - MLCT/LC (C ^N) - LC (N ^N)
17	32245,24	310,12	0,0469	H-3->L+1 (17%), H-2->L+2 (17%), H-2->L+3 (29%), H-1->L+1 (17%)	MLLCT - MLCT/LC (C ^N)
18	32770,31	305,15	0,0145	H-1->L+2 (32%), H-1->L+3 (48%)	MLLCT - MLCT/LC (C ^N)
19	32984,85	303,17	0,0012	H-7->LUMO (88%)	LC (N ^N)
20	33077,60	302,32	0,2642	H-6->LUMO (18%), H-2->L+2 (25%), H-2->L+3 (34%)	MLLCT - MLCT/LC (C ^N) - LC (N ^N)
21	33226,01	300,97	0,0095	H-3->L+1 (50%), H-2->L+2 (11%)	MLLCT - MLCT/LC (C ^N)
22	33447,01	298,98	0,0985	H-3->L+2 (35%), H-3->L+3 (29%)	MLLCT / MLCT/LC (C ^N)
S ₀ to T _x	Energy (cm ⁻¹)	Wavelength (nm)	Osc. Strength	Major contributions	Attribution
1	19266,97	519,02	0	HOMO->LUMO (97%)	MLLCT
2	22406,08	446,31	0	HOMO->L+1 (54%)	MLLCT - MLCT/LC (C ^N)
3	22449,64	445,44	0	H-6->LUMO (41%), H-4->LUMO (13%), H-2->LUMO (19%)	MLLCT - MLCT/LC (C ^N) - LC (N ^N)
4	22758,55	439,40	0	H-1->L+1 (27%), HOMO->L+2 (23%), HOMO->L+3 (27%)	MLLCT - MLCT/LC (C ^N)
5	24204,70	413,14	0	H-5->LUMO (10%), H-3->LUMO (42%), H-1->LUMO (40%)	MLLCT
6	25323,39	394,89	0	H-6->LUMO (32%), H-2->LUMO (57%)	MLLCT - LC (N ^N)
7	25923,47	385,75	0	H-3->LUMO (18%), H-1->LUMO (33%)	MLLCT - MLCT/LC (C ^N)
8	26042,84	383,98	0	H-2->L+1 (21%), HOMO->L+1 (27%)	MLLCT - MLCT/LC (C ^N)
9	26195,27	381,75	0	H-3->LUMO (18%), H-1->LUMO (20%), HOMO->L+2 (18%)	MLLCT - MLCT/LC (C ^N)
10	26768,73	373,57	0	HOMO->L+2 (40%), HOMO->L+3 (49%)	MLLCT - MLCT/LC (C ^N)

Table S26. Singlet-singlet transitions above 300nm and 10 first singlet-triplet transitions predicted for IrppyF₂-2244tpy in MeCN with their oscillator strength and major orbitals contributions

S ₀ to S _x	Energy (cm ⁻¹)	Wavelength (nm)	Osc. Strength	Major contributions	Attribution
1	21732,61	460,14	0,0008	HOMO->LUMO (98%)	MLCT
2	26354,97	379,44	0,0359	H-1->LUMO (91%)	ILCT
3	26418,69	378,52	0,0009	H-3->LUMO (36%), H-2->LUMO (53%)	MLCT
4	27230,08	367,24	0,0554	HOMO->L+2 (96%)	MLCT/LC (C ^N)
5	27940,66	357,90	0,0017	HOMO->L+1 (59%), HOMO->L+3 (37%)	MLLCT -MLCT/LC (C ^N)
6	28013,25	356,97	0,0089	H-3->LUMO (55%), H-2->LUMO (40%)	MLLCT
7	28143,91	355,32	0,037	H-4->LUMO (45%), HOMO->L+1 (20%), HOMO->L+3 (27%)	MLLCT - MLCT/LC (C ^N)
8	28568,16	350,04	0,088	H-4->LUMO (39%), HOMO->L+1 (17%), HOMO->L+3 (30%)	MLLCT - MLCT/LC (C ^N)
9	30334,51	329,66	0,008	H-5->LUMO (91%)	MLLCT
10	30964,43	322,95	0,0057	HOMO->L+4 (95%)	MLLCT
11	31974,24	312,75	0,0367	H-3->L+2 (10%), H-2->L+2 (10%), H-1->L+1 (26%), H-1->L+2 (34%)	MLLCT - MLCT/LC (C ^N)
12	32114,58	311,39	0,0269	H-4->L+2 (11%), H-3->L+2 (12%), H-2->L+2 (28%), H-1->L+2 (29%)	MLCT/LC (C ^N)
13	32270,24	309,88	0,0152	H-2->L+2 (10%), H-1->L+1 (58%), H-1->L+2 (11%)	MLLCT - MLCT/LC (C ^N)
14	32663,03	306,16	0,0682	H-2->L+1 (22%), H-1->L+3 (42%)	MLLCT - MLCT/LC (C ^N)
15	32796,92	304,91	0,0023	H-6->LUMO (32%), H-2->L+1 (11%), H-1->L+3 (20%)	MLLCT - MLCT/LC (C ^N) - LC (N ^N)
16	32968,72	303,32	0,0237	H-7->LUMO (19%), H-6->LUMO (29%), H-2->L+1 (27%)	ILCT - LC (N ^N)
17	33173,58	301,44	0,0492	H-3->L+3 (25%), H-2->L+3 (45%), H-1->L+2 (10%)	MLCT/LC (C ^N)
S ₀ to T _x	Energy (cm ⁻¹)	Wavelength (nm)	Osc. Strength	Major contributions	Attribution
1	21455,96	466,07	0	HOMO->LUMO (94%)	MLCT
2	23442,50	426,58	0	H-2->L+2 (12%), H-1->L+3 (24%), HOMO->L+2 (46%)	MLCT/LC (C ^N)
3	23586,88	423,96	0	H-7->LUMO (12%), H-6->LUMO (12%), H-3->LUMO (35%)	MLLCT - LC (N ^N)
4	23645,76	422,91	0	H-2->L+3 (12%), H-1->L+2 (35%), HOMO->L+3 (36%)	MLCT/LC (C ^N)
5	25062,87	399,00	0	H-4->LUMO (40%), H-1->LUMO (36%)	MLLCT
6	26618,72	375,68	0	H-7->LUMO (13%), H-6->LUMO (14%), H-3->LUMO (10%), H-2->LUMO (53%)	MLLCT - LC (N ^N)
7	27005,06	370,30	0	H-4->LUMO (24%), H-1->LUMO (57%)	MLLCT
8	27198,63	367,67	0	H-2->L+2 (23%), H-1->L+3 (10%), HOMO->L+2 (41%)	MLCT/LC (C ^N)
9	27416,40	364,75	0	H-2->L+3 (15%), HOMO->L+3 (42%)	MLCT/LC (C ^N)
10	27977,76	357,43	0	HOMO->L+1 (75%)	MLLCT

Table S27. Singlet-singlet transitions above 300nm and 10 first singlet-triplet transitions predicted for IrppyF₂-2254tpy in MeCN with their oscillator strength and major orbitals contributions

S ₀ to S _x	Energy (cm ⁻¹)	Wavelength (nm)	Osc. Strength	Major contributions	Attribution
1	21551,94	464,00	0,0001	HOMO->LUMO (98%)	MLCT
2	26082,36	383,40	0,0155	H-1->LUMO (95%)	ILCT
3	26217,05	381,43	0,0011	H-3->LUMO (40%), H-2->LUMO (58%)	MLCT
4	27272,02	366,68	0,0556	HOMO->L+1 (95%)	MLCT/LC (C ^N)
5	27730,15	360,62	0,0049	H-3->LUMO (57%), H-2->LUMO (41%)	MLCT
6	27986,63	357,31	0,0269	H-4->LUMO (46%), HOMO->L+2 (42%)	MLCT - MLCT/LC (C ^N)
7	28268,93	353,75	0,0374	H-4->LUMO (40%), HOMO->L+2 (49%)	MLCT - MLCT/LC (C ^N)
8	29218,24	342,25	0,0015	HOMO->L+3 (92%)	MLCT - MLCT/LC (C ^N)
9	30062,70	332,64	0,0041	H-5->LUMO (89%)	MLCT
10	31794,38	314,52	0,0266	HOMO->L+4 (91%)	MLCT
11	32037,15	312,14	0,379	H-6->LUMO (57%)	MLCT/LC (C ^N) - LC (N ^N)
12	32133,94	311,20	0,1268	H-6->LUMO (26%), H-3->L+1 (12%), H-2->L+1 (18%), H-1->L+1 (27%)	MLCT/LC (C ^N) - LC (N ^N)
13	32182,33	310,73	0,026	H-3->L+1 (12%), H-2->L+1 (21%), H-1->L+1 (40%)	MLCT/LC (C ^N)
14	32680,78	305,99	0,0078	H-7->LUMO (70%), H-1->L+2 (14%)	MLCT mixte
15	32718,69	305,64	0,1541	H-7->LUMO (21%), H-1->L+2 (47%)	MLCT/LC (C ^N) - LC (N ^N)
16	33119,54	301,94	0,0541	H-3->L+2 (20%), H-2->L+2 (40%), H-1->L+1 (10%)	MLCT - MLCT/LC (C ^N)
17	33318,76	300,13	0,0005	H-3->L+1 (13%), HOMO->L+5 (69%)	MLCT - MLCT/LC (C ^N)
S ₀ to T _x	Energy (cm ⁻¹)	Wavelength (nm)	Osc. Strength	Major contributions	Attribution
1	21292,23	469,65	0	HOMO->LUMO (91%)	MLCT
2	22719,03	440,16	0	H-6->LUMO (51%), H-3->LUMO (26%)	MLCT - LC (N ^N)
3	23452,99	426,38	0	H-2->L+1 (12%), H-1->L+2 (22%), HOMO->L+1 (48%)	MLCT - MLCT/LC (C ^N)
4	23640,92	423,00	0	H-2->L+2 (10%), H-1->L+1 (34%), HOMO->L+2 (32%)	MLCT - MLCT/LC (C ^N)
5	25184,66	397,07	0	H-4->LUMO (31%), H-1->LUMO (51%)	MLCT
6	26121,88	382,82	0	H-6->LUMO (20%), H-3->LUMO (20%), H-2->LUMO (54%)	MLCT - LC (N ^N)
7	26926,01	371,39	0	H-4->LUMO (39%), H-1->LUMO (44%)	MLCT
8	27231,70	367,22	0	H-2->L+1 (24%), HOMO->L+1 (42%)	MLCT/LC (C ^N)
9	27483,34	363,86	0	H-2->L+2 (14%), HOMO->L+2 (44%)	MLCT - MLCT/LC (C ^N)
10	27767,25	360,14	0	H-6->LUMO (11%), H-3->LUMO (41%), H-2->LUMO (40%)	MLCT - LC (N ^N)

Table S28. Singlet-singlet transitions above 300nm and 10 first singlet-triplet transitions predicted for Irpiq-2244tpy in MeCN with their oscillator strength and major orbitals contributions

S ₀ to S _x	Energy (cm ⁻¹)	Wavelength (nm)	Osc. Strength	Major contributions	Attribution
1	19602,50	510,14	0,0009	HOMO->LUMO (98%)	MLCT
2	21985,06	454,85	0,0976	HOMO->L+1 (97%)	MLCT/LC (C^N)
3	22997,29	434,83	0	HOMO->L+2 (96%)	MLCT/LC (C^N)
4	23909,50	418,24	0,0374	H-1->LUMO (96%)	ILCT
5	24522,48	407,79	0,0008	H-4->LUMO (10%), H-2->LUMO (84%)	MLLCT
6	25930,72	385,64	0,0001	HOMO->L+3 (96%)	MLLCT
7	26601,78	375,91	0,0377	H-1->L+1 (85%)	MLCT/LC (C^N)
8	26926,82	371,38	0,0599	H-3->LUMO (80%)	MLLCT
9	27020,38	370,09	0,0515	H-2->L+1 (39%), H-1->L+2 (37%)	MLCT/LC (C^N)
10	27290,58	366,43	0,0293	H-4->LUMO (80%)	MLLCT - MLCT/LC (C^N)
11	27625,30	361,99	0,0908	H-2->L+1 (33%), H-1->L+2 (53%)	MLCT/LC (C^N)
12	28315,71	353,16	0,0351	H-2->L+2 (69%)	MLCT/LC (C^N)
13	28802,06	347,20	0,0072	HOMO->L+4 (88%)	MLLCT
14	29085,16	343,82	0,0062	H-5->LUMO (75%)	MLLCT
15	29467,47	339,36	0,0193	H-3->L+1 (64%), H-2->L+2 (10%)	MLCT/LC (C^N)
16	29732,82	336,33	0,0466	H-3->L+2 (10%), H-1->L+3 (80%)	MLLCT - MLCT/LC (C^N)
17	29765,89	335,96	0,0932	H-3->L+2 (73%), H-1->L+3 (12%)	MLCT/LC (C^N)
18	29919,94	334,23	0,2156	H-4->L+1 (74%), H-2->L+1 (12%)	MLCT/LC (C^N)
19	30526,47	327,58	0,0287	H-5->L+1 (11%), H-4->L+2 (61%)	MLCT/LC (C^N)
20	30899,10	323,63	0,031	H-2->L+3 (81%)	MLLCT
21	31102,35	321,52	0,0149	H-5->L+1 (65%), H-4->L+2 (10%)	MLCT/LC (C^N)
22	31551,60	316,94	0,0457	H-5->L+2 (23%), HOMO->L+5 (18%), HOMO->L+6 (43%)	MLCT/LC (C^N)
23	31852,45	313,95	0,002	HOMO->L+5 (72%), HOMO->L+6 (11%)	MLCT/LC (C^N)
24	31966,17	312,83	0,065	H-5->L+2 (56%), HOMO->L+6 (36%)	MLCT/LC (C^N)
25	32701,75	305,79	0,0028	H-8->LUMO (13%), H-4->L+3 (13%), H-3->L+3 (43%), H-1->L+4 (12%)	MLLCT
26	32860,64	304,32	0,0052	H-6->LUMO (17%), H-1->L+4 (66%)	ILCT
27	32867,90	304,25	0,0061	H-6->LUMO (69%), H-3->L+3 (22%)	ILCT
28	33143,74	301,72	0,0193	H-8->LUMO (23%), H-4->L+3 (31%), H-3->L+3 (14%)	MLLCT - LC (N^N)
S ₀ to T _x	Energy (cm ⁻¹)	Wavelength (nm)	Osc. Strength	Major contributions	Attribution
1	18125,70	551,70	0	H-2->L+1 (15%), H-1->L+2 (31%), HOMO->L+1 (43%)	MLCT/LC (C^N)
2	18298,30	546,50	0	H-2->L+2 (15%), H-1->L+1 (41%), HOMO->L+2 (33%)	MLCT/LC (C^N)
3	19386,34	515,83	0	HOMO->LUMO (94%)	MLLCT
4	21806,01	458,59	0	H-2->L+1 (25%), H-1->L+2 (13%), HOMO->L+1 (46%)	MLCT/LC (C^N)
5	22288,33	448,67	0	H-2->L+2 (18%), H-1->L+1 (10%), HOMO->L+2 (56%)	MLCT/LC (C^N)
6	22750,48	439,55	0	H-4->LUMO (19%), H-2->LUMO (15%), H-1->LUMO (40%)	MLLCT
7	23390,08	427,53	0	H-3->LUMO (10%), H-2->LUMO (21%), H-1->LUMO (34%)	MLLCT
8	25272,58	395,69	0	H-8->LUMO (20%), H-2->LUMO (47%)	MLLCT - LC (N^N)
9	25649,24	389,88	0	H-3->LUMO (48%), H-1->LUMO (20%)	MLLCT
10	25809,74	387,45	0	HOMO->L+3 (91%)	MLLCT

Table S29. Singlet-singlet transitions above 300nm and 10 first singlet-triplet transitions predicted for Irpiq-2254tpy in MeCN with their oscillator strength and major orbitals contributions

S ₀ to S _x	Energy (cm ⁻¹)	Wavelength (nm)	Osc. Strength	Major contributions	Attribution
1	19368,60	516,30	0,001	HOMO->LUMO (98%)	MLLCT
2	22009,26	454,35	0,0957	HOMO->L+1 (97%)	MLCT/LC (C^N)
3	22998,09	434,82	0,0001	HOMO->L+2 (95%)	MLCT/LC (C^N)
4	23565,10	424,36	0,0179	H-1->LUMO (95%)	ILCT
5	24251,48	412,35	0,0008	H-2->LUMO (86%)	MLLCT
6	26565,48	376,43	0,0622	H-3->LUMO (75%), H-1->L+1 (12%)	MLLCT - MLCT/LC (C^N)
7	26675,98	374,87	0,0055	H-3->LUMO (11%), H-1->L+1 (77%)	MLLCT - MLCT/LC (C^N)
8	26901,01	371,73	0,0156	H-4->LUMO (50%), HOMO->L+3 (21%)	MLLCT - MLCT/LC (C^N)
9	27070,39	369,41	0,0374	H-4->LUMO (10%), H-2->L+1 (37%), H-1->L+2 (30%)	MLLCT - MLCT/LC (C^N)
10	27184,11	367,86	0,0049	H-4->LUMO (27%), HOMO->L+3 (67%)	MLLCT
11	27636,59	361,84	0,0805	H-2->L+1 (33%), H-1->L+2 (54%)	MLCT/LC (C^N)
12	28297,96	353,38	0,0435	H-2->L+2 (70%)	MLCT/LC (C^N)
13	28794,80	347,28	0,0047	H-5->LUMO (86%)	MLLCT
14	29394,07	340,20	0,0137	H-3->L+1 (54%), HOMO->L+4 (24%)	MLLCT - MLCT/LC (C^N)
15	29602,16	337,81	0,0564	H-3->L+1 (16%), H-3->L+2 (10%), HOMO->L+4 (61%)	MLLCT - MLCT/LC (C^N)
16	29778,80	335,81	0,0646	H-3->L+2 (71%)	MLCT/LC (C^N)
17	29975,60	333,60	0,2104	H-4->L+1 (67%)	MLCT/LC (C^N)
18	30547,44	327,36	0,0476	H-5->L+1 (10%), H-4->L+2 (63%)	MLCT/LC (C^N)
19	31117,68	321,36	0,0101	H-5->L+1 (33%), H-4->L+2 (12%), H-1->L+3 (35%)	MLLCT - MLCT/LC (C^N)
20	31181,39	320,70	0,0039	H-5->L+1 (33%), H-1->L+3 (54%)	MLLCT - MLCT/LC (C^N)
21	31445,94	318,01	0,0552	H-5->L+2 (13%), HOMO->L+5 (66%)	MLLCT - MLCT/LC (C^N)
22	31757,27	314,89	0,1669	H-6->LUMO (30%), H-2->L+3 (35%)	MLLCT - MLCT/LC (C^N) - LC (N^N)
23	31921,00	313,27	0,0277	HOMO->L+6 (66%)	MLCT/LC (C^N)
24	31943,59	313,05	0,0735	H-5->L+2 (56%), HOMO->L+5 (14%), HOMO->L+6 (16%)	MLCT/LC (C^N)
25	32356,54	309,06	0,2784	H-6->LUMO (49%), H-2->L+3 (36%)	MLLCT - LC (N^N)
26	32543,66	307,28	0,0934	H-7->LUMO (86%)	ILCT
27	32988,88	303,13	0,0082	H-9->LUMO (90%)	LC (N^N)
28	33202,62	301,18	0,0014	H-8->LUMO (94%)	ILCT
S ₀ to T _x	Energy (cm ⁻¹)	Wavelength (nm)	Osc. Strength	Major contributions	Attribution
1	18121,66	551,83	0	H-2->L+1 (15%), H-1->L+2 (31%), HOMO->L+1 (42%)	MLCT/LC (C^N)
2	18302,33	546,38	0	H-2->L+2 (16%), H-1->L+1 (41%), HOMO->L+2 (33%)	MLCT/LC (C^N)
3	19191,16	521,07	0	HOMO->LUMO (93%)	MLLCT
4	21814,88	458,40	0	H-2->L+1 (24%), H-1->L+2 (13%), HOMO->L+1 (46%)	MLCT/LC (C^N)
5	22306,07	448,31	0	H-2->L+2 (18%), HOMO->L+2 (52%)	MLCT/LC (C^N)
6	22406,08	446,31	0	H-6->LUMO (35%), H-4->LUMO (19%), H-2->LUMO (16%)	MLLCT - LC (N^N)
7	22990,83	434,96	0	H-3->LUMO (11%), H-1->LUMO (74%)	MLLCT
8	24473,28	408,61	0	H-6->LUMO (25%), H-2->LUMO (65%)	MLLCT - LC (N^N)
9	25571,00	391,07	0	H-3->LUMO (57%), H-1->LUMO (16%)	MLLCT
10	26146,88	382,45	0	H-4->L+1 (10%), H-3->L+1 (10%), H-2->L+1 (16%), H-1->L+1 (13%), H-1->L+2 (17%)	MLCT/LC (C^N)

Table S30. Singlet-singlet transitions above 300nm and 10 first singlet-triplet transitions predicted for the protonated form of Irppy-2244tpy in MeCN with their oscillator strength and major orbitals contributions

S ₀ to S _x	Energy (cm ⁻¹)	Wavelength (nm)	Osc. Strength	Major contributions	Attribution
1	15385,83	649,95	0,0021	HOMO->LUMO (97%)	MLLCT - LC (C [^] N)
2	20872,82	479,09	0,0129	H-1->LUMO (96%)	ILCT
3	21404,34	467,19	0,0106	H-4->LUMO (12%), H-2->LUMO (60%), HOMO->L+1 (21%)	MLLCT - LC (C [^] N)
4	21472,90	465,70	0,003	H-2->LUMO (20%), HOMO->L+1 (74%)	MLLCT - LC (C [^] N)
5	22874,69	437,16	0,0892	H-3->LUMO (88%)	MLLCT - LC (C [^] N)
6	23422,34	426,94	0,0367	H-4->LUMO (77%), H-2->LUMO (13%)	MLLCT - LC (C [^] N)
7	24531,35	407,64	0,0302	H-5->LUMO (91%)	MLLCT - LC (C [^] N)
8	25695,21	389,18	0,061	HOMO->L+3 (95%)	MLCT/LC (C [^] N)
9	26615,49	375,72	0,0006	HOMO->L+4 (94%)	MLCT/LC (C [^] N)
10	27041,35	369,80	0,0051	H-1->L+1 (89%)	ILCT
11	27390,59	365,09	0,0184	H-4->L+1 (19%), H-2->L+1 (73%)	MLLCT
12	27846,29	359,11	0,0016	HOMO->L+2 (20%), HOMO->L+5 (76%)	MLLCT
13	28422,98	351,83	0,0005	HOMO->L+2 (76%), HOMO->L+5 (19%)	MLLCT
14	28536,70	350,43	0,0158	H-5->L+1 (10%), H-3->L+1 (68%)	MLLCT - LC (N [^] N)
15	29465,05	339,39	0,0493	H-6->LUMO (63%), H-4->L+1 (16%), H-3->L+1 (10%)	MLLCT
16	29702,98	336,67	0,0294	H-6->LUMO (24%), H-4->L+1 (60%), H-2->L+1 (13%)	MLLCT - LC (N [^] N)
17	30457,91	328,32	0,0031	HOMO->L+6 (96%)	MLLCT
18	30741,82	325,29	0,0055	H-5->L+1 (84%), H-3->L+1 (12%)	MLLCT
19	31303,99	319,45	0,0096	HOMO->L+7 (93%)	MLCT/LC (C [^] N)
20	31529,83	317,16	0,0236	H-2->L+3 (22%), H-1->L+3 (48%)	MLCT/LC (C [^] N)
21	31669,36	315,76	0,03	H-4->L+3 (11%), H-2->L+3 (39%), H-1->L+3 (29%)	MLCT/LC (C [^] N)
22	31742,76	315,03	0,0017	H-7->LUMO (18%), HOMO->L+8 (74%)	MLCT/LC (C [^] N) - MLLCT - LC (N [^] N)
23	31809,70	314,37	0,0086	H-7->LUMO (72%), HOMO->L+8 (19%)	MLCT/LC (C [^] N) - MLLCT - LC (N [^] N)
24	32233,95	310,23	0,0582	H-1->L+4 (75%)	LC (C [^] N)
25	32466,24	308,01	0,0107	H-4->L+4 (15%), H-3->L+3 (24%), H-2->L+4 (46%)	MLCT/LC (C [^] N)
26	33143,74	301,72	0,0045	H-8->LUMO (87%)	MLCT/LC (C [^] N) - MLLCT - LC (N [^] N)
27	33205,04	301,16	0,0034	H-1->L+2 (70%), H-1->L+5 (19%)	ILCT
S ₀ to T _x	Energy (cm ⁻¹)	Wavelength (nm)	Osc. Strength	Major contributions	Attribution
1	15216,46	657,18	0	HOMO->LUMO (96%)	MLLCT - LC (C [^] N)
2	20184,83	495,42	0	H-3->LUMO (18%), H-2->LUMO (20%), H-1->LUMO (36%)	MLLCT - LC (C [^] N)
3	20734,90	482,28	0	H-4->LUMO (15%), H-2->LUMO (33%), H-1->LUMO (39%)	MLLCT - LC (C [^] N)
4	21354,34	468,29	0	HOMO->L+1 (92%)	MLLCT
5	21754,39	459,68	0	H-5->LUMO (11%), H-3->LUMO (52%), H-1->LUMO (22%)	MLLCT - LC (C [^] N)
6	22479,48	444,85	0	H-1->L+4 (18%), HOMO->L+3 (60%)	MLCT/LC (C [^] N)
7	22827,10	438,08	0	H-1->L+3 (28%), HOMO->L+4 (49%)	MLCT/LC (C [^] N)
8	23077,94	433,31	0	H-4->LUMO (49%), H-2->LUMO (30%)	MLLCT - LC (C [^] N)
9	24321,65	411,16	0	H-5->LUMO (72%), H-3->LUMO (19%)	MLLCT - LC (C [^] N)
10	24535,39	407,57	0	H-6->LUMO (34%), H-6->L+1 (33%), H-4->LUMO (18%)	MLLCT

Table S31. Singlet-singlet transitions above 300nm and 10 first singlet-triplet transitions predicted for the protonated form of Irppy-2254tpy in MeCN with their oscillator strength and major orbitals contributions

S ₀ to S _x	Energy (cm ⁻¹)	Wavelength (nm)	Osc. Strength	Major contributions	Attribution
1	15107,57	661,92	0,0005	HOMO->LUMO (98%)	MLLCT - LC (C ⁴ N)
2	20530,04	487,09	0,0045	H-1->LUMO (97%)	ILCT - LC C ⁴ N)
3	21138,18	473,08	0,0013	H-4->LUMO (14%), H-2->LUMO (83%)	MLLCT - LC (C ⁴ N)
4	22360,11	447,23	0,0229	H-3->LUMO (78%), HOMO->L+1 (15%)	MLLCT - LC (C ⁴ N)
5	22578,68	442,90	0,0023	H-3->LUMO (14%), HOMO->L+1 (74%)	MLLCT
6	23080,36	433,27	0,003	H-4->LUMO (74%), H-2->LUMO (12%)	MLLCT - LC (C ⁴ N)
7	24186,95	413,45	0,0048	H-5->LUMO (86%)	MLLCT - LC (C ⁴ N)
8	25659,72	389,72	0,0599	HOMO->L+3 (93%)	MLCT/LC (C ⁴ N)
9	26567,90	376,39	0,0014	HOMO->L+4 (75%), HOMO->L+5 (15%)	MLLCT - LC (C ⁴ N)
10	27164,75	368,12	0,0011	HOMO->L+2 (62%), HOMO->L+5 (34%)	MLLCT - LC (C ⁴ N)
11	28376,20	352,41	0,0158	H-1->L+1 (87%)	ILCT
12	28473,79	351,20	0,0015	H-2->L+1 (11%), HOMO->L+2 (20%), HOMO->L+4 (16%), HOMO->L+5 (38%)	MLLCT - LC (C ⁴ N)
13	28499,60	350,88	0,0009	H-4->L+1 (14%), H-2->L+1 (58%)	MLLCT - LC (C ⁴ N)
14	29258,57	341,78	0,0011	HOMO->L+6 (89%)	MLLCT
15	29666,69	337,08	0,6152	H-6->LUMO (91%)	LC
16	30166,75	331,49	0,0609	H-3->L+1 (77%)	MLLCT
17	30883,78	323,79	0,0136	H-4->L+1 (71%), H-2->L+1 (20%)	MLLCT
18	31327,38	319,21	0,0071	HOMO->L+7 (88%)	MLLCT - LC (C ⁴ N)
19	31470,95	317,75	0,0172	H-7->LUMO (18%), H-2->L+3 (24%), H-1->L+3 (25%)	MLCT/LC (C ⁴ N) - MLLCT - LC (N ⁴ N)
20	31498,37	317,48	0,0153	H-7->LUMO (70%), H-1->L+3 (10%)	MLCT/LC (C ⁴ N) - MLLCT - LC (N ⁴ N)
21	31663,71	315,82	0,0243	H-2->L+3 (32%), H-1->L+3 (38%)	MLCT/LC (C ⁴ N)
22	31751,63	314,94	0,0006	HOMO->L+8 (90%)	MLCT/LC (C ⁴ N)
23	32053,28	311,98	0,0154	H-5->L+1 (73%)	MLLCT - LC (C ⁴ N)
24	32224,27	310,33	0,0687	H-1->L+2 (13%), H-1->L+4 (51%)	MLLCT - LC (C ⁴ N)
25	32496,88	307,72	0,0048	H-2->L+4 (12%), H-1->L+2 (39%), H-1->L+5 (14%)	MLLCT - LC (C ⁴ N)
26	32517,05	307,53	0,009	H-3->L+3 (15%), H-2->L+4 (18%), H-1->L+2 (25%), H-1->L+5 (11%)	MLLCT - LC (C ⁴ N)
27	32859,03	304,33	0,0028	H-8->LUMO (90%)	MLLCT - LC (C ⁴ N)
28	33162,29	301,55	0,0166	H-2->L+2 (47%), H-2->L+5 (27%)	MLLCT - LC (C ⁴ N)
<hr/>					
S ₀ to T _x	Energy (cm ⁻¹)	Wavelength (nm)	Osc. Strength	Major contributions	Attribution
1	15022,08	665,69	0	HOMO->LUMO (98%)	MLLCT - LC (C ⁴ N)
2	20248,55	493,86	0	H-3->LUMO (10%), H-1->LUMO (74%)	MLLCT - LC (C ⁴ N)
3	20450,99	488,97	0	H-4->LUMO (22%), H-2->LUMO (48%), H-1->LUMO (11%)	MLLCT - LC (C ⁴ N)
4	21615,66	462,63	0	H-5->LUMO (11%), H-3->LUMO (62%), H-1->LUMO (10%)	MLLCT - LC (C ⁴ N)
5	22190,73	450,64	0	H-2->LUMO (14%), HOMO->L+1 (35%), HOMO->L+3 (11%)	MLLCT - LC (C ⁴ N)
6	22481,09	444,82	0	H-6->LUMO (23%), H-2->LUMO (19%), HOMO->L+1 (20%), HOMO->L+3 (13%)	MLLCT - LC (C ⁴ N) - LC (N ⁴ N)
7	22533,52	443,78	0	H-1->L+4 (10%), HOMO->L+1 (29%), HOMO->L+3 (34%)	MLLCT - LC (C ⁴ N)
8	22865,82	437,33	0	H-1->L+3 (26%), HOMO->L+4 (30%), HOMO->L+5 (13%)	MLLCT - LC (C ⁴ N)
9	23457,02	426,31	0	H-6->LUMO (36%), H-4->LUMO (47%)	MLLCT - LC (C ⁴ N) - LC (N ⁴ N)
10	24059,52	415,64	0	H-5->LUMO (73%), H-3->LUMO (12%)	MLLCT - LC (C ⁴ N)

Table S32. Singlet-singlet transitions above 300nm and 10 first singlet-triplet transitions predicted for the protonated form of IrppyF₂-2244tpy in MeCN with their oscillator strength and major orbitals contributions

S ₀ to S _x	Energy (cm ⁻¹)	Wavelength (nm)	Osc. Strength	Major contributions	Attribution
1	17426,41	573,84	0,0021	HOMO->LUMO (97%)	MLLCT - LC (C [^] N)
2	21488,22	465,37	0,0136	H-1->LUMO (96%)	ILCT
3	22182,67	450,80	0,0031	H-3->LUMO (13%), H-2->LUMO (83%)	MLLCT - LC (C [^] N)
4	23373,14	427,84	0,004	H-3->LUMO (60%), HOMO->L+1 (25%)	MLLCT - LC (C [^] N)
5	23662,69	422,61	0,0004	H-3->LUMO (22%), HOMO->L+1 (70%)	MLLCT
6	24345,04	410,76	0,145	H-5->LUMO (13%), H-4->LUMO (82%)	MLLCT - LC (C [^] N)
7	25432,27	393,20	0,0203	H-5->LUMO (84%), H-4->LUMO (14%)	MLLCT - LC (C [^] N)
8	27387,36	365,13	0,0579	HOMO->L+2 (26%), HOMO->L+3 (70%)	MLLCT - LC (C [^] N)
9	27748,70	360,38	0,0026	H-1->L+1 (94%)	ILCT
10	28318,13	353,13	0	H-2->L+1 (14%), HOMO->L+4 (74%)	MLLCT - LC (C [^] N)
11	28401,20	352,10	0,0114	H-3->L+1 (15%), H-2->L+1 (57%), HOMO->L+4 (20%)	MLLCT - LC (C [^] N)
12	29246,47	341,92	0,027	H-6->LUMO (62%), H-4->L+1 (10%), H-2->L+1 (13%)	MLLCT - LC (N [^] N)
13	29760,25	336,02	0,0412	H-6->LUMO (12%), H-3->L+1 (67%), H-2->L+1 (14%)	MLLCT - LC (N [^] N)
14	29955,43	333,83	0,005	H-4->L+1 (10%), HOMO->L+2 (13%), HOMO->L+5 (65%)	MLLCT - LC (C [^] N)
15	30214,34	330,97	0,0506	H-6->LUMO (18%), H-5->L+1 (14%), H-4->L+1 (49%)	MLLCT - LC (N [^] N)
16	30902,33	323,60	0,0004	HOMO->L+2 (55%), HOMO->L+3 (21%), HOMO->L+5 (22%)	MLLCT - LC (C [^] N)
17	31744,37	315,02	0,002	H-5->L+1 (74%), H-4->L+1 (23%)	MLLCT
18	32160,55	310,94	0,0368	H-1->L+2 (23%), H-1->L+3 (51%)	ILCT - LC (C [^] N)
19	32373,48	308,89	0,0282	H-3->L+3 (17%), H-2->L+2 (12%), H-2->L+3 (31%), H-1->L+4 (13%)	MLLCT - LC (C [^] N)
20	32686,42	305,94	0,003	HOMO->L+6 (90%)	MLLCT - LC (C [^] N)
21	32800,96	304,87	0,1016	H-2->L+3 (10%), H-1->L+4 (66%)	MLLCT - LC (C [^] N)
22	33330,06	300,03	0,0579	H-3->L+4 (20%), H-2->L+4 (53%)	MLLCT - LC (C [^] N)
<hr/>					
S ₀ to T _x	Energy (cm ⁻¹)	Wavelength (nm)	Osc. Strength	Major contributions	Attribution
S ₀ to T _x	Energy (cm ⁻¹)	Wavelength (nm)	Osc. Strength	Major contributions	Attribution
1	17256,23	579,50	0	HOMO->LUMO (96%)	MLLCT - LC (C [^] N)
2	20980,09	476,64	0	H-4->LUMO (13%), H-1->LUMO (55%)	MLLCT - LC (C [^] N)
3	21621,30	462,51	0	H-3->LUMO (32%), H-2->LUMO (21%), H-1->LUMO (31%)	MLLCT - LC (C [^] N)
4	22521,42	444,02	0	H-5->LUMO (10%), H-4->LUMO (16%), H-2->LUMO (56%)	MLLCT - LC (C [^] N)
5	23043,26	433,97	0	H-5->LUMO (11%), H-4->LUMO (27%), H-3->LUMO (25%)	MLLCT - LC (C [^] N)
6	23444,92	426,53	0	H-1->L+4 (19%), HOMO->L+1 (25%), HOMO->L+3 (24%)	MLLCT - LC (C [^] N)
7	23576,39	424,15	0	HOMO->L+1 (50%), HOMO->L+3 (11%)	MLLCT - LC (C [^] N)
8	23694,96	422,03	0	H-2->L+4 (10%), H-1->L+3 (23%), HOMO->L+1 (11%), HOMO->L+4 (30%)	MLLCT - LC (C [^] N)
9	24736,22	404,27	0	H-6->LUMO (40%), H-6->L+1 (29%), H-3->LUMO (21%)	MLLCT - LC (N [^] N)
10	25299,19	395,27	0	H-5->LUMO (64%), H-4->LUMO (33%)	MLLCT - LC (C [^] N)

Table S33. Singlet-singlet transitions above 300nm and 10 first singlet-triplet transitions predicted for the protonated form of IrppyF₂-2254tpy in MeCN with their oscillator strength and major orbitals contributions

S ₀ to S _x	Energy (cm ⁻¹)	Wavelength (nm)	Osc. Strength	Major contributions	Attribution
1	17415,93	574,19	0,0005	HOMO->LUMO (98%)	MLLCT - LC (C [^] N)
2	21380,14	467,72	0,0038	H-1->LUMO (93%)	ILCT
3	22117,34	452,13	0,0003	H-3->LUMO (11%), H-2->LUMO (83%)	MLLCT - LC (C [^] N)
4	23390,88	427,52	0,0051	H-3->LUMO (82%), H-2->LUMO (11%)	MLLCT - LC (C [^] N)
5	23983,70	416,95	0,0285	H-5->LUMO (13%), H-4->LUMO (80%)	MLLCT - LC (C [^] N)
6	24695,08	404,94	0,0017	HOMO->L+1 (88%)	MLLCT
7	25351,62	394,45	0,0029	H-5->LUMO (78%), H-4->LUMO (15%)	MLLCT - LC (C [^] N)
8	27397,04	365,00	0,0562	HOMO->L+2 (31%), HOMO->L+3 (64%)	MLLCT - LC (C [^] N)
9	28297,96	353,38	0,002	HOMO->L+4 (89%)	MLLCT - LC (C [^] N)
10	29066,61	344,04	0,0122	H-1->L+1 (94%)	ILCT
11	29382,78	340,34	0,0053	HOMO->L+2 (44%), HOMO->L+3 (22%), HOMO->L+5 (27%)	MLLCT - LC (C [^] N)
12	29486,02	339,14	0,0382	H-6->LUMO (11%), H-3->L+1 (24%), H-2->L+1 (58%)	MLLCT - LC (C [^] N)
13	29892,52	334,53	0,5638	H-6->LUMO (84%), H-2->L+1 (11%)	MLLCT - LC (C [^] N) - LC (N [^] N)
14	30790,22	324,78	0,0274	H-3->L+1 (41%), H-2->L+1 (16%), HOMO->L+5 (21%)	MLLCT - LC (C [^] N)
15	30888,61	323,74	0,0073	H-3->L+1 (24%), HOMO->L+5 (44%)	MLLCT - LC (C [^] N)
16	31262,05	319,88	0,0195	H-4->L+1 (34%), HOMO->L+6 (47%)	MLLCT
17	31602,42	316,43	0,0642	H-5->L+1 (11%), H-4->L+1 (37%), HOMO->L+6 (39%)	MLLCT
18	32146,03	311,08	0,022	H-1->L+2 (21%), H-1->L+3 (39%)	MLLCT - LC (C [^] N)
19	32408,97	308,56	0,0249	H-3->L+3 (12%), H-2->L+2 (10%), H-2->L+3 (27%), H-1->L+3 (18%)	MLLCT - LC (C [^] N)
20	32809,02	304,79	0,1191	H-1->L+4 (62%)	MLLCT - LC (C [^] N)
21	32934,04	303,64	0,0126	H-5->L+1 (69%), H-4->L+1 (16%)	MLLCT - LC (C [^] N)
22	33258,27	300,68	0,0064	H-2->L+4 (12%), H-1->L+2 (33%), H-1->L+3 (23%), H-1->L+5 (12%)	MLLCT - LC (C [^] N)
S ₀ to T _x	Energy (cm ⁻¹)	Wavelength (nm)	Osc. Strength	Major contributions	Attribution
1	17323,18	577,26	0	HOMO->LUMO (97%)	MLLCT - LC (C [^] N)
2	21175,28	472,25	0	H-1->LUMO (76%)	MLLCT - LC (C [^] N)
3	21387,40	467,56	0	H-6->LUMO (23%), H-3->LUMO (36%), H-2->LUMO (12%), H-1->LUMO (13%)	MLLCT - LC (N [^] N)
4	22315,75	448,11	0	H-6->LUMO (14%), H-2->LUMO (72%)	MLLCT - LC (N [^] N)
5	23083,59	433,21	0	H-5->LUMO (17%), H-4->LUMO (53%), H-3->LUMO (12%)	MLLCT - LC (C [^] N)
6	23473,15	426,02	0	H-1->L+4 (23%), HOMO->L+2 (16%), HOMO->L+3 (29%)	MLLCT - LC (C [^] N)
7	23676,41	422,36	0	H-2->L+4 (10%), H-1->L+2 (11%), H-1->L+3 (21%), HOMO->L+4 (34%)	MLLCT - LC (C [^] N)
8	23943,37	417,65	0	H-6->LUMO (37%), H-3->LUMO (41%)	MLLCT - LC (N [^] N)
9	24525,71	407,74	0	HOMO->L+1 (85%)	MLLCT
10	25262,09	395,85	0	H-5->LUMO (67%), H-4->LUMO (26%)	MLLCT

Table S34. Singlet-singlet transitions above 300nm and 10 first singlet-triplet transitions predicted for the protonated form of Irpiq-2244tpy in MeCN with their oscillator strength and major orbitals contributions

S ₀ to S _x	Energy (cm ⁻¹)	Wavelength (nm)	Osc. Strength	Major contributionss	Attribution
1	15043,85	664,72	0,001	HOMO->LUMO (97%)	MLLCT
2	18820,14	531,35	0,0183	H-1->LUMO (98%)	ILCT
3	19979,16	500,52	0,0067	H-2->LUMO (93%)	MLLCT
4	21312,39	469,21	0,0059	HOMO->L+1 (95%)	MLLCT
5	22136,69	451,74	0,0583	H-3->LUMO (36%), HOMO->L+2 (50%)	MLLCT - LC (C ^N)
6	22247,19	449,49	0,0482	H-3->LUMO (45%), HOMO->L+2 (46%)	MLLCT - LC (C ^N)
7	22798,87	438,62	0,0839	H-4->LUMO (67%), HOMO->L+3 (18%)	MLLCT - LC (C ^N)
8	23291,68	429,34	0,0251	H-4->LUMO (13%), HOMO->L+3 (78%)	MLLCT - LC (C ^N)
9	24058,71	415,65	0,0379	H-5->LUMO (92%)	MLLCT
10	25202,41	396,79	0,0053	H-1->L+1 (96%)	ILCT
11	26275,12	380,59	0,0119	H-2->L+1 (88%)	MLLCT
12	26759,06	373,71	0,0198	H-1->L+2 (92%)	LC (C ^N)
13	27240,57	367,10	0,0459	H-2->L+2 (34%), H-1->L+3 (51%)	MLCT/LC (C ^N)
14	27385,75	365,15	0,002	H-7->LUMO (11%), H-6->LUMO (86%)	ILCT
15	27790,64	359,83	0,0329	H-2->L+2 (16%), H-1->L+3 (18%), HOMO->L+4 (29%), HOMO->L+5 (28%)	MLLCT - LC (N ^N) - LC (C ^N)
16	27805,16	359,65	0,0503	H-2->L+2 (29%), H-1->L+3 (23%), HOMO->L+4 (19%), HOMO->L+5 (20%)	MLLCT - LC (N ^N) - LC (C ^N)
17	28178,59	354,88	0,0014	H-7->LUMO (87%), H-6->LUMO (11%)	ILCT
18	28314,90	353,17	0,0025	H-3->L+1 (21%), HOMO->L+4 (40%), HOMO->L+5 (31%)	MLLCT
19	28379,42	352,37	0,0198	H-3->L+1 (50%), HOMO->L+4 (11%), HOMO->L+5 (15%)	MLLCT
20	28524,60	350,57	0,0378	H-2->L+3 (73%)	MLCT/LC (C ^N)
21	28739,95	347,95	0,0181	H-8->LUMO (12%), H-4->L+1 (66%)	MLLCT - LC (N ^N)
22	29405,36	340,07	0,0755	H-8->LUMO (75%), H-4->L+1 (17%)	MLLCT - LC (N ^N)
23	29671,52	337,02	0,0432	H-3->L+2 (73%)	MLCT/LC (C ^N)
24	29973,18	333,63	0,0334	H-4->L+2 (17%), H-3->L+3 (66%)	MLCT/LC (C ^N)
25	30101,42	332,21	0,243	H-4->L+2 (56%), H-3->L+3 (16%)	MLCT/LC (C ^N)
26	30347,42	329,52	0,0048	H-5->L+1 (70%)	MLCT/LC (C ^N)
27	30408,72	328,85	0,0079	HOMO->L+6 (89%)	MLLCT
28	30724,88	325,47	0,038	H-5->L+1 (14%), H-4->L+3 (58%)	MLLCT - LC (C ^N)
29	31207,20	320,44	0,0131	H-5->L+2 (61%), H-4->L+3 (12%)	MLCT/LC (C ^N)
30	31280,60	319,69	0,0008	H-1->L+4 (93%)	ILCT
31	31458,04	317,88	0,0219	H-11->LUMO (16%), H-9->LUMO (73%)	MLLCT
32	31616,93	316,29	0,0306	H-5->L+3 (34%), HOMO->L+7 (32%), HOMO->L+8 (12%)	MLLCT - LC (C ^N)
33	31992,79	312,57	0,0293	H-5->L+3 (16%), H-1->L+5 (22%), HOMO->L+7 (42%)	MLLCT - LC (C ^N)
34	32079,09	311,73	0,0554	H-5->L+3 (25%), H-1->L+5 (34%), HOMO->L+8 (24%)	MLLCT - LC (C ^N)
35	32132,32	311,21	0,01	H-1->L+5 (33%), HOMO->L+8 (49%)	MLLCT - LC (C ^N)
36	32513,82	307,56	0,0361	H-10->LUMO (81%)	MLLCT
37	32667,87	306,11	0,0162	H-2->L+4 (66%), H-2->L+5 (21%)	MLLCT
38	33154,23	301,62	0,0229	H-2->L+4 (27%), H-2->L+5 (57%)	MLLCT
39	33261,50	300,65	0,0209	H-11->LUMO (66%), H-9->LUMO (17%)	MLLCT

S_0 to T_x	Energy (cm ⁻¹)	Wavelength (nm)	Osc. Strength	Major contributions	Attribution
1	14886,58	671,75	0	HOMO->LUMO (96%)	MLLCT
2	18161,19	550,62	0	H-2->L+2 (14%), H-1->L+3 (31%), HOMO->L+2 (40%)	MLLCT - LC (C^N)
3	18303,14	546,35	0	H-2->L+3 (12%), H-1->LUMO (20%), H-1->L+2 (31%), HOMO->L+3 (26%)	MLLCT - LC (C^N)
4	18470,10	541,42	0	H-1->LUMO (64%)	MLLCT - LC (C^N)
5	19622,66	509,61	0	H-4->LUMO (11%), H-2->LUMO (76%)	MLLCT
6	21117,21	473,55	0	H-4->LUMO (17%), HOMO->L+1 (62%)	MLLCT
7	21383,37	467,65	0	H-5->LUMO (13%), H-4->LUMO (11%), H-3->LUMO (41%), HOMO->L+1 (21%)	MLLCT
8	21920,54	456,19	0	H-4->LUMO (19%), H-3->LUMO (13%), H-2->L+2 (13%), HOMO->L+2 (20%)	MLLCT - LC (C^N)
9	21976,19	455,04	0	H-4->LUMO (17%), H-3->LUMO (19%), H-2->L+2 (11%), HOMO->L+2 (28%)	MLLCT - LC (C^N)
10	22467,38	445,09	0	H-2->L+3 (19%), HOMO->L+3 (56%)	MLLCT - LC (C^N)

Table S35. Singlet-singlet transitions above 300nm and 10 first singlet-triplet transitions predicted for the protonated form of Irpiq-2254tpy in MeCN with their oscillator strength and major orbitals contributions

S ₀ to S _x	Energy (cm ⁻¹)	Wavelength (nm)	Osc. Strength	Major contributions	Attribution
1	14901,90	671,06	0,001	HOMO->LUMO (98%)	MLLCT - LC (C ⁴ N)
2	18574,95	538,36	0,0035	H-1->LUMO (97%)	ILCT
3	19777,52	505,62	0,0003	H-2->LUMO (93%)	MLLCT - LC (C ⁴ N)
4	21985,87	454,84	0,0206	H-3->LUMO (74%), HOMO->L+1 (10%), HOMO->L+2 (12%)	MLLCT - LC (C ⁴ N)
5	22015,71	454,22	0,0493	H-3->LUMO (18%), HOMO->L+1 (21%), HOMO->L+2 (48%)	MLLCT - LC (C ⁴ N)
6	22262,52	449,19	0,0368	H-4->LUMO (34%), HOMO->L+1 (27%), HOMO->L+2 (33%)	MLLCT - LC (C ⁴ N)
7	22622,24	442,04	0,0179	H-4->LUMO (49%), HOMO->L+1 (37%)	MLLCT
8	23345,72	428,34	0,0006	HOMO->L+3 (91%)	MLLCT - LC (C ⁴ N)
9	23864,33	419,04	0,0083	H-5->LUMO (88%)	MLLCT - LC (C ⁴ N)
10	26471,92	377,76	0,0192	H-1->L+1 (92%)	ILCT - LC (C ⁴ N)
11	26712,28	374,36	0,0321	H-1->L+2 (86%)	LC (C ⁴ N)
12	27033,28	369,91	0,0004	HOMO->L+4 (73%), HOMO->L+5 (20%)	MLLCT
13	27122,01	368,70	0,0093	H-7->LUMO (12%), H-6->LUMO (45%), H-2->L+1 (14%), H-2->L+2 (11%)	ILCT - LC (C ⁴ N)
14	27172,82	368,01	0,0158	H-6->LUMO (29%), H-2->L+1 (12%), H-2->L+2 (23%), H-1->L+3 (15%)	MLLCT - LC (C ⁴ N)
15	27477,70	363,93	0,0228	H-2->L+1 (58%), H-2->L+2 (13%), H-1->L+3 (13%)	MLLCT - LC (C ⁴ N)
16	27799,51	359,72	0,0678	H-2->L+2 (31%), H-1->L+3 (57%)	MLCT/LC (C ⁴ N)
17	28000,34	357,14	0,0007	H-7->LUMO (78%), H-6->LUMO (21%)	ILCT
18	28442,34	351,59	0,0011	HOMO->L+4 (19%), HOMO->L+5 (75%)	MLLCT
19	28561,71	350,12	0,0537	H-2->L+3 (73%)	MLCT/LC (C ⁴ N)
20	29088,39	343,78	0,0068	HOMO->L+6 (83%)	MLLCT
21	29292,44	341,38	0,2033	H-8->LUMO (29%), H-3->L+1 (23%), H-3->L+2 (31%)	MLLCT - LC (C ⁴ N) - LC (N ⁴ N)
22	29569,09	338,19	0,0692	H-4->L+1 (11%), H-3->L+1 (14%), H-3->L+2 (39%)	MLLCT - LC (C ⁴ N)
23	29673,94	337,00	0,3084	H-8->LUMO (52%), H-3->L+1 (18%), H-3->L+3 (10%)	MLLCT - LC (C ⁴ N) - LC (N ⁴ N)
24	30057,06	332,70	0,272	H-4->L+2 (56%), H-3->L+3 (15%)	MLCT/LC (C ⁴ N)
25	30146,58	331,71	0,1198	H-4->L+1 (52%), H-4->L+2 (10%), H-3->L+3 (13%)	MLLCT - LC (C ⁴ N)
26	30418,39	328,75	0,0451	H-4->L+1 (20%), H-3->L+1 (20%), H-3->L+3 (39%)	MLLCT - LC (C ⁴ N)
27	30578,90	327,02	0,0161	H-4->L+3 (15%), H-1->L+4 (62%), H-1->L+5 (10%)	MLLCT - LC (C ⁴ N)
28	30757,15	325,13	0,0147	H-5->L+2 (16%), H-4->L+3 (40%), H-1->L+4 (22%)	MLLCT - LC (C ⁴ N)
29	31221,72	320,29	0,0056	H-5->L+2 (57%), H-4->L+3 (21%)	MLCT/LC (C ⁴ N)
30	31234,63	320,16	0,0137	H-11->LUMO (15%), H-9->LUMO (56%), H-5->L+1 (14%)	MLLCT - LC (C ⁴ N)
31	31457,24	317,89	0,0059	H-9->LUMO (12%), H-5->L+1 (41%), H-5->L+3 (16%)	MLLCT - LC (C ⁴ N)
32	31822,60	314,24	0,046	H-5->L+1 (11%), H-2->L+4 (27%), H-1->L+5 (10%), HOMO->L+7 (20%)	MLLCT - LC (C ⁴ N)
33	31921,81	313,27	0,0381	H-2->L+4 (28%), HOMO->L+7 (31%)	MLLCT - LC (C ⁴ N)
34	31983,11	312,67	0,0037	H-2->L+4 (12%), H-1->L+4 (11%), H-1->L+5 (59%)	MLLCT
35	32068,60	311,83	0,0002	HOMO->L+7 (28%), HOMO->L+8 (44%)	MLLCT - LC (C ⁴ N)
36	32321,86	309,39	0,0468	H-5->L+1 (12%), H-5->L+3 (50%), HOMO->L+8 (20%)	MLLCT - LC (C ⁴ N)
37	32363,80	308,99	0,0012	H-10->LUMO (80%)	MLLCT - LC (C ⁴ N)
38	33086,48	302,24	0,0029	H-12->LUMO (10%), H-11->LUMO (60%), H-9->LUMO (19%)	MLLCT - LC (C ⁴ N)
39	33129,22	301,85	0,0242	H-2->L+5 (13%), H-1->L+6 (70%)	MLLCT
40	33292,95	300,36	0,0197	H-2->L+4 (14%), H-2->L+5 (56%), H-1->L+6 (17%)	MLLCT

S ₀ to T _x	Energy (cm ⁻¹)	Wavelength (nm)	Osc. Strength	Major contributions	Attribution
1	14813,18	675,07	0	HOMO->LUMO (98%)	MLLCT
2	18097,47	552,56	0	H-1->LUMO (25%), H-1->L+2 (14%), H-1->L+3 (13%), HOMO->L+2 (24%)	MLLCT - LC (C [^] N)
3	18224,90	548,70	0	H-1->LUMO (16%), H-1->L+2 (11%), H-1->L+3 (15%), HOMO->L+2 (18%), HOMO->L+3 (15%)	MLLCT - LC (C [^] N)
4	18563,66	538,69	0	H-1->LUMO (53%), H-1->L+2 (19%), HOMO->L+3 (12%)	MLLCT - LC (C [^] N)
5	19554,11	511,40	0	H-2->LUMO (82%)	MLLCT - LC (C [^] N)
6	21364,82	468,06	0	H-8->LUMO (22%), H-4->LUMO (42%), H-2->LUMO (12%)	MLLCT - LC (N [^] N)
7	21480,16	465,55	0	H-5->LUMO (11%), H-3->LUMO (75%)	MLLCT - LC (C [^] N)
8	21751,16	459,75	0	H-2->L+2 (17%), HOMO->L+1 (23%), HOMO->L+2 (35%)	MLLCT - LC (C [^] N)
9	22252,84	449,38	0	HOMO->L+1 (37%), HOMO->L+2 (12%)	MLCT/LC (C [^] N)
10	22752,90	439,50	0	HOMO->L+1 (22%), HOMO->L+3 (50%)	MLLCT - LC (C [^] N)

Figure S78. Experimental spectra and calculated transitions for Irppy-bpy in MeCN

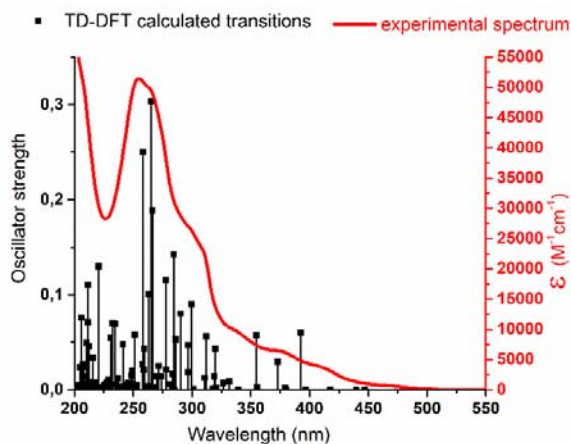


Figure S79. Experimental spectra and calculated transitions for IrppyF₂-bpy in MeCN

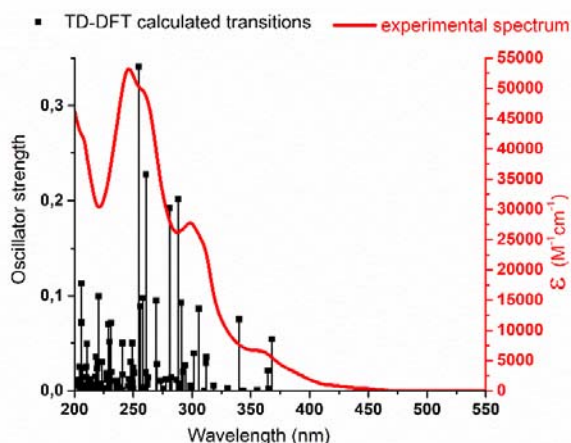


Figure S80. Experimental spectra and calculated transitions for Irpiq-bpy in MeCN

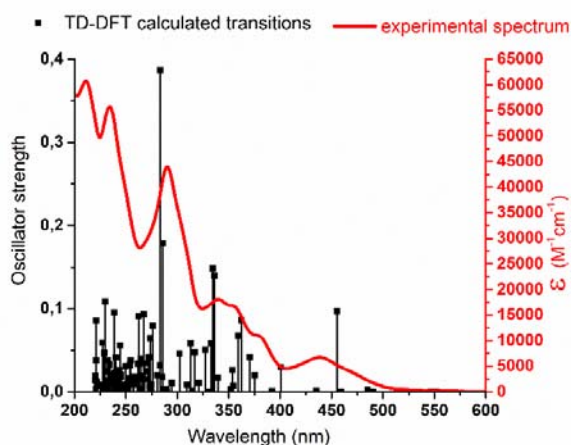


Figure S81. Experimental spectra and calculated transitions for Irppy-2244tpy in MeCN

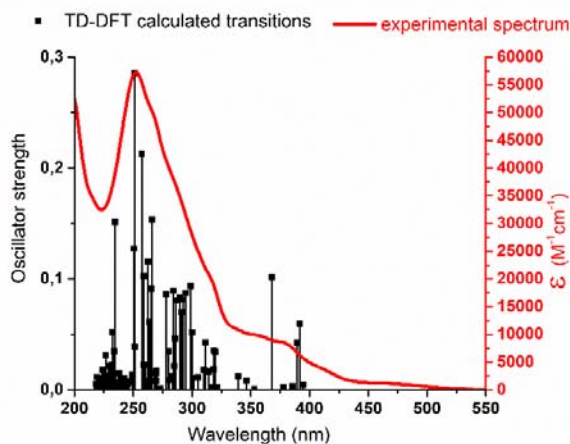


Figure S82. Experimental spectra and calculated transitions for Irppy-2254tpy in MeCN

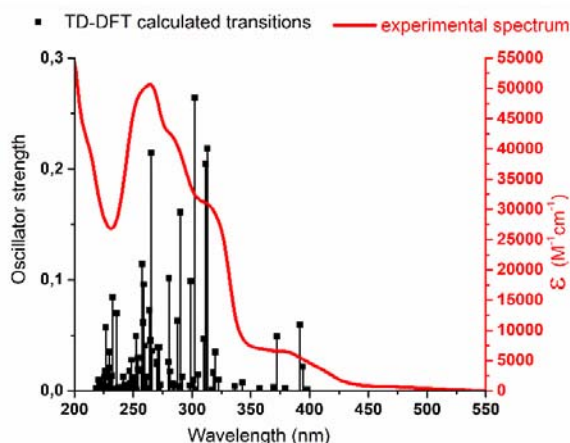


Figure S83. Experimental spectra and calculated transitions for IrppyF₂-2244tpy in MeCN

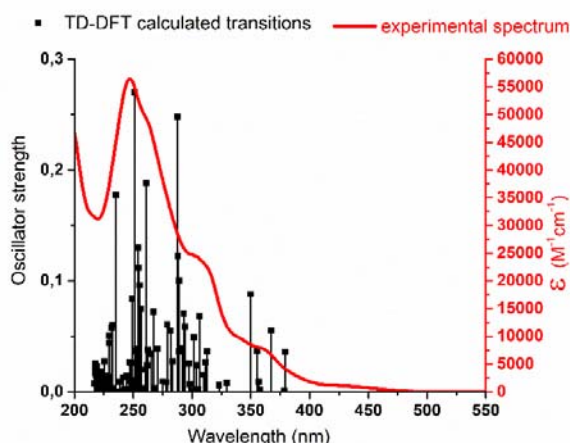


Figure S84. Experimental spectra and calculated transitions for IrppyF₂-2254tpy in MeCN

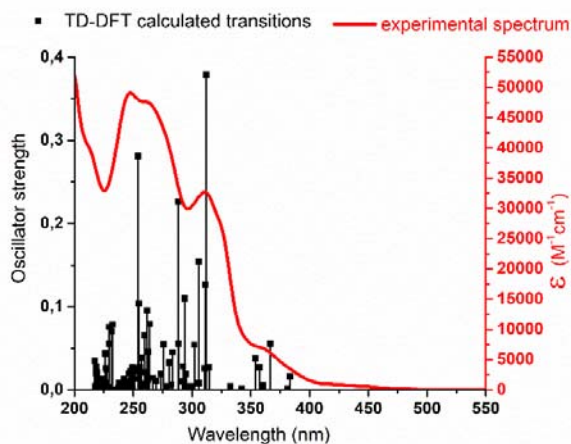


Figure S85. Experimental spectra and calculated transitions for Irpiq-2244tpy in MeCN

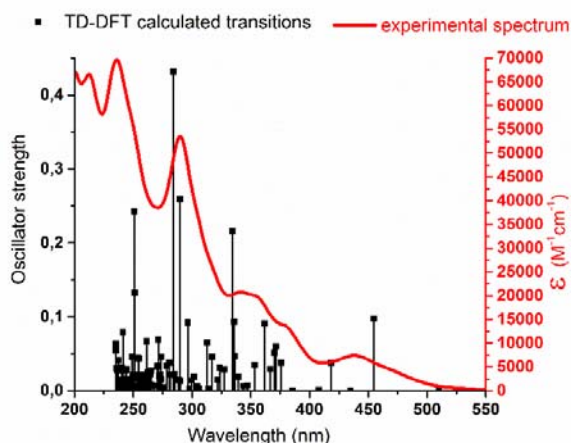


Figure S86. Experimental spectra and calculated transitions for Irpiq-2254tpy in MeCN

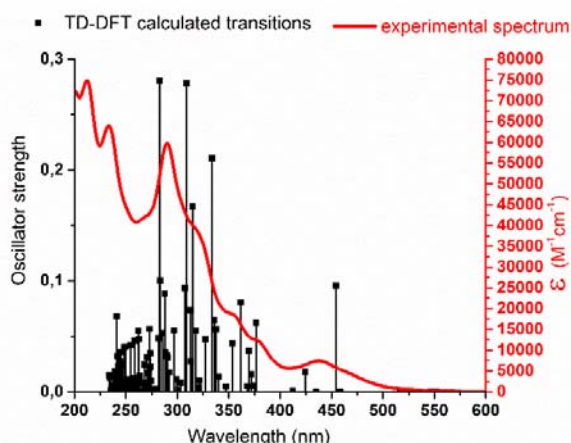


Figure S87. Experimental spectra and calculated transitions for Irppy-2244tpy-H⁺ in MeCN

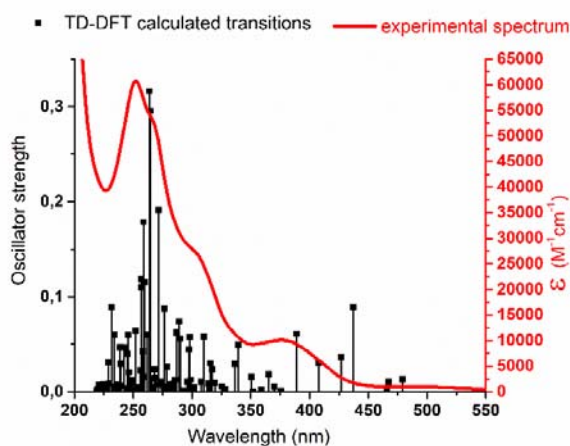


Figure S88. Experimental spectra and calculated transitions for Irppy-2254tpy-H⁺ in MeCN

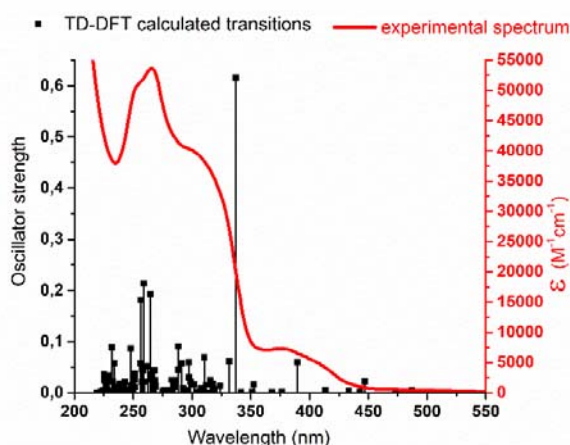


Figure S89. Experimental spectra and calculated transitions for the IrppyF₂-2244tpy-H⁺ in MeCN

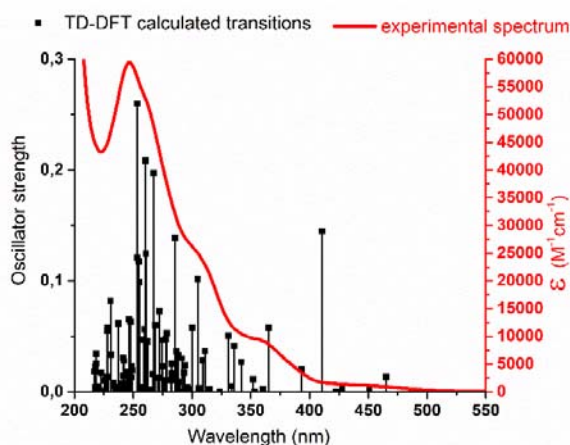


Figure S90. Experimental spectra and calculated transitions for IrppyF₂-2254-H⁺ in MeCN

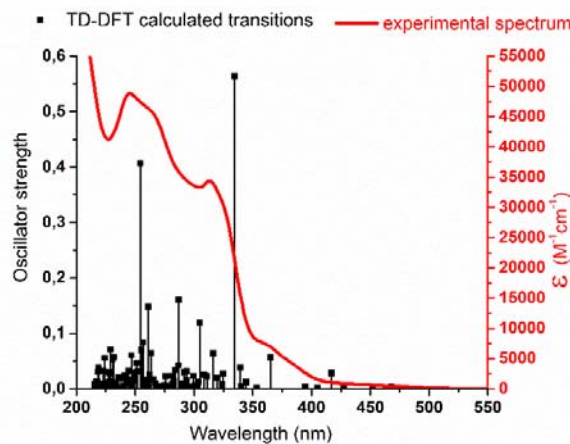


Figure S91. Experimental spectra and calculated transitions for Irpiq-2244-H⁺ in MeCN

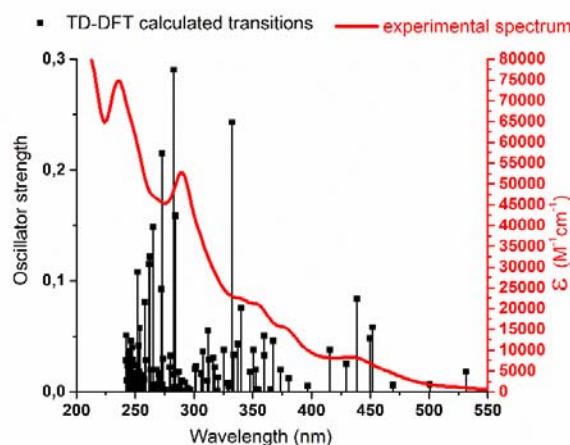


Figure S92. Experimental spectra and calculated transitions for Irpiq-2254tpy-H⁺ in MeCN

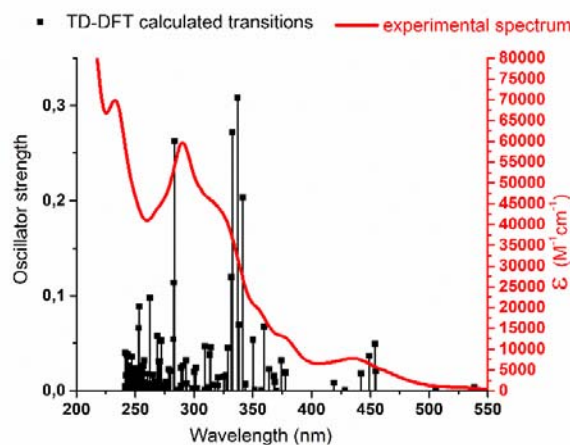


Photo-catalyzed hydrogen production

Co(dmgH)₂ClPyr. Co(dmgH)₂ClPyr is synthetized by a procedure as reported⁴.

CoCl₂.6H₂O (150 mg, 0.65 mmol), dimethylglyoxime (167 mg, 1.4 mmol) and NaOH (26.0 mg, 0.65 mmol) were dissolved in 95% ethanol (5.0 mL) and heated to 70 °C. Pyridine (51 mg, 0.65 mmol) were then added and the resulting solution cooled to room temperature. A stream of air was then passed through the solution for 30 min, which caused precipitation of a brown solid. The suspension was stirred for 1 h and filtered. The precipitate was successively washed with water (10 mL), ethanol (10 mL), and diethyl ether (10 mL). The product was then extracted with acetone (15 mL) and the solution is let to a slow evaporation (m = 130 mg 49%). Elemental Analysis: calc for C₁₃H₁₉ClCoN₅O₄ C= 38, 68 % H=4, 74 % N=17.35 %, found C=38,59 % H=4,82 % N=17.12 %

Set up of gas chromatography

Monitoring of hydrogen evolution is measured using a Perkin Elmer Clarus-580 gas chromatograph (GC) with a thermal conductivity detector, argon as carrier and eluent gas, a 7' HayeSep N 60/80 pre-column, a 9' molecular sieve 13x45/60 column and a 1 mL injection loop. Three distinct solutions for photosensitizer, for catalyst and last for sacrificial donor and acid source (HBF₄ 48% water) or two distinct solutions when Ir(III)-Co(III) dyads are used : the dyad solution and the electron and proton source solutions are mixed together to obtain 5 mL of sample solutions in standard 20 mL headspace vials. In DMF, the resulting molar concentration of photocatalytic components are: 1 M for triethanolamine (TEOA), 0.1 M for (HBF₄), 0.56 M for water, 0.1 mM for the dyad Ir-Co or 0.1 mM for the photosensitizer [Ir(ppy)₂(bpy)](PF₆)₂ and 0.1 mM for Co(dmgH)₂PyrCl. (pH apparent= 8.9) Those vials are placed on LED panel in a thermostatic bath set at 20°C. They were sealed with a rubber septum pierced with two stainless steel tubes. The first tube carried an argon flow pre-bubbled in spectrograde solvent. The flow was set to 10 mL/min (unless otherwise specified) (adjusted with a manual flow controller (Porter, 1000) and referenced with a digital flowmeter (Perkin Elmer FlowMark). The second tube lead the flow to the GC sample loop through a 2 mL overflow protection vial, then through a 8-port stream select valve (VICCI) and finally to GC sample loop. A microprocessor (Arduino Uno) coupled with a custom PC interface allowed for timed injections. For general calibration, stock cylinders of known concentration of H₂ in nitrogen replaced the nitrogen flow (inserted at the pre-bubbler, to keep the vapor matrix consistent). The measured results, independent of flow rate (under same pressure) can be easily converted into a rate of hydrogen following equation 1. For calibration of H₂ production, a nitrogen bottle of 100 ppm hydrogen certified is set to deliver a specific flow. H₂ production rate at a specific nitrogen flow, a syringe pump (New Era Pump) equipped with a gas-tight syringe (SGE) and a 26s gauge needle (Hamilton) was used to bubble different rates of pure hydrogen gas into the sample, to a minimum of 0.5 μL /minute. This gave a linear fit for peak area for H₂ versus the flow rates of H₂.

$$\text{(Eq. 1) H}_2 \text{ rate } (\mu\text{L}/\text{min}) = [\text{H}_2 \text{ standard}] \text{ (ppm)} \times \text{N}_2 \text{ flow rate (L/min)}$$

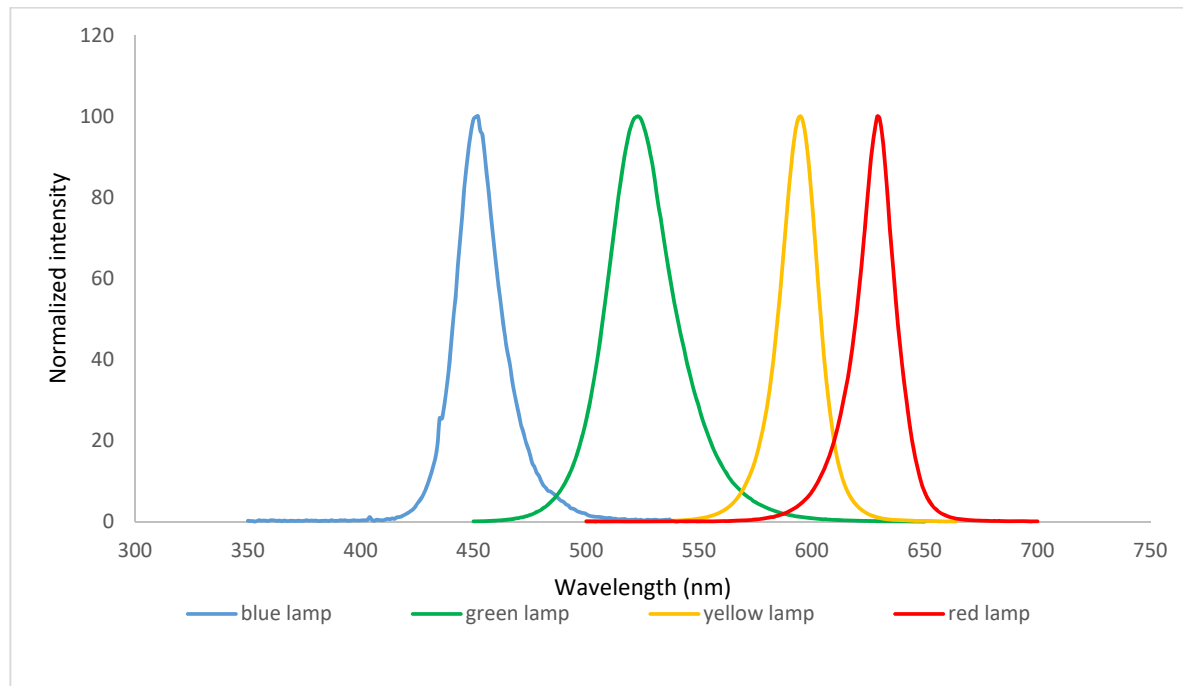


Figure S93: Emission spectra of light-emitting diodes used as irradiation sources (blue, green, yellow, red).

Table S36. Maxima, width band of emission spectra and photon flux of used L.E.D.'s.

	Blue	Green	Yellow	Red
$\lambda_{\text{max em}}$ (nm)	452	525	595	630
$\Delta\lambda$ (nm)	150	170	85	125
Photon flux in $\mu\text{Einstein} \cdot \text{min}^{-1} \cdot \text{cm}^{-2}$ [a]	20.5	10.1	13.9	24.5

[a] An analog power-meter PM100A (THORLABS) associated with a compact photodiode power head with silicon detector S120C is used to evaluate the photon flux for each LEDs. Photo-diode detector is placed at the same distance from the LED surface than the bottom of illuminated vial (0.7 cm for blue, green and red LED panels and 1.2 cm for yellow LED).

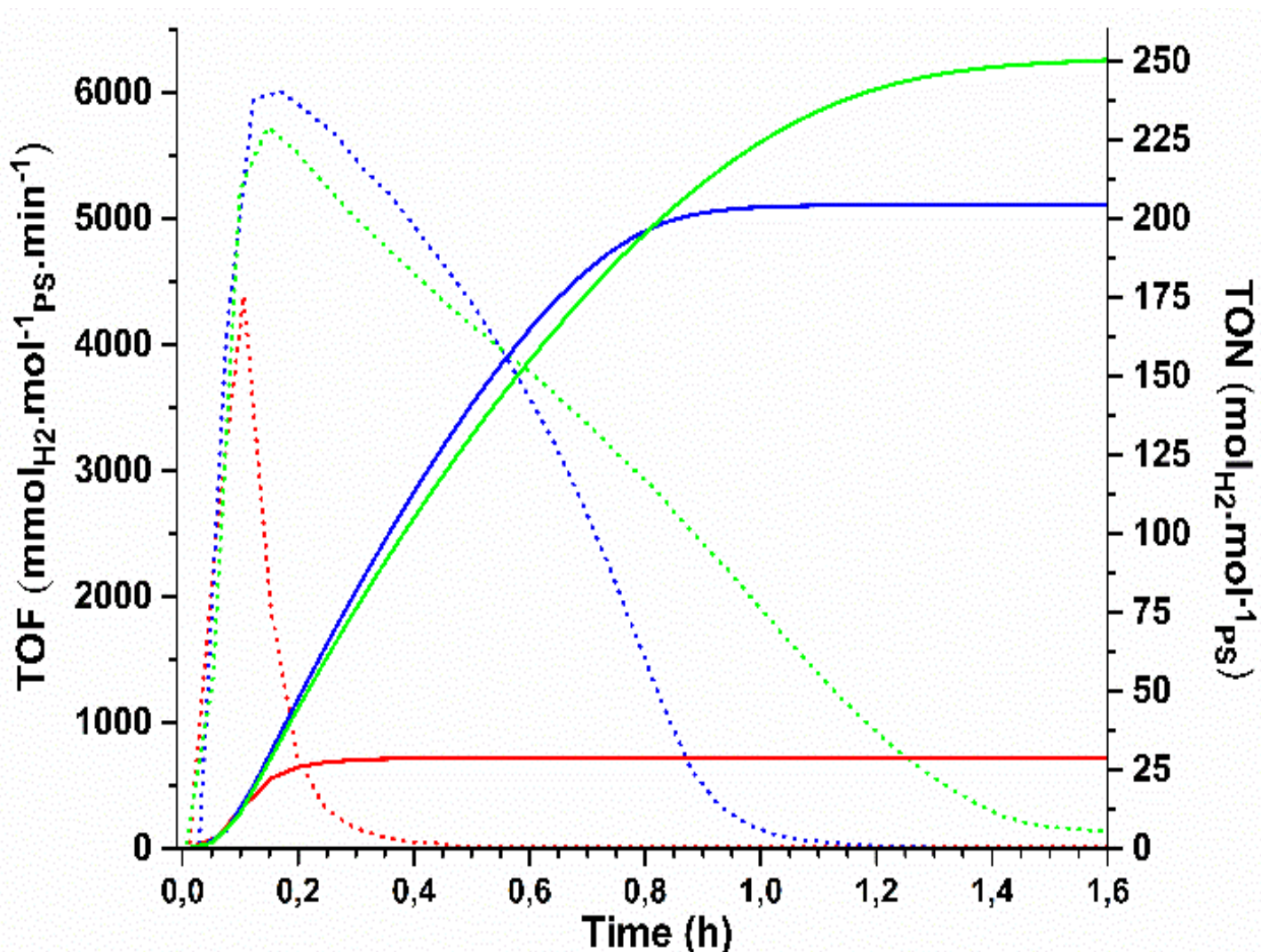


Figure 94. Hydrogen evolution of Irppy-2244tpy-Co(blue), Irppy-2254tpy-Co (green) ad dissociated system Irppy-bpy with Co(dmgH)₂PyCl (Red). Solid line : TON, dashed line : TOF. Blue LED irradiation centered at 452 nm. (blue light).

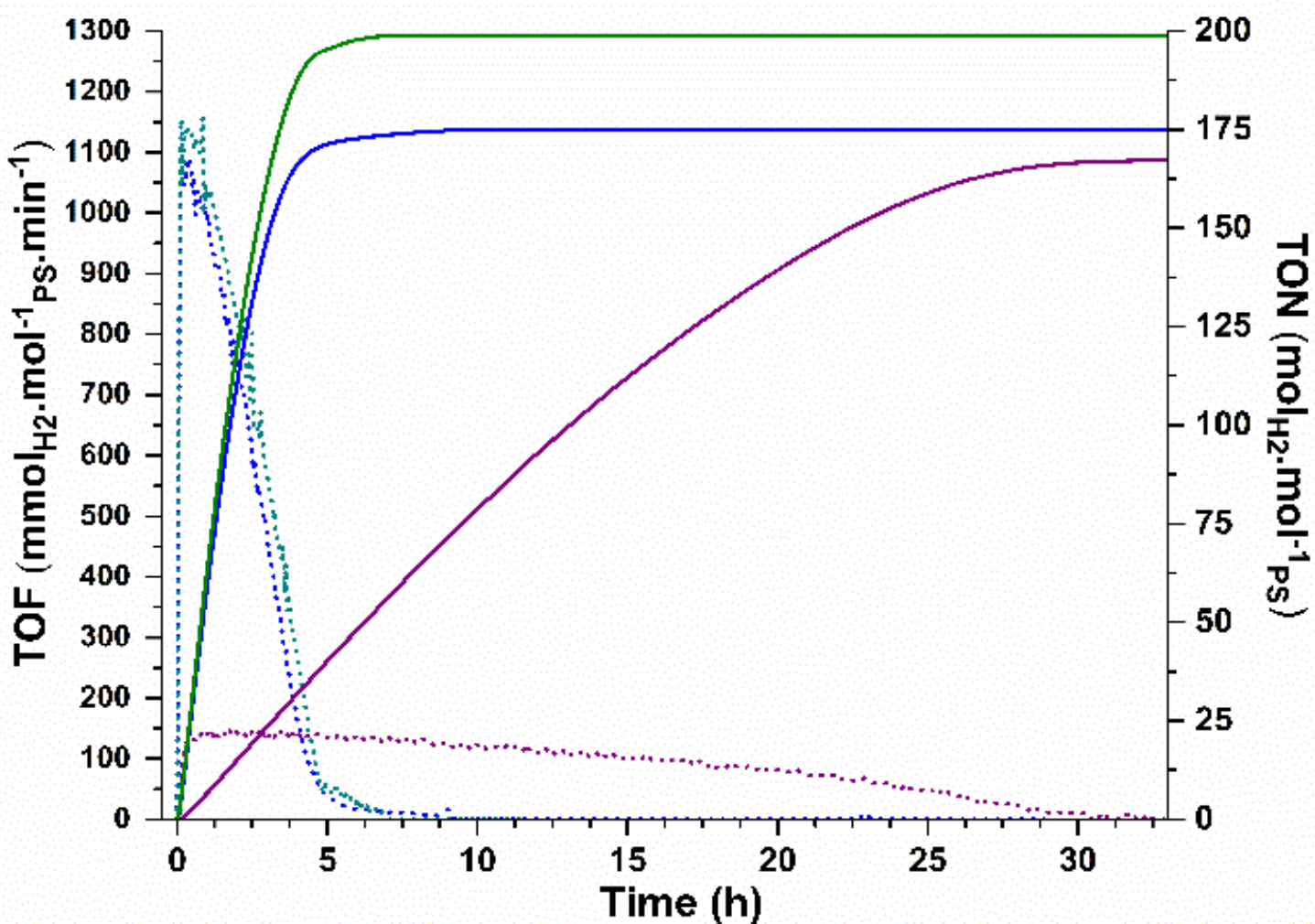


Figure 95. Hydrogen evolution of Irppy-2244tpy-Co (blue), Irppy₂-2244tpy-Co (purple) and Irpiq-2244tpy-Co (olive). Solid line: TON, dashed line: TOF. Irradiation centered at 525 nm (green light).

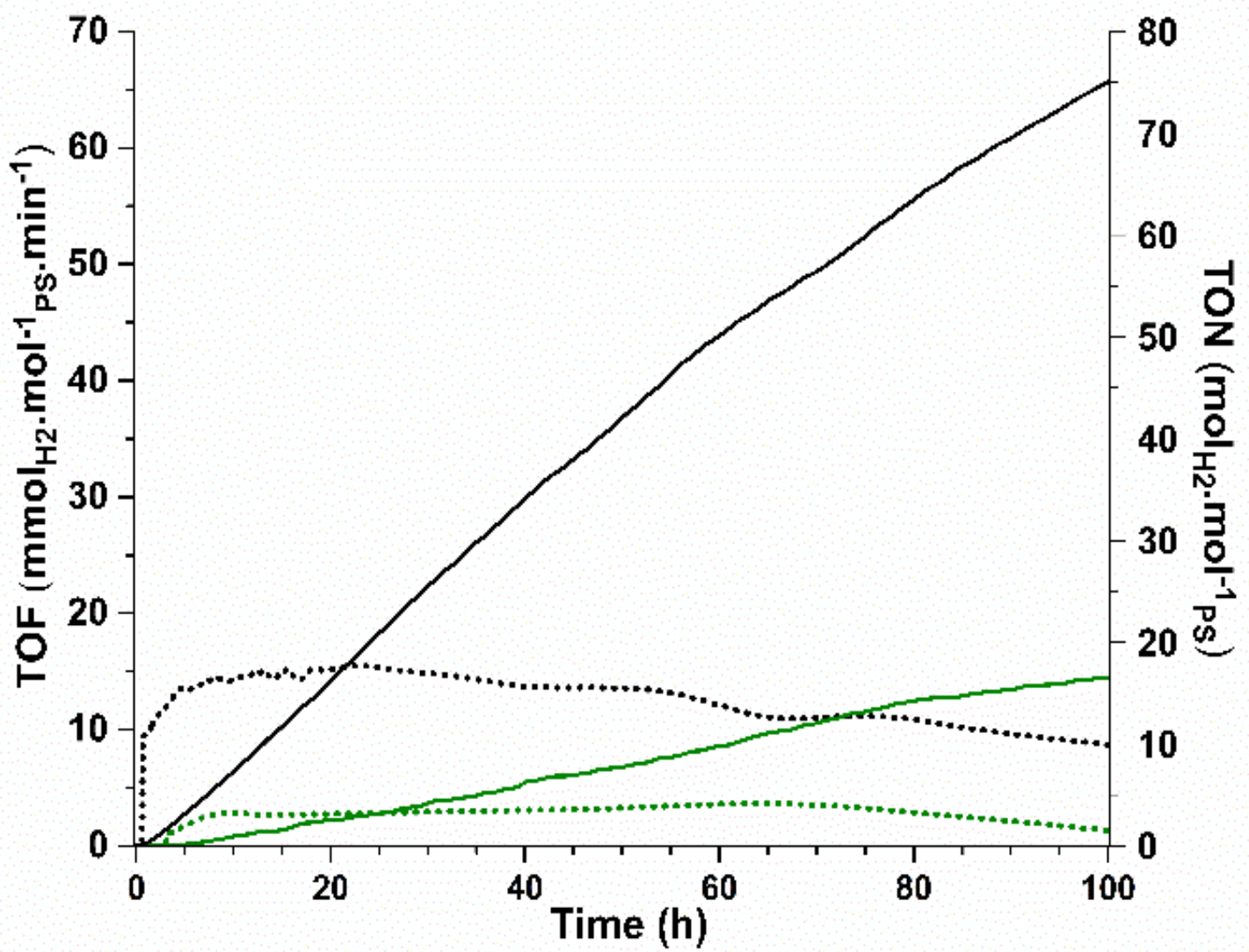


Figure 96. Hydrogen evolution of Irppy-2244tpy-Co (blue), IrppyF₂-2244tpy-Co (purple) and Irpiq-2244tpy-Co (olive). Solid line: TON, dashed line: TOF. Irradiation centered at 525 nm (green light).

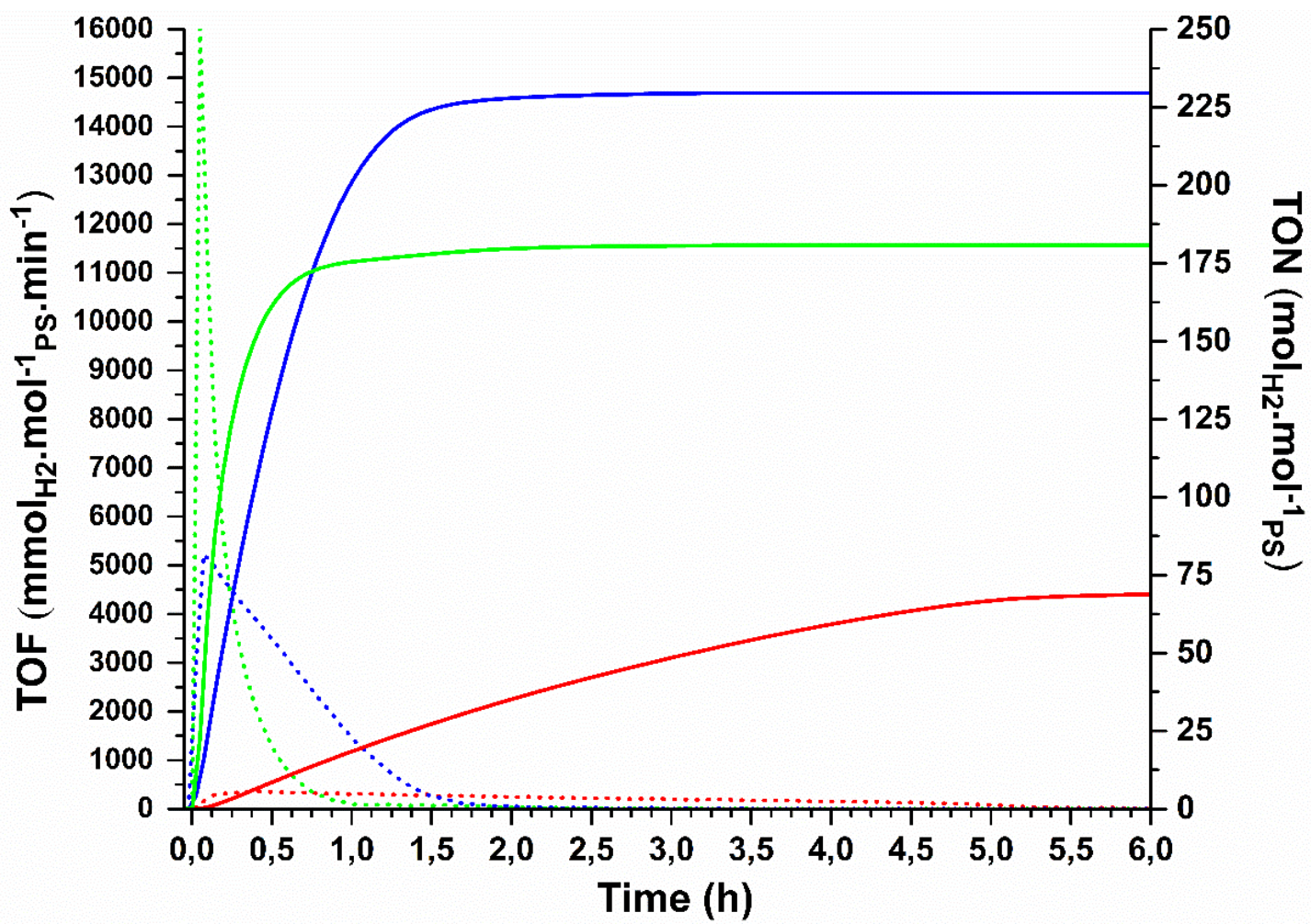


Figure S97. Hydrogen evolution of Irpiq-2244tpy-Co (blue), Irpiq-2254tpy-Co (green) and Irpiq-bpy/Co(dmgH)₂PyrCl (red). Solid line: TON, dashed line: TOF. Irradiation centered at 452 nm (blue light).

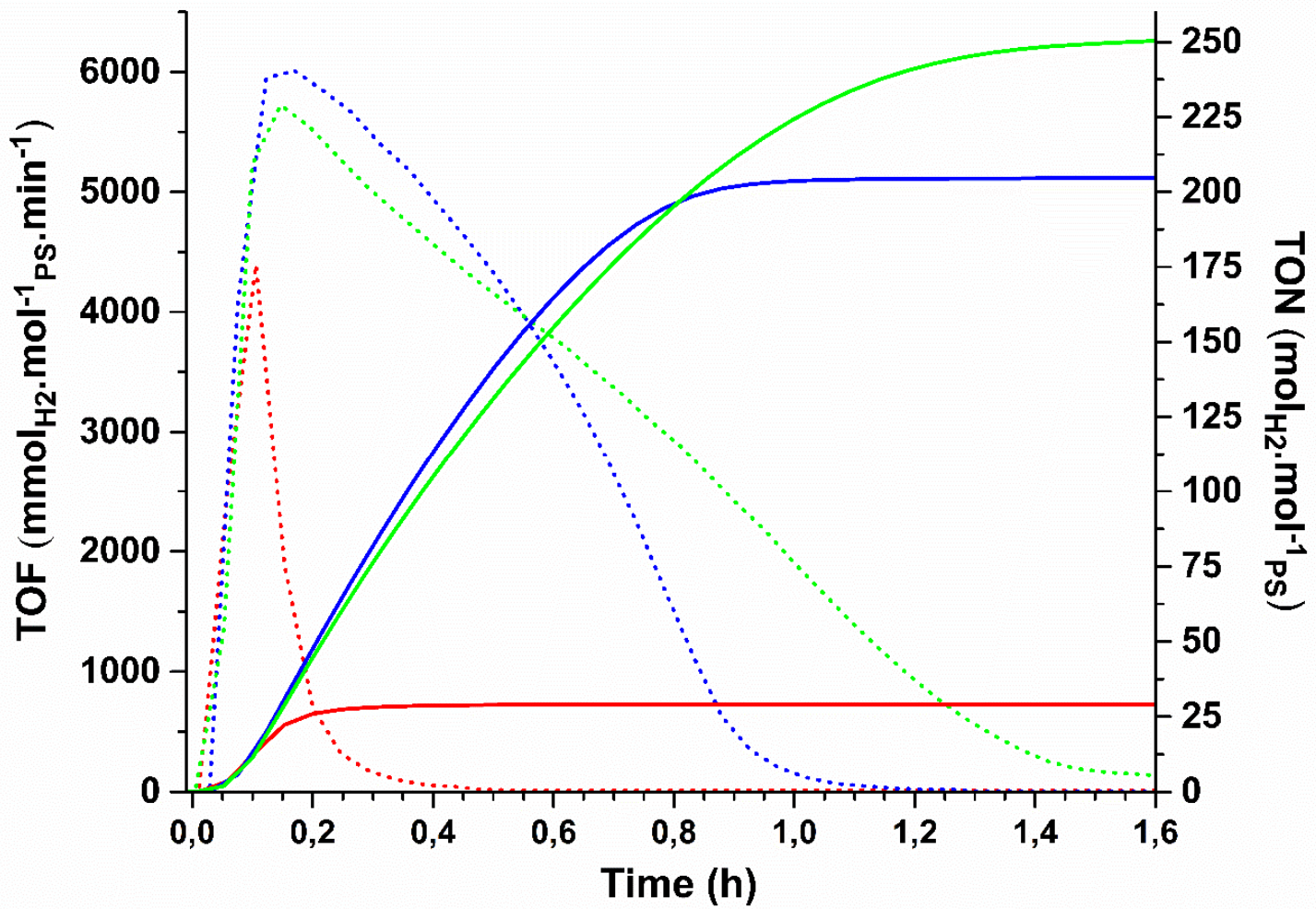


Figure S98. Hydrogen evolution of Irppy-2244tpy-Co (blue), Irppy-2254tpy-Co (green) and Irppy-bpy/Co(dmgH)₂PyrCl (red). Solid line: TON, dashed line: TOF. Irradiation centered at 452 nm (blue light).

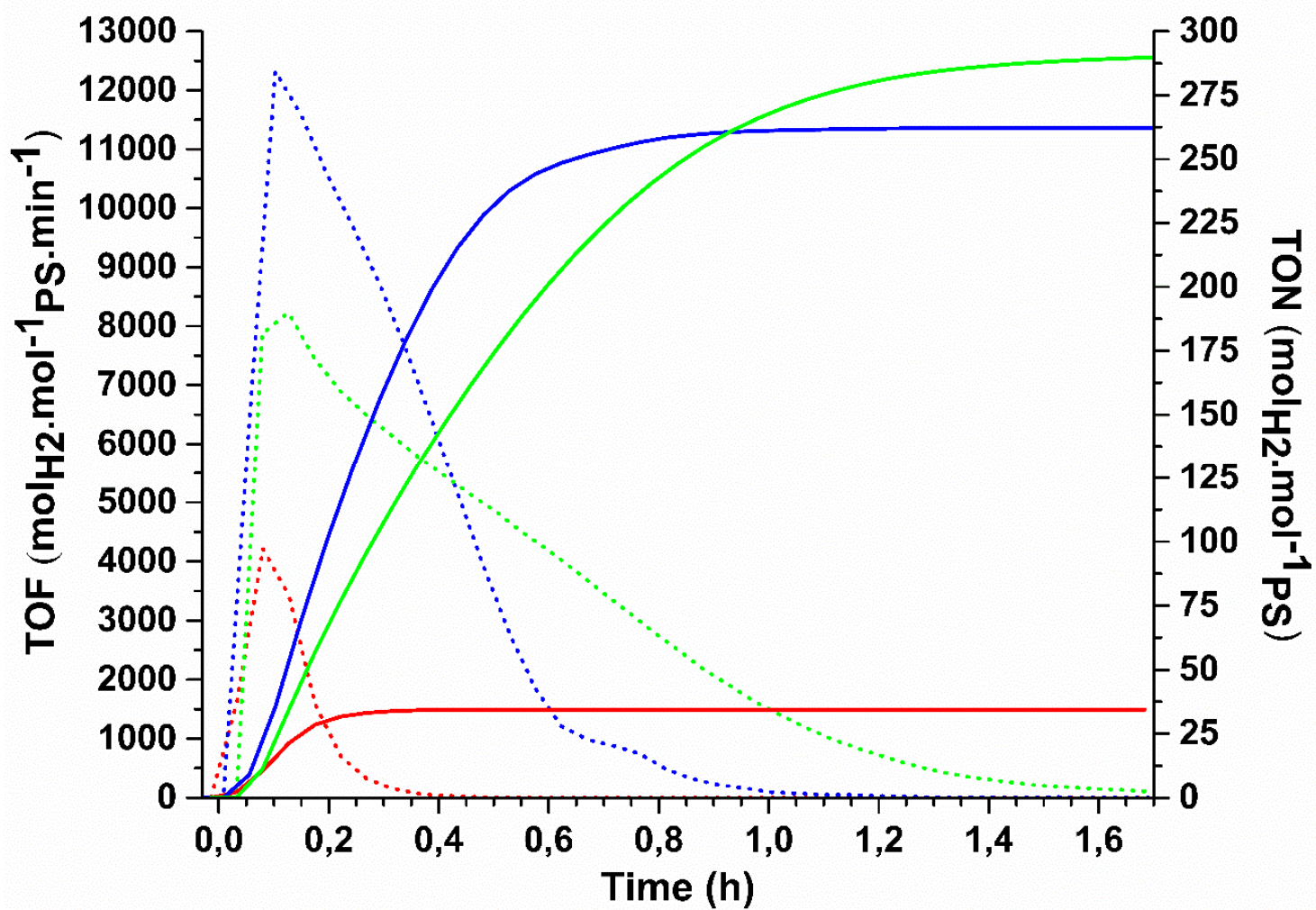


Figure S99. Hydrogen evolution of IrppyF₂-2244tpy-Co (blue), IrppyF₂-2254tpy-Co (green) and IrppyF₂-bpy /Co(dmgH)₂PyrCl (red). Solid line: TON, dashed line: TOF. Irradiation centered at 452 nm (blue light).

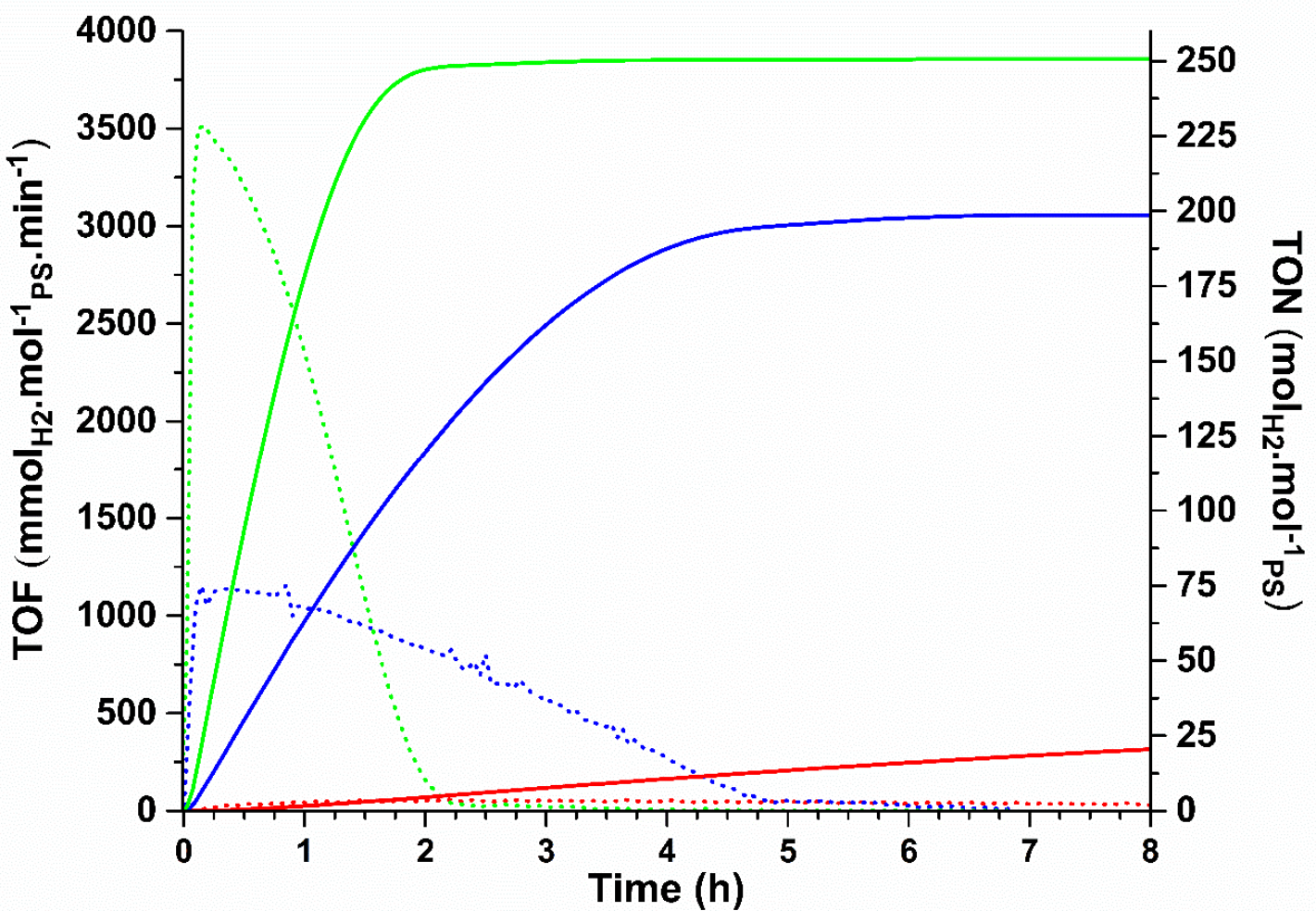


Figure S100. Hydrogen evolution of Irpiq-2244tpy-Co (blue), Irpiq-2254tpy-Co (green) and Irpiq-bpy/Co(dmgH)₂PyrCl (red). Solid line: TON, dashed line: TOF, Irradiation centered at 523 nm (green light).

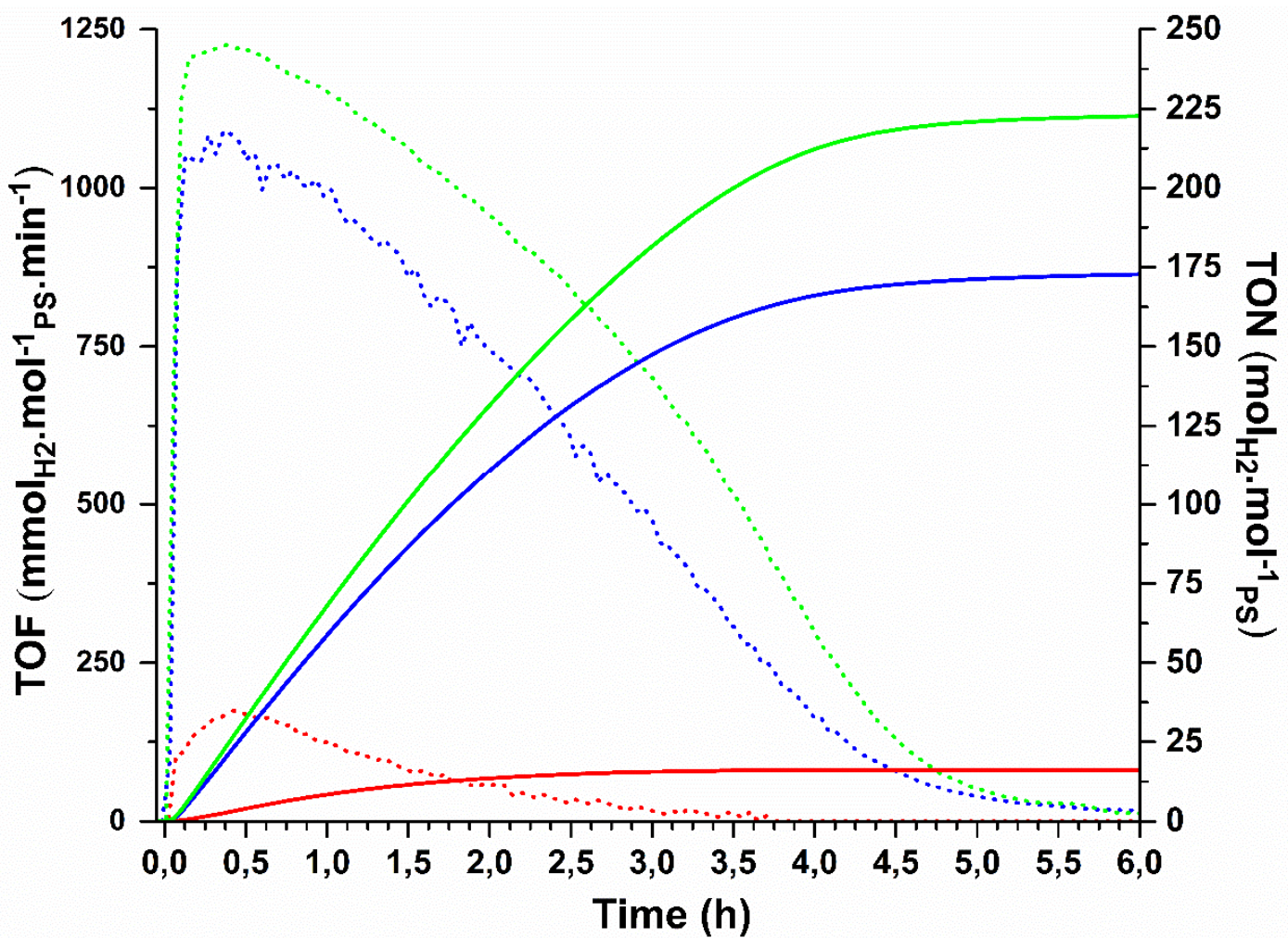


Figure S101. Hydrogen evolution of Irppy-2244tpy-Co (blue), Irppy-2254tpy-Co (green) and Irppy-bpy/Co(dmgH)₂PyrCl (red). Solid line: TON, dashed line: TOF. Irradiation centered at 523 nm (green light).

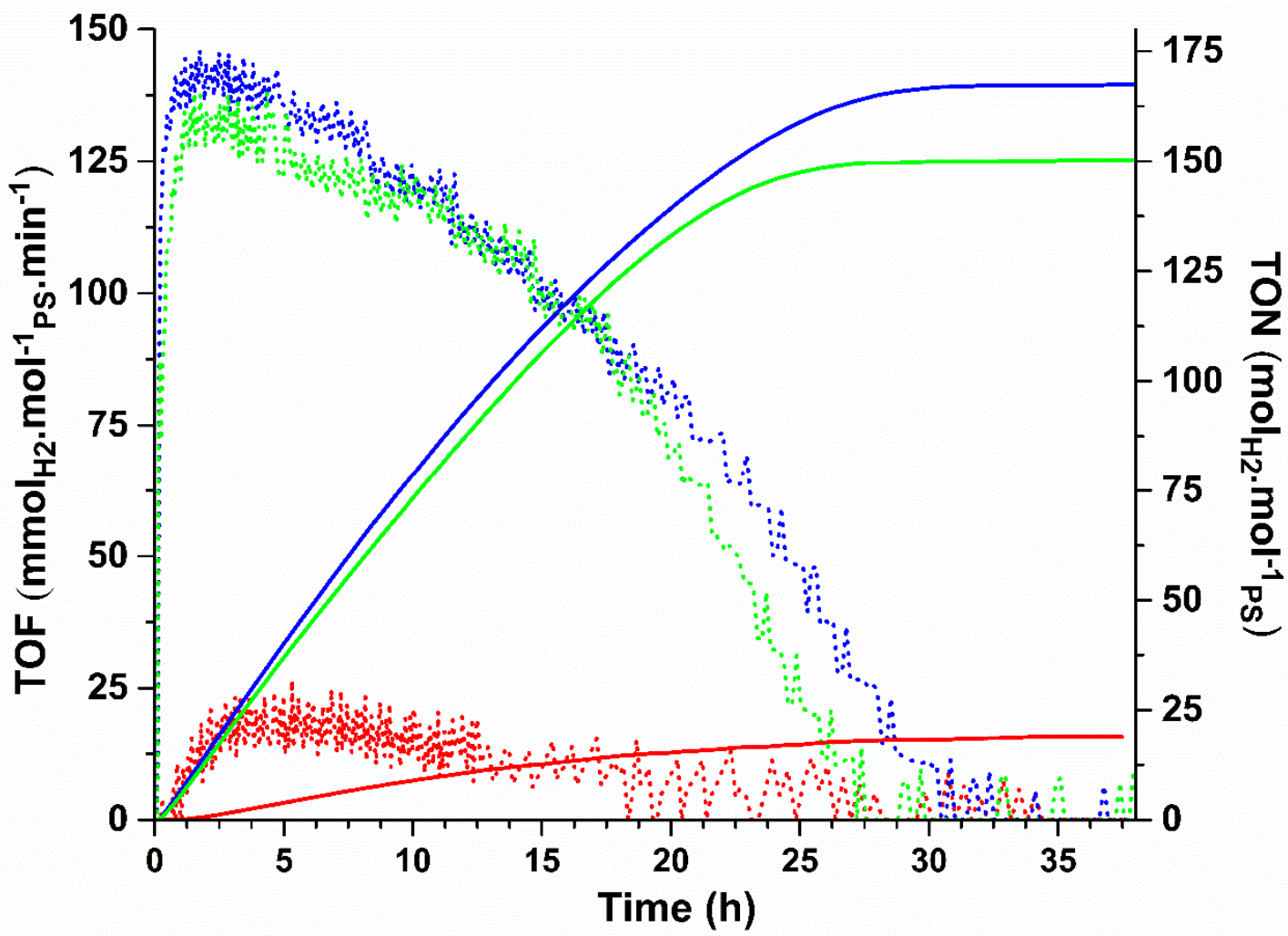


Figure S102. Hydrogen evolution of IrppyF₂-2244tpy-Co (blue), IrppyF₂-2254tpy-Co (green) and IrppyF₂-bpy/Co(dmgH)₂PyrCl (red). Solid line: TON, dashed line: TOF. Irradiation centered at 523 nm (green light)

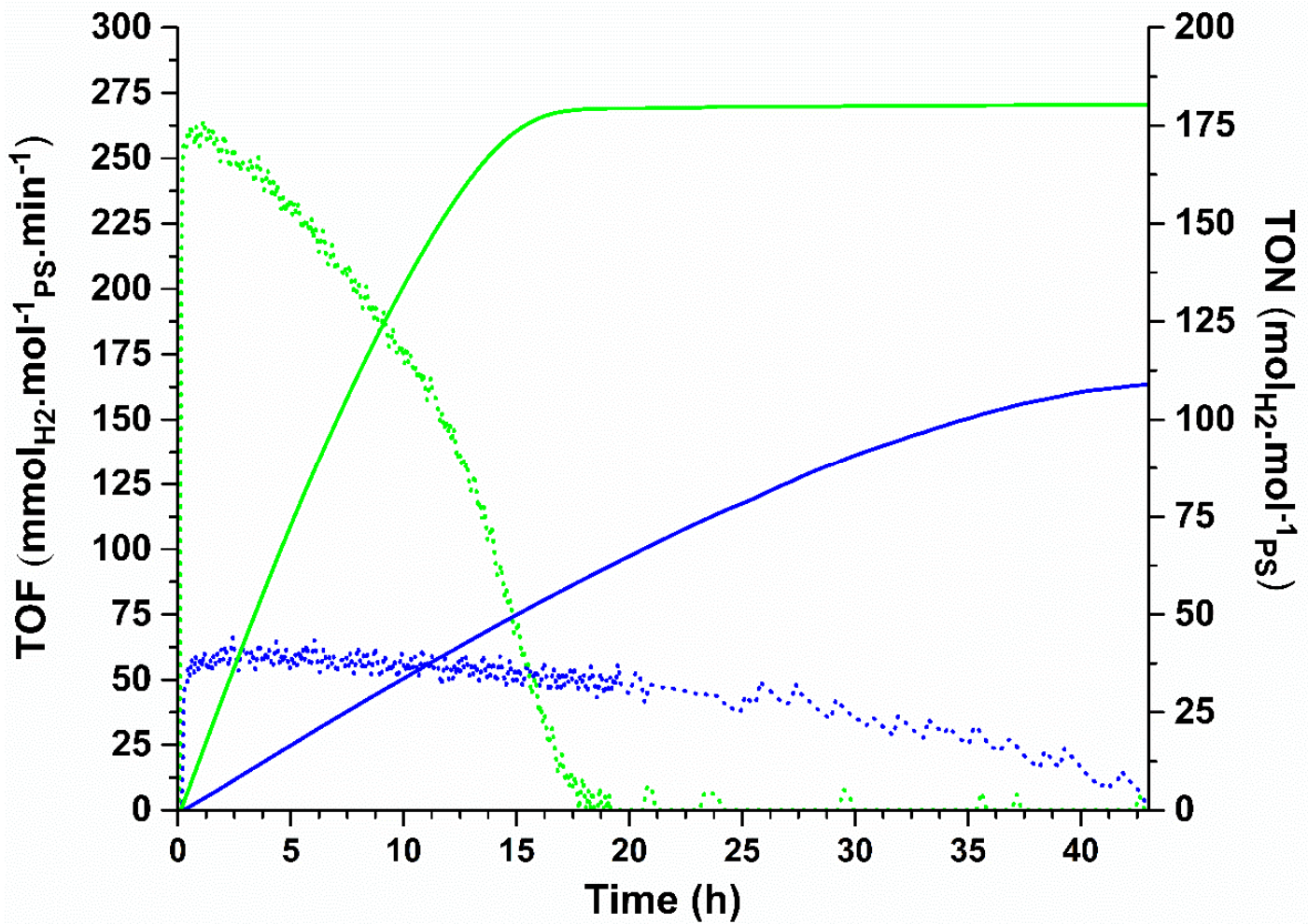


Figure S103. Hydrogen evolution of Irpiq-2244tpy-Co (blue), Irpiq-2254tpy-Co (green). Solid line: TON, dashed line: TOF, Irradiation centered at 595 nm (Yellow light).

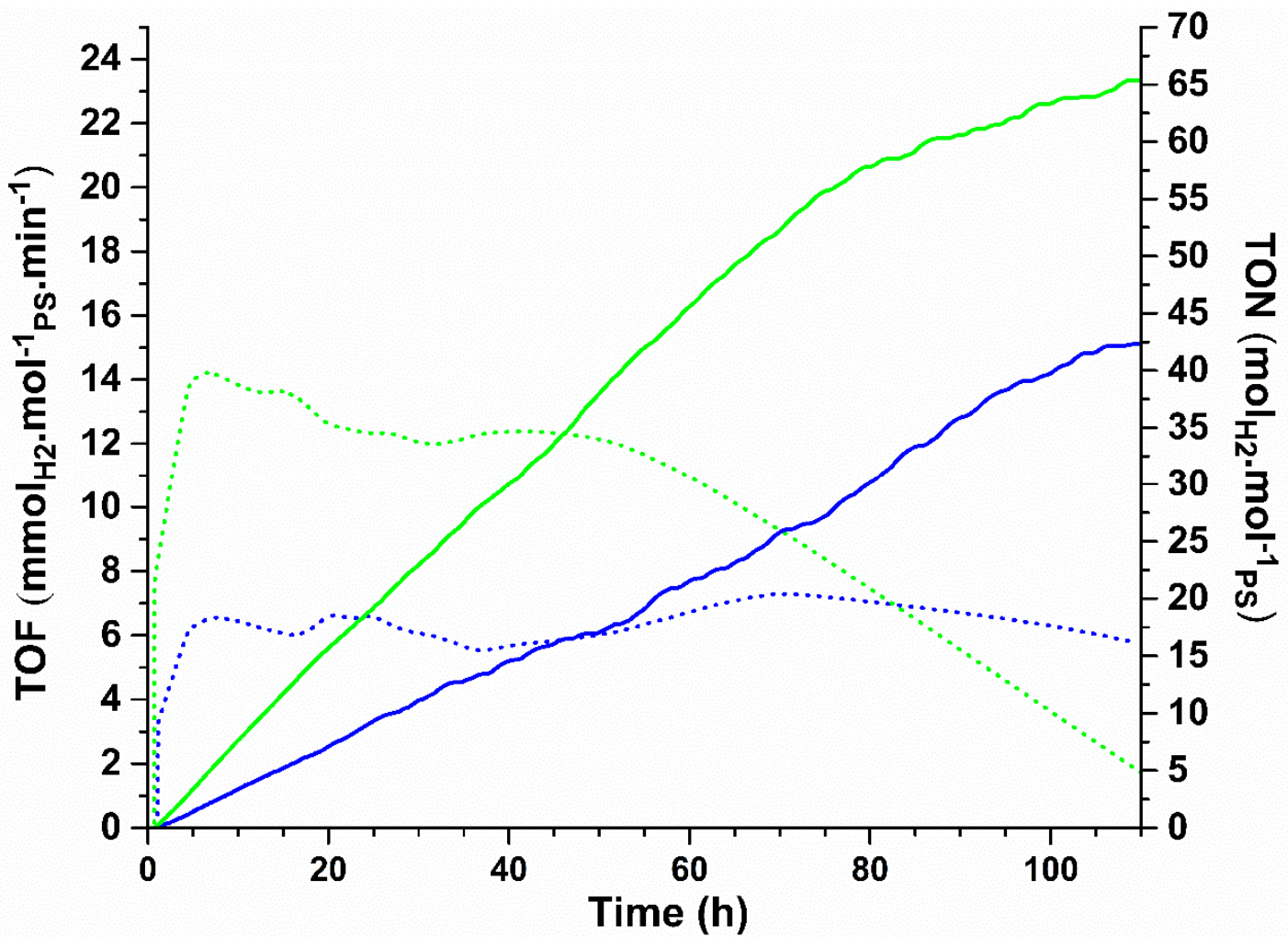


Figure S104. Hydrogen evolution of Irppy-2244tpy-Co (blue), Irppy-2254tpy-Co (green). Solid line : TON, dashed line: TOF, Irradiation centered at 595 nm (Yellow light). A data smoothing with the ORIGIN software is performed on the TOF data.

Table S37. Performances of photo-catalytic systems under yellow and red LEDs.

Compounds	Yellow LED Centered at 595 nm		Red LED Centered at 630 nm	
	TON	TOFmax	TON	TOFmax
Irppy-2244tpy-Co	43 ¹ (110 h)	7 (9 h)	No detection of hydrogen	No detection of hydrogen
Irppy-2254tpy-Co	66 ² (110 h)	14 (9 h)	No detection of hydrogen	No detection of hydrogen
Irpiq-2244tpy-Co	109 (42 h)	66 (2,4 h)	16 (100 h) ³	4 (66 h)
Irpiq-2254tpy-Co	180 (17 h)	263 (0,6 h)	75 (100 h) ⁴	15 (23 h)

TON in mol_{H2}.mol⁻¹_{ps}. TOF in mmol_{H2}. mol⁻¹_{ps}.min⁻¹; ¹ 1 hour of induction time; ² 40 minutes of induction time; ³ 3 hours 15 min of induction time; ⁴ 40 min of induction time.

References

1. K. Kodama, A. Kobayashi and T. Hirose, *Tetrahedron Lett.*, 2013, **54**, 5514-5517.
2. C. Brotschi, G. Mathis and C. J. Leumann, *Chem. - Eur. J.*, 2005, **11**, 1911-1923.
3. N. Matsuo, *Bull. Chem. Soc. Jpn.*, 1974, **47**, 767-768.
4. (a) M. Razavet, V. Artero and M. Fontecave, *Inorg. Chem.*, 2005, **44**, 4786-4795; (b) P. Du, J. Schneider, G. Luo, W. W. Brennessel and R. Eisenberg, *Inorg. Chem.*, 2009, **48**, 4952-4962.
5. *Bruker SADABS and TWINABS*, Bruker AXS Inc.: Madison, Wisconsin, USA., 2001.
6. (a) G. M. Sheldrick, *Acta Crystallogr., Sect. A*, 2008, **64**, 112-122; (b) G. M. Sheldrick, *Acta Crystallogr., Sect. A*, 2015, **71**, 3-8.
7. A. L. Spek, *Acta Crystallogr., Sect. D*, 2009, **65**, 148-155.
8. *CCDC Mercury 3.1 - 3.3, 2001-2003*.
9. S.-J. Liu, Q. Zhao, Q.-L. Fan and W. Huang, *Eur. J. Inorg. Chem.*, 2008, **2008**, 2177-2185.
10. R. D. Costa, E. Orti, H. J. Bolink, S. Gruber, S. Schaffner, M. Neuburger, C. E. Housecroft and E. C. Constable, *Adv. Funct. Mater.*, 2009, **19**, 3456-3463.
11. Gaussian 09 Revision E01, M. J. Frisch, G. W. Trucks and G. E. S. H. B. Schlegel, M. A. Robb, J. R. Cheeseman, G. Scalmani, V. Barone, G. A. Petersson, H. Nakatsuji, X. Li, M. Caricato, A. Marenich, J. Bloino, B. G. Janesko, R. Gomperts, B. Mennucci, H. P. Hratchian, J. V. Ortiz, A. F. Izmaylov, J. L. Sonnenberg, D. Williams-Young, F. Ding, F. Lipparini, F. Egidi, J. Goings, B. Peng, A. Petrone, T. Henderson, D. Ranasinghe, V. G. Zakrzewski, J. Gao, N. Rega, G. Zheng, W. Liang, M. Hada, M. Ehara, K. Toyota, R. Fukuda, J. Hasegawa, M. Ishida, T. Nakajima, Y. Honda, O. Kitao, H. Nakai, T. Vreven, K. Throssell, J. A. Montgomery, Jr., J. E. Peralta, F. Ogliaro, M. Bearpark, J. J. Heyd, E. Brothers, K. N. Kudin, V. N. Staroverov, T. Keith, R. Kobayashi, J. Normand, K. Raghavachari, A. Rendell, J. C. Burant, S. S. Iyengar, J. Tomasi, M. Cossi, J. M. Millam, M. Klene, C. Adamo, R. Cammi, J. W. Ochterski, R. L. Martin, K. Morokuma, O. Farkas, J. B. Foresman, and D. J. Fox, Gaussian, Inc., Wallingford CT, 2016.
12. (a) C. Lee, W. Yang and R. G. Parr, *Phys. Rev. B*, 1988, **37**, 785-789; (b) B. Miehlich, A. Savin, H. Stoll and H. Preuss, *Chem. Phys. Lett.*, 1989, **157**, 200-206; (c) A. D. Becke, *J. Chem. Phys.*, 1993, **98**, 5648-5652.
13. A. V. Mitin, J. Baker and P. Pulay, *J. Chem. Phys.*, 2003, **118**, 7775-7782.
14. (a) J. S. Binkley, J. A. Pople and W. J. Hehre, *J. Am. Chem. Soc.*, 1980, **102**, 939-947; (b) W. J. Stevens, H. Basch and M. Krauss, *J. Chem. Phys.*, 1984, **81**, 6026-6033; (c) W. J. Stevens, M. Krauss, H. Basch and P. G. Jasien, *Can. J. Chem.*, 1992, **70**, 612-630; (d) T. R. Cundari and W. J. Stevens, *J. Chem. Phys.*, 1993, **98**, 5555-5565.
15. N. M. O'boyle, A. L. Tenderholt and K. M. Langner, *J. Comput. Chem.*, 2008, **29**, 839-845.
16. L. Skripnikov, *Chemissian, version 4.43*, 2005–2016.
17. (a) S. Miertuš, E. Scrocco and J. Tomasi, *Chem. Phys.*, 1981, **55**, 117-129; (b) J. Tomasi, B. Mennucci and R. Cammi, *Chem. Rev.*, 2005, **105**, 2999-3094.